NTNU – Trondheim
Norwegian University of
Science and Technology

Surrogate Models for Integrated Reforming Combined Cycle Optimization

Surrogat-modeller til optimalisering av
naturgassbaserte kraftverk med integrert
reformering

Mohammad Ostadi

NTNU

Norwegian University
of Science and Technology

Department of Energy
and Process Engineering

EPT-M-2013-87

MASTER THESIS

for

Stud.techn. Mohammad Ostadi

Spring 2013

Surrogate Models for Integrated Reforming Combined Cycle Optimization

Surrogat-modeller til optimalisering av naturgassbaserte kraftverk med integrert reformering

Background and objective

Natural gas combined cycle power plants with CO_2 capture are expected to play an important role in mitigating carbon emissions. Integrated Reforming Combined Cycle (IRCC) is a promising route for combined power generation and hydrogen production with CO_2 capture from natural gas. The design of an IRCC involves many parameters that interact in complex relationships. A modeling and optimization approach to design IRCC processes has been under development at NTNU and SINTEF. This methodology includes physical insight gained from engineering judgement, and a superstructure (i.e. multiple flowsheets drawn in one diagram with discrete decision variables making the selection of a single process flowsheet possible) has been developed with different possible combinations for an air blown or oxygen based IRCC.

The reforming process, which is an important part of an Integrated Reforming Combined Cycle plant, is a chemical process for fuel conversion. The process model involves chemical equilibrium and reaction kinetics. A first principles based model of this process used in an optimization framework will be very complex and computationally expensive. A so-called surrogate model is a multivariable general mapping that can be used in an optimization framework to reduce the model complexity and thus reduce the computational load in the optimization to something that is manageable. There are many different methods for developing surrogate models varying from "simple" polynomial models to more complicated models such as Kriging models. Kriging is a group of geostatistical techniques to interpolate the value of a random field, and Kriging belongs to the family of linear least squares estimation algorithms.

The <u>main objective</u> of this master thesis project is to develop surrogate models for the reforming section of an IRCC for use in a deterministic optimization framework that reflect a good trade-off between accuracy and computational cost.

The following tasks are to be considered:

1. A brief literature study should be undertaken about Integrated Reforming Combined Cycle processes as well as Surrogate Models.
2. Develop a reforming section model in HYSYS, including pre-reformer, air-blown ATR, oxygen-blown ATR, standard 2 step shift reactors, and an advanced ECN shift system design.
3. Identify operating parameters and data collection schemes for surrogate model development.
4. Develop surrogate models of two types:
   a. Polynomial models
   b. Kriging type models
5. Compare the accuracy of polynomial and Kriging type models
6. Compare the computational cost for the two types of models from an optimization point of view.
7. Present recommendations for which surrogate model to be used.

-- " --

Within 14 days of receiving the written text on the master thesis, the candidate shall submit a research plan for his project to the department.

When the thesis is evaluated, emphasis is put on processing of the results, and that they are presented in tabular and/or graphic form in a clear manner, and that they are analyzed carefully.

The thesis should be formulated as a research report with summary both in English and Norwegian, conclusion, literature references, table of contents etc. During the preparation of the text, the candidate should make an effort to produce a well-structured and easily readable report. In order to ease the evaluation of the thesis, it is important that the cross-references are correct. In the making of the report, strong emphasis should be placed on both a thorough discussion of the results and an orderly presentation.

The candidate is requested to initiate and keep close contact with his/her academic supervisor(s) throughout the working period. The candidate must follow the rules and regulations of NTNU as well as passive directions given by the Department of Energy and Process Engineering.

Risk assessment of the candidate's work shall be carried out according to the department's procedures. The risk assessment must be documented and included as part of the final report. Events related to the candidate's work adversely affecting the health, safety or security, must be documented and included as part of the final report. If the documentation on risk assessment represents a large number of pages, the full version is to be submitted electronically to the supervisor and an excerpt is included in the report.

Pursuant to "Regulations concerning the supplementary provisions to the technology study program/Master of Science" at NTNU §20, the Department reserves the permission to utilize all the results and data for teaching and research purposes as well as in future publications.

The final report is to be submitted digitally in DAIM. An executive summary of the thesis including title, student's name, supervisor's name, year, department name, and NTNU's logo and name, shall be submitted to the department as a separate pdf file. Based on an agreement with the supervisor, the final report and other material and documents may be given to the supervisor in digital format.

☐ Work to be done in lab (Water power lab, Fluids engineering lab, Thermal engineering lab)
☐ Field work

Department of Energy and Process Engineering, 23 January 2013

Olav Bolland
Department Head

Truls Gundersen
Academic Supervisor

Research Advisor:

PhD Rahul Anantharaman, SINTEF Energy Research

Preface

This master thesis ends my two year master studies in Natural Gas Technology at the Norwegian University of Science and Technology (NTNU). The thesis was written at the Department of Energy and Process Engineering.

Working on this thesis was challenging and exciting, and the method discussed in this report may play a significant role in the future of optimization software. Even though this master thesis presents many results, the work is far from finished, and there are many possibilities yet to explore. Hopefully this report can serve as a starting point for future student projects.

I would like to thank my supervisor, Professor Truls Gundersen for letting me work with this project, for his guidance in general and for sharing his valuable expertise and useful comments and insights.

I am also thankful to researcher Rahul Anantharaman at SINTEF Energy Research for answering my questions and his positive view on the problems encountered during the work.

I would thank Prof. Olav Bolland, for providing a nice reading place and all equipment necessary to have exciting two-year studies at NTNU.

Finally, I am immensely grateful to my parents and friends who never left me alone in all kind of difficulties. I dedicate my thesis to them for their endless love.

Any questions regarding the contents of the report can be sent to my e-mail address:

Ostadi.petroleum@gmail.com

Trondheim, 24 June 2013

Mohammad Ostadi

Abstract

In the light of increasing concerns about climate change, greenhouse gas mitigation technologies have gained growing attention. Integrated Reforming Combined Cycle (IRCC) is one of the processes for reducing CO_2 emissions from natural gas (NG) power plants, which could help attenuate the rise in atmospheric temperature.

The reforming process, an important part of an IRCC, is a chemical process for fuel conversion and the process model involves chemical equilibrium and reaction kinetics. A first principles model of this process in an optimization framework will be very complex and may involve solving of hundreds (or thousands) of nonlinear equations and therefore is computationally expensive. A so-called surrogate model (or metamodel) is a multivariable general purpose mapping that can be used in an optimization framework to reduce the model complexity and thus reduce computational load in the optimization to something that is manageable. There are many different methods for developing surrogate models varying from "simple" polynomial models to complicated models such a Kriging etc.

Objectives for the thesis work were development of Kriging and Polynomial surrogate models for two configurations of IRCC process: air blown and oxygen blown ATR. The figure below gives a brief overview of possible alternatives in the design of an IRCC with CO_2 capture.
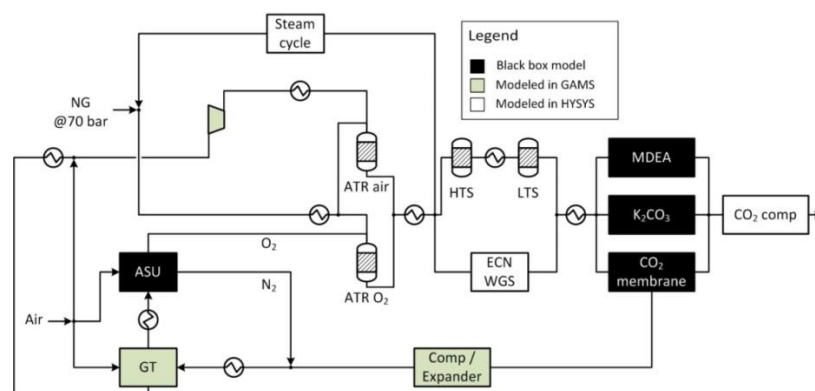
A total of 30 cases were considered for metamodel building with different sample sizes and different number of inputs to metamodels. The built metamodels were compared based on their accuracy in predicting the outputs. Kriging models yield results that are equal or slightly better than Polynomial models in accuracy. One Polynomial and Kriging model were tested in an existing optimization framework to identify a model with best computational cost-accuracy trade-off. The Polynomial model demonstrated faster performance than the Kriging model. Polynomial models with a predictive accuracy close to Kriging models but with an advantage of less computational time will most likely be used for optimization of IRCC plants. The contribution that this thesis has made is better understanding of the process and metamodel building. Recommendations for future work are given in Chapter 7.

Table of Contents

1 Introduction

1. Motivation for carbon capture

Global temperature rise in the past years has been mainly due to increase in anthropogenic greenhouse gases. Figure 1-1 shows the increase in CO_2 concentration in the atmosphere measured in Mauna Loa observatory in Hawaii. It is getting close to 400 parts per million (ppm) for the first time in human history. In that respect greenhouse gas mitigation technologies, particularly with respect to CO_2 have attracted much attention nowadays.

Figure 1-1: CO_2 concentration measured at Mauna Loa, Hawaii [1]
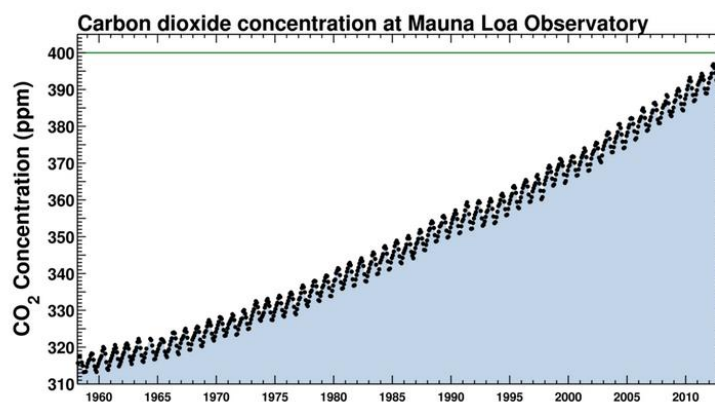
Power generating sectors such as coal and gas fired power plants are of primary targets for Carbon Capture and Storage (CCS), because they create large and concentrated amounts of CO_2. Figure 1-2 shows that we cannot completely live fossil-fuel-free in near future and our dependency will increase as we need more energy.
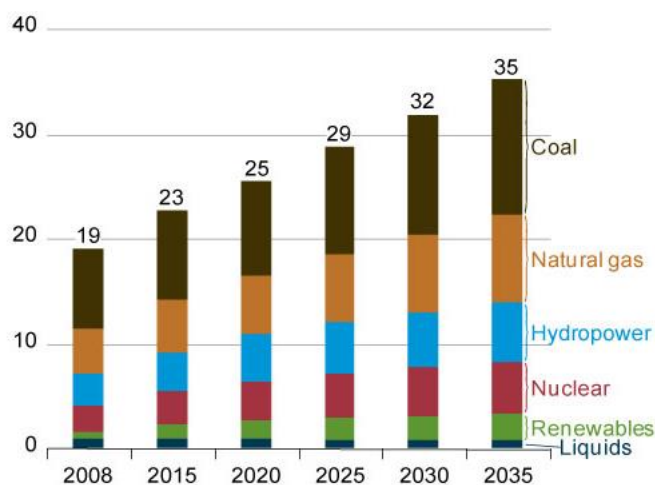
Figure 1-2: World net electricity generation by fuel type (trillion kilo watt hours) [2]

The energy demand of a process can be reduced by applying heat integration methods and use of optimization techniques. Through optimization, one can find the most efficient process design, both with respect to heat integration and power generation. This is however a complicated task. A mathematical description of the process may be highly nonlinear and very complex from optimization point of view. One way to reduce the complexities is to use approximating methods in which difficult correlations are replaced by simpler ones.

The goal of this work is to make Polynomial and Kriging metamodels for an integrated reforming combined cycle (IRCC) process with CO_2 capture, and then compare them with respect to computational cost and model accuracy.
The first reported work for use of metamodels in chemical flowsheets in the literature is by Palmer and Realf [3]. According to them if the approximation model is made carefully, this approach can be fruitful in optimization of flow sheets.

1.1. Thesis Organization:

The thesis comprises of seven chapters covering the following topics:

Chapter 1, Introduction: Motivation for working on this topic is presented.

Chapter 2, Technical background: CO_2 capturing methods are described first, followed by presenting different sections in the integrated reforming combined cycle process with CO_2 capture. Then introduction to surrogate models is given. At the end statistical information is provided.

Chapter 3, Process design and modeling: Presented in this chapter are details of IRCC process modeling.

Chapter 4, Identification of operating parameters: Presented in this Chapter are sensitivity analysis on the inputs and outputs of the process and degree of freedom analysis for IRCC process units.

Chapter 5, Metamodel building: This chapter presents the work that has been done on metamodeling.

Chapter 6, Comparison of Polynomial vs. Kriging models: This chapter compares Polynomial and Kriging models in terms of model accuracy and computational costs. Comparisons available in the literature between Polynomial and Kriging models are also included.

Chapter 7, Conclusions and future work

2 Technical Background

CO_2 capturing methods are presented first in this chapter, followed by an overview of different sections in the integrated reforming combined cycle process with CO_2 capture. Then an introduction into surrogate modeling is given. At the end of the chapter some statistical background information is provided.

2.1 CO_2 Capturing methods

Methods for capturing CO_2 from fossil fuel power generation plants can be divided into three main categories:

1) Pre-combustion: Carbon of the fuel is removed before combustion and the fuel heating value is given to Hydrogen [4]. Fossil fuel which is converted to syngas is separated before the combustion takes place. There exist many different possible configurations for a pre-combustion plant [5]. IRCC is one of such possibilities.

2) Oxy fuel combustion: The combustion oxidant is oxygen (97%+ purity) instead of air. The advantage of this method is lower volume of the combustion products which are mainly CO_2 and steam due to the omittance of nitrogen from air. The disadvantage of course is the need for large amounts of pure oxygen which would add significant cost and complexity to the plant. Another obstacle is the high combustion temperature while burning pure oxygen. This can be overcome by recycling part of the flue gas into the combustor or by injecting water or steam[6].

3) Post combustion: In this method, CO_2 is separated after combustion. CO_2 often is captured by Chemical absorption and use of Amine solutions. This technique may be the best option for capturing in existing power plants [6]. One of the main challenges of this method is the handling of large volume of flue gases with a relatively low pressure.

2.2 IRCC Design

The IRCC process reforms natural gas to syngas and then converts CO to CO_2 in the water-gas shift reactors and separates CO_2 in the capture unit. The resulting Hydrogen-rich fuel is used for the gas turbine in a combined cycle configuration. IRCC is part of the pre-combustion capture method in which CO_2 is captured before burning the fuel. The technology comprises of three steps to covert Hydrocarbon molecules to H_2 and CO_2:

–Conversion of fossil fuel to a mixture containing H_2, CO_2 and CO (Syngas);

– Shifting the produced mixture to a mixture with CO_2 and H_2;

– Separation of CO_2 and Hydrogen.

Figure 2-1 shows schematic diagram of IRCC process with CO_2 capture. We will go through the most important unit operations in the IRCC design in the following sections.
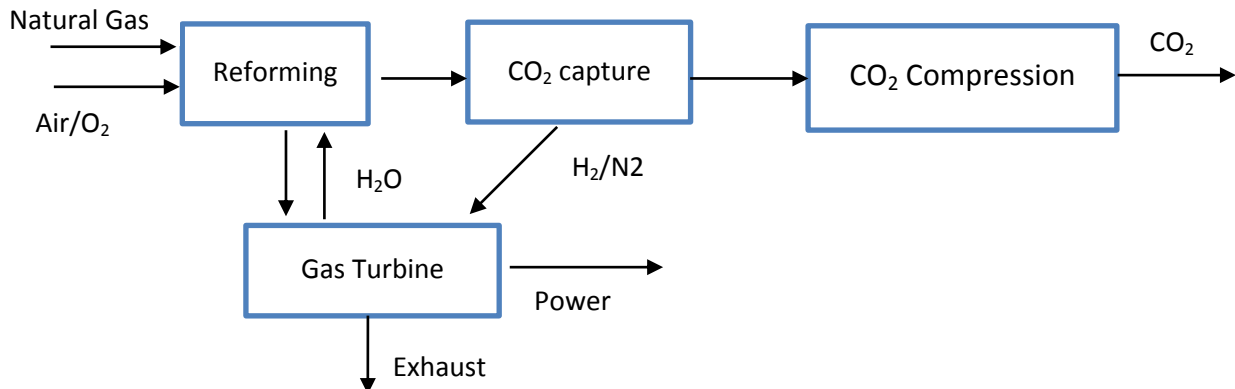
Figure 2-1: Schematic diagram of IRCC process with CO_2 capture

2.2.1 Reforming section:

In order to convert heavier hydrocarbons to a mixture of H_2, CH_4, CO_2 and CO, pre-reformer is used. This is mainly done to avoid cock formation in the reformer. For ATR applications, pre-reformer is needed especially when operating at low steam-to-carbon ratio (S/C) or with high preheat temperatures [6]. A catalytic pre-reformer usually operates at approximately 500°C, which increases the overall fuel conversion efficiency. A nickel-based catalyst is typically used in the pre-reformer [6]. The main reformer which follows the pre-reformer preferably converts methane to CO and H_2.

The main reactions for syngas production are:

- **Heavy Hydrocarbon conversion:**

$$C_nH_m + nH_2O \longrightarrow nCO + (n+\frac{m}{2})H_2 \quad \Delta H = -1175 \; (C_7) \; \left[kJ/mol\right] \qquad \text{Equation 2-1}$$

- **Steam reforming:**

$$CH_4 + H_2O \rightleftharpoons CO + 3H_2 \qquad \Delta H = 205.9 \; \left[kJ/mol\right] \qquad \text{Equation 2-2}$$

- **Partial Oxidation:**

$$CH_4 + \frac{1}{2}O_2 \rightleftharpoons CO + 2H_2 \qquad \Delta H = -35.9 \; \left[kJ/mol\right] \qquad \text{Equation 2-3}$$

- **Water gas shift reaction:**

$$CO + H_2O \rightleftharpoons CO_2 + H_2 \qquad \Delta H = -41.2 \; \left[kJ/mol\right] \qquad \text{Equation 2-4}$$
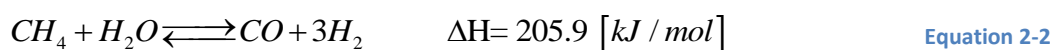
These reactions are involved in one or several steps of the IRCC process. The aim of the Reforming section is to produce syngas. Syngas is converted to a mixture with CO_2 and H_2 through two shift reactors which are High temperature shift (HTS) and Low temperature shift (LTS) reactors. Main reactions in the reforming stage are divided into conversion and equilibrium reactions. Equation 2-1 represents a range of syngas formation reactions from heavy hydrocarbons. Steam reforming reaction Equation 2-2 is preferred to react under high temperature and low pressure in order to obtain a high equilibrium conversion.

There are several syngas production technologies available which are listed in Table 2-1.

Table 2-1: Gas reforming technologies

Gas Reforming technologies
Conventional Steam Methane Reforming (SMR)
Heat exchange reformer (HER)/ gas heated reformer (GHR)
Pressurized combustion reforming
(Non- catalytic) partial oxidation (POX)
Catalytic partial oxidation (CPO)
Autothermal reforming (ATR)

The features of commercially available reforming technologies are summarized in Table 2-2 [5].

Table 2-2: Features of commercially available reforming technologies [5]

	Steam reforming	Partial oxidation	Autothermal reforming
Abbreviation	SMR	POX	ATR, CPO
Catalyst	Ni	---	Partial oxidation:- Steam reforming: Ni
Pressure	15-40 bar	->150 bar	20-40 bar
Temperature	750-900°C	1200-1600°C	850-1100°C
Reaction	$CH_4 + H_2O \rightleftharpoons CO + 3H_2$	$CH_4 + \frac{1}{2}O_2 \rightleftharpoons CO + 2H_2$	$CH_4 + \frac{1}{2}O_2 \rightleftharpoons CO + 2H_2$ $CH_4 + H_2O \rightleftharpoons CO + 3H_2$
H_2/CO ratio	3-6	1.8	1.8-3.7

The type of the feedstock mainly determines which reforming technology to choose. In this study Auto Thermal Reformer (ATR) is used as the gas reformer. ATR has high efficiency for high temperature reactions [7]. In ATR three main reactions occur: Partial oxidation (Equation 2-3), Steam reforming (Equation 2-2) and Water Gas Shift reaction (Equation 2-4).

Gas mixture from the pre-reformer is mixed with oxygen, or air in the burner. Partial oxidation takes place in the combustion chamber. It follows by methane steam reforming reaction and shift conversion to equilibrium over the catalyst bed. The overall reaction is exothermic, resulting in a high outlet temperature, typically 850°C-1000°C. There are different choices of oxidants which are air, oxygen, and oxygen enriched air. The advantage of using oxygen or oxygen enriched air is the reduced amount of inert gas which results in reduced equipment size downstream of ATR.

Due to volume flow, oxygen blown reformer has the advantage of a more compact design compared to an air-blown reformer. This, however, comes at a price and in most cases steam is required to avoid very high temperatures in the reformer. Also, before combustion of hydrogen in the gas turbine, nitrogen diluent from ASU needs to be introduced to the hydrogen fuel. In addition, the high electricity consumption of an air separation unit (ASU), reduced thermal efficiency of the plant and increased operating costs are the negative points [5].

The added oxygen supplies and controls the heat of reaction in ATR. The extent of the other two reactions (Equation 2-2) and (Equation 2-4) depend on the amount of heat released by the oxidation reaction and on the amount of steam added which is referred to by Steam to carbon ratio. Steam to carbon ratio is the molar ratio of steam to hydrocarbons.

If the feedstock is coal instead of natural gas, Gasification replaces Reforming process and IRCC becomes IGCC (Integrated Gasification Combined Cycle) as is shown in Figure 2-2. In IGCC process coal is turned into syngas in a gasifier. The rest of the process is essentially the same as IRCC.
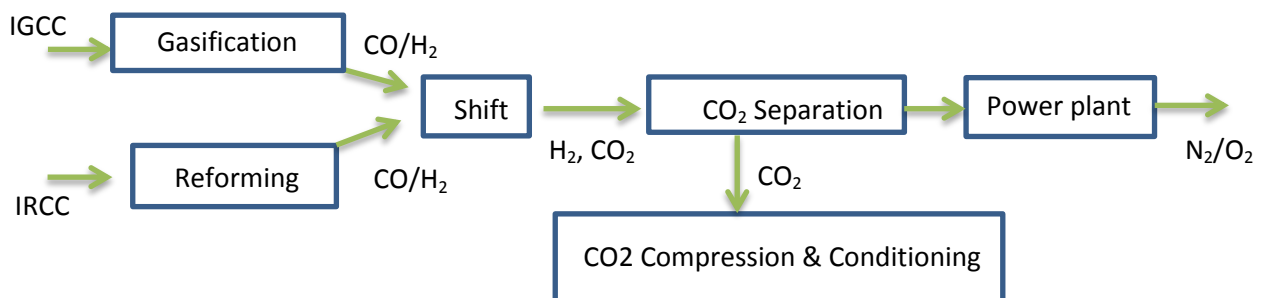
Figure 2-2: Schematic diagram for IRCC and IGCC processes

2.2.2 CO- Conversion (Water Gas Shift Reactors):

In the CO-conversion step, CO generated from the reforming section is converted into H_2 and CO_2 by water gas shift reaction (Equation 2-4). Mostly used configuration is a two-step method consisting of High Temperature Shift (HTS) and Low Temperature Shift (LTS) reactors. The major conversion takes place in HTS reactor and rest of the conversion takes place in LTS. Use of LTS and HTS reactors is to achieve high CO conversion. The main alternative to this would be one medium-temperature shift reactor [5].

High temperature shift typically operates at 350°C and Low temperature shift typically operates at 190-210°C [5]. The equilibrium is favored by low temperatures and thus a cooler is placed before each reactor. The cooler has the ability to produce part of the steam required in the process. In this study the heat integration of the process is not considered but it can be a subject for further investigation.

2.2.3 CO_2 Removal (Carbon Capture Unit (CCU))

After CO-conversion step and removal of process condensate (mostly H_2O), the process gas mainly consists of hydrogen and carbon dioxide. In the air blown ATR case, large amounts of nitrogen will also be present. Traces of unconverted CO and methane will also be found. The objective of the IRCC process is to produce as much hydrogen as possible. Now comes the removal of CO_2. Some of the carbon dioxide removal techniques are [5]:

- Chemical absorption
- Pressure swing adsorption
- Cryogenic separation
- Physical absorption using Selexol or Rectisol
- Membrane separation

In this study, Amine absorption is used in CCU but the choice of CO_2 removal is not considered to be important, since most of our focus is on the reforming section of the process.

2.2.4　Combustor

After the Carbon Capture Unit, the gas mixture is fired in the gas turbine. This mixture mainly consists of hydrogen in the oxygen blown reformer and both nitrogen and hydrogen in the air blown reformer. The flue gas of the gas turbine has a very low content of CO_2. Hydrogen is completely combusted with air as in reaction (Equation 2-5). There will also be some H_2O, CO, CH_4 and CO_2 left in the syngas. CH_4 and CO will react according to equations (Equation 2-6) and (Equation 2-7) respectively. The heat of reaction is then utilized in the gas turbine.

$$H_2 + \frac{1}{2}O_2 \longrightarrow H_2O \qquad \Delta H = -241.8 \left[kJ/mol \right] \qquad \text{Equation 2-5}$$

$$CH_4 + 2O_2 \longrightarrow 2H_2O + CO_2 \qquad \Delta H = -890.4 \left[kJ/mol \right] \qquad \text{Equation 2-6}$$

$$CO + \frac{1}{2}O_2 \longrightarrow CO_2 \qquad \Delta H = -283.0 \left[kJ/mol \right] \qquad \text{Equation 2-7}$$
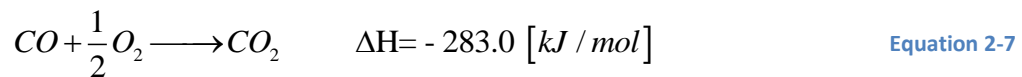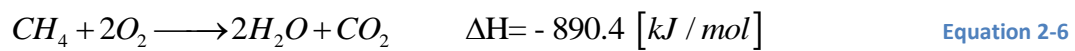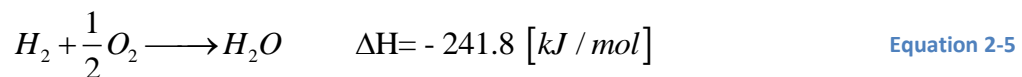
The main differences between an IRCC gas turbine and regular gas turbine is related to the inlet capacity, burner design, turbine inlet and exhaust temperatures, compressor air extraction and control system design [6]. The use of hydrogen as gas turbine fuel is investigated by Chiesa et al. [8].

2.2.5　Air/Oxygen compressors

In order to run the ATR at desired pressures, air/ oxygen must be compressed accordingly to the system pressure. Three stage compression is utilized to reach the desired operating pressure. The outlet temperatures of the compressors satisfy the limit of 250°C by use of two intercoolers to avoid exceeding this limit.

2.3   Surrogate models (Metamodels):

Nowadays computer based simulation is used extensively in different areas of engineering. Despite their increasing speed and power, the computational complexity and cost of running these complex simulations limit their use in important areas such as design optimization. Single evaluations of CFD or finite-element analyses can take a long time from minutes to hours and days. Statistical approximation techniques have become widely used in engineering instead of running such computer simulations. These methods show good promise in trade-off between computational cost and accuracy.

As Figure 2-3 shows, metamodel is a simplification of the real process which gives us almost the same understanding but with less computation time and effort.

Figure 2-3: Metamodeling of a real phenomenon
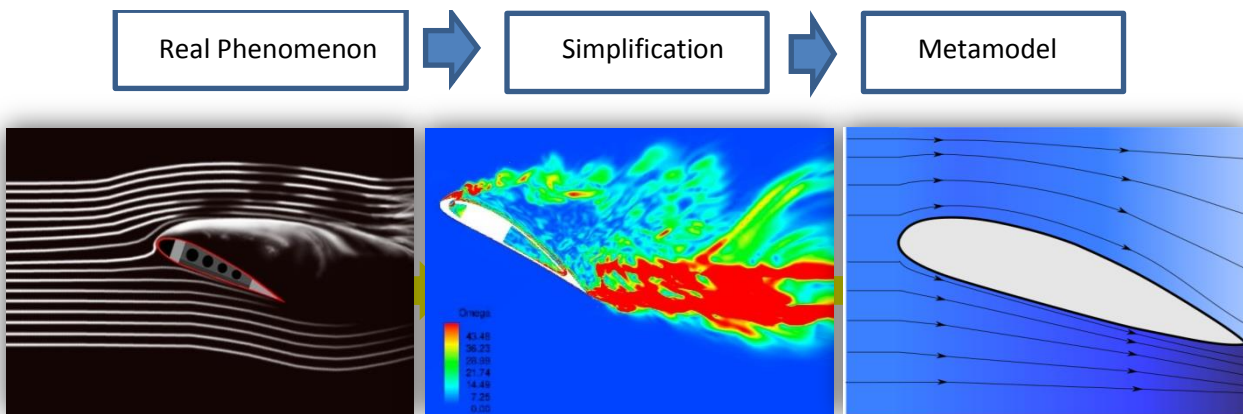
In the past two decades, approximation methods have attracted much attention. With this approach computation demanding simulations are approximated with simple models. This simple model is often called metamodel; and the process of constructing a metamodel is called metamodeling. Since the approximation model acts as a surrogate for the original code, it is often referred to as a surrogate model, surrogate approximation, approximation model, or metamodel (i.e. model of a model) [9].

If the true output of a computer analysis code is: $y = f(x)$

Then a metamodel of the simulation code will be of the form: $y = g(x)$ and $y = y + \varepsilon$

Where ε represents approximation errors. Metamodels are more efficient to run and provide insight into the relationship between inputs and outputs.
 A variety of approximation models exist (e.g. Polynomial Response Surfaces (PRS), Kriging models, Radial Basis Functions, Neural Networks, Multivariate Adaptive Regression Splines), and reviews and comparisons of many of these approximation model types are available in the literature ([10]; [11]; [12]; [13]; [14]; [15]). There has been growing number of investigations in recent years in use of metamodels in design optimization and reliability

analysis. Figure 2-4 illustrates number of publications related to the use of metamodels in design optimization and reliability analysis applications.

Figure 2-4: Use of metamodels in design optimization and reliability analysis [16]
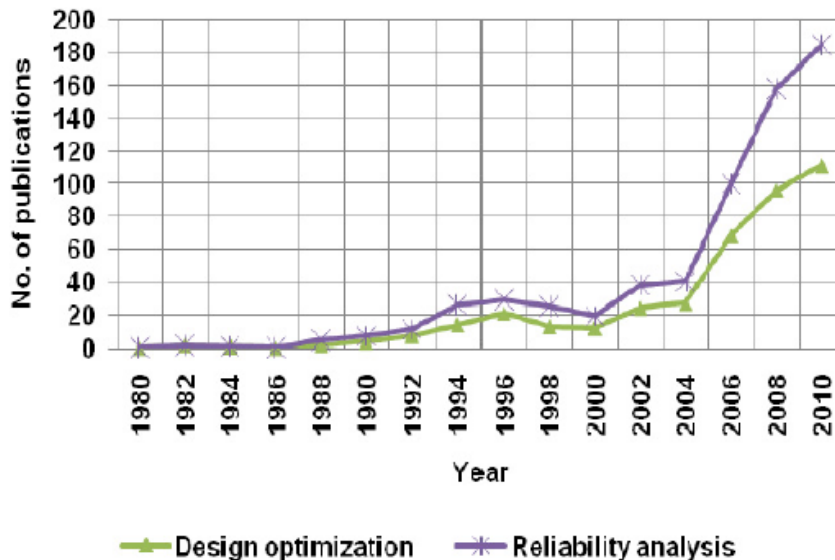
A comprehensive review of metamodeling applications in mechanical and aerospace systems is done by Simpson et al. [17]. A review of metamodeling applications in structural optimization can be found in the paper by Barthelemy and Haftka [13]; Sobieszczanski-Sobieski and Haftka [12] investigated metamodeling applications in multidisciplinary design optimization.

Simpson et al. [18] compared Kriging models against Polynomial models for a multidisciplinary design optimization. Giunta et al. [19] compared Kriging and Polynomial models for two test problems. Varadarajan et al. [20] compared ANN methods with Polynomial regression models for an engine design problem involving nonlinear thermodynamic behavior.

Wag and Shan [15] in their review of metamodeling techniques provide an overall picture of the current research and development in metamodel-based design optimization.

Simpson et al. [21] give a review on metamodel based design optimization (MBDO) through different sampling methods and metamodels.

In Palmer and Realff [3], Polynomial and Kriging models are investigated and the importance of a smart sampling scheme to get as much information as possible from few simulations is highlighted. In their second article [22], they present heuristics to solve the optimization problems. They were the first to report the use of metamodels for chemical processes.

Jin et al. [11] investigated the advantages and disadvantages of four metamodeling techniques: Polynomial, Kriging, Multivariate adaptive Regression Splines (MARS) and Radial

Basis Functions. The models were compared on different test problems based on different criteria (e.g. accuracy, transparency, robustness, etc.).

Simpson et al. [10] compared Polynomial and Kriging models for multidisciplinary design optimization.

2.3.1 Roles of Metamodeling in Design Optimization

Numerous researches have been done in employing metamodeling techniques in design optimization. These include research on different areas such as sampling, metamodels, model fitting techniques and model validation.

The list of areas that metamodeling can play an important rule are [15]:

1) Model approximation.
2) Design space exploration. To enhance the understanding of the design problem by working on a cheap-to-run metamodel.
3) Problem formulation. Metamodel can assist the formulation of an optimization problem that is easier to solve or is more accurate.
4) Optimization support.
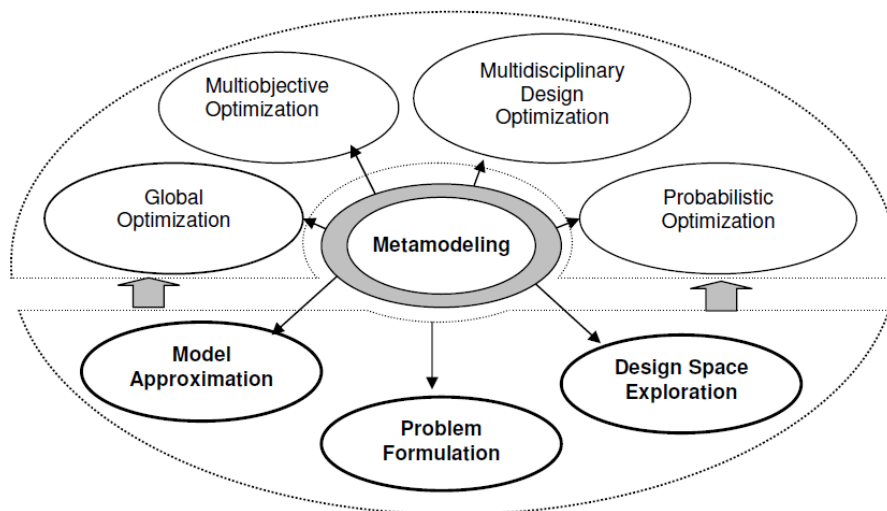
Figure 2-5: Metamodeling and its role in support of engineering design optimization [15]

Figure 2-5 illustrates various support activities that metamodeling can provide in design optimization. The bottom half includes model approximation, problem formulation, and design space exploration, which form a common supportive base for all types of optimization problems [15]. The upper half lists four major types of optimization problems of interests to design engineers. Metamodeling is the key to metamodel-based design optimization (MBDO).

The three main steps in making metamodels are shown in Figure 2-6. We will go through experimental design, model choice and model fitting in the following sections.

Table 2-3 categorizes the metamodeling techniques according to sampling, model types, and model fitting [5].

Figure 2-6 : Main steps in Metamodeling

Experimental Design $\longrightarrow$ Metamodel Choice $\longrightarrow$ Model fitting

Table 2-3: Techniques for metamodeling [21]

EXPERIMENTAL DESIGN	MODEL CHOICE	MODEL FITTING	SAMPLE APPROXIMATION TECHNIQUES
(Fractional) Factorial	Polynomial (linear, quadratic)	Least Squares Regression	Response Surface Methodology
Central Composite	Splines (linear, cubic)	Weighted Least Squares Regression	
Box-Behnken			
D-Optimal	Realization of a Stochastic Process	Best Linear Unbiased Predictor	Kriging
G-Optimal			
Orthogonal Array	Kernel Smoothing	Best Linear Predictor	
Plackett-Burman	Radial Basis Functions		
Hexagon		Log-Likelihood	
Hybrid			
Latin Hypercube	Network of Neurons	Backpropagation	Neural Networks
Select By Hand			
Random Selection	Rulebase or Decision Tree	Entropy (info.-theoretic)	Inductive Learning

2.3.2 Design of experiments (DOE)

Experimental design techniques were initially developed for physical experiments. The aim of DOE is to collect sufficient data points that are representative of the input space and thus accurately estimate model parameters. Experimental designs are also used in reducing the dimensionality of the problem [23].

The basic concept in design of experiments is to treat the simulation as "computer experiments", and then choose the input points to study the impact of process inputs (for example ATR temperature) on outputs (H_2 concentration in ATR outlet).

The region of interest for the inputs is referred to as design space. It is very important how to choose the design points for simulation runs, because they can to a great extent determine the success or failure of a metamodel.

Table 2-4 shows different experimental design methods used in metamodel building. Comparisons of experimental design strategies are available in the literature [23], [24], [25].

Table 2-4: Experimental design methods

Experimental Design Methods		
Classical methods	Factorial	
	Central Composite	
	Box-Behnken	
	Alphabetical optimal	
	Plackett-Burman	
Spacefilling designs	Simple Grids	
	Latin Hypercube	
	Orthogonal Arrays	
	Hammersley Sequence	
	Uniform designs	
	Minimax and Maximin	
Hybrid methods		
Random methods		
Importance sampling		
Directional simulation		
Discriminative sampling		
Sequential or adaptive methods		

In DOE there are two design criteria: "Classical" and "Space filling". "Classical" design of physical experiments, has two main features: first, random variation in sample points by spreading the sample points out in the design space and second, taking multiple data points (or replicates).

Figure 2-7 shows the difference between classical and space filling designs. Sacks et al. [26] state that in deterministic computer experiments (which do not have random error), randomization and replication are irrelevant and the sample points should be chosen to be space filling. Thus many researchers use "Space filling" designs to treat all regions of the design space equally [27].
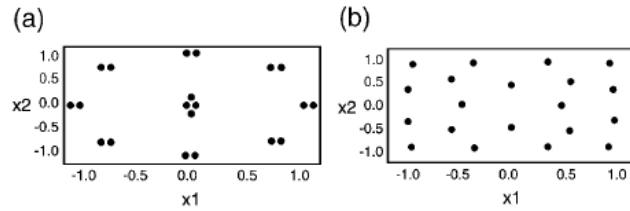
(a) 'Classical' and (b) 'Space filling' designs.

Figure 2-8 shows six different experimental designs for the two variables x_1 and x_2 [28]. Some of the designs like orthogonal arrays and face centered designs take samples on the border of the design space while other methods focus more inside the design space. Koehler and Owen [28] describe some of the "space filling" designs such as Latin Hypercubes, maximum entropy designs, mean squared error designs, etc. Each of these designs has specific characteristics and there have been many studies comparing them [29], [21].

14
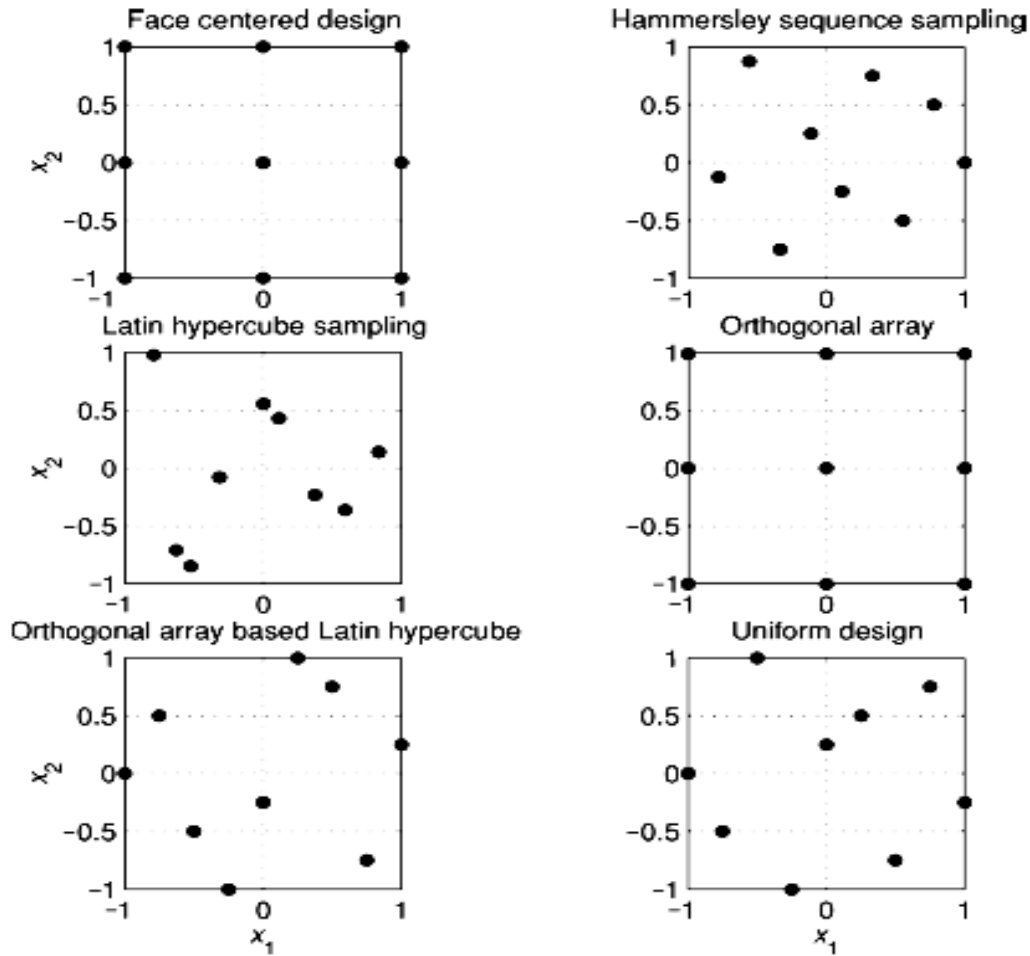
Figure 2-8: Six different experimental designs for two variables x_1 and x_2 [28]

In this study Latin Hypercube Sampling (LHS) was used as a technique to select points for running simulations. LHS was developed by McKay et al. [25] and is the first type of design proposed specifically for computer experiments [25]. Latin Hypercube offer flexible sample sizes while distributing points randomly over the design space. Sacks et al. [26] recommended the use of Latin Hypercube Sampling (LHS) with which they fit their Kriging model.

MATLAB program was utilized to generate LHS sample points by use of the following command line:

$$X = lhsdesign\,(N, P)$$ Equation 2-8

It generates a Latin Hypercube sample X containing N values on each of the P input variables. N is the sample size we want to make metamodel with.

LHS is made by dividing the range for each input variable into N equally large — or equally probable — interval per simulation to be performed. Then, for each simulation, the value of

15

each input variable is taken from a randomly selected interval under the condition that the interval is not used in any other simulation. If each input variable's range is taken to be [-1,+1], then the sample values for each variable, $i = 1, \ldots, m$ are given by

$$x_{iu} = \frac{2u - N - 2w}{N}$$

<div align="right">**Equation 2-9**</div>

Where $u = 1, \ldots, N$ and $w \sim U(0,1)$. A new value for w is used to generate each sample value. The sample values are then randomly matched, selecting one value for each variable without replacement, to create the N sample points.

The maximum number of combinations for a Latin Hypercube of N divisions and P variables (i.e., dimensions) can be computed with the following formula:

$$\left(\prod_{n=0}^{N-1} (N-n) \right)^{P-1} = (N!)^{P-1}$$

<div align="right">**Equation 2-10**</div>

For example, a Latin Hypercube of $M = 4$ divisions with $N = 2$ variables will have 24 possible combinations. A Latin hypercube of $M = 4$ divisions with $N = 3$ variables will have 576 possible combinations.

2.4   Metamodeling Techniques

There are different techniques to fit data and make metamodels as shown in Table 2-3. Polynomial models ([30], [31]), and Artificial Neural Network (ANN) methods ([32], [33]) are two well-known approaches for constructing simple approximations of complex computer codes. Kriging models are becoming widely used for the design and analysis of computer experiments ([26], [34]). Other statistical techniques that show a great deal of promise, such as multivariate adaptive regression splines [35] and radial basis function approximations ([36], [37]) are in the focus of many researchers. There are many researches in the literature that compared metamodel's performance in different engineering applications.

Table 2-5 shows the size of data points required for building metamodels. Kriging and Polynomial model forms are usually generated from small data sets. Regression splines [35] often require moderately sized data sets, while neural networks typically require quite large data sets [3].

Table 2-5: Sample data sizes for different metamodels

Metamodel	Data points required
Polynomial	Small
Kriging	Small
Regression Splines	Moderate sized
Neural Network	Large

Now we focus on the metamodels that are used in this work. The Polynomial, Kriging and ANN models are presented in the following sections.

2.4.1   Polynomial Modeling

Polynomial models form the basis of response surface models. Response surface models were originally developed to analyze the results of physical experiments [38]. Although both Polynomial and Kriging models are approximations to the true response surface, and thus are response surface models, but in the literature the term "Response surface" is reserved for Polynomial models [19].

Polynomial models are the most basic form of empirical models used in statistics and are well established and easy to use. Box and Draper [30] and many other researchers [17], [38], [31] have described its use. Typically, second-order Polynomials, or their reduced versions are used. First and second order polynomials are of the following form:

$$y(x) = \beta_0 \sum_{i=1}^{m} \beta_i x_i$$

Equation 2-11

$$y(x) = \beta_0 + \sum_{i=1}^{m} \beta_i x_i + \sum_{i=1}^{m} \beta_{ii} x_i^2 + \sum_{i=1}^{m-1} \sum_{j=i+1}^{m} \beta_{ij} x_i x_j$$

Where $y(x)$ is the output, x_i are the input variables, and β_i are the regression parameters. β_i is called the linear effect parameter and β_{ii} is the quadratic effect parameter. In the statistical literature x is called the independent variable or predictor and y is called the dependent variable or response.

The β parameters are calculated using least squares regression. Least squares regression minimizes the sum of the squares of the deviations of predicted values from the true values:

$$\beta = \left[X'X\right]^{-1} X' y$$

Equation 2-12

Where X is the design matrix of sample data points, X' is its transpose, and y is the vector of the responses at each sample point.

In this study, it is decided to use second order Polynomial models to fit the data, because increasing the power of x will bring in more coefficients to the model which will be

17

computationally more expensive and time consuming. It may also be difficult to take sufficient sample data to estimate all of the coefficients in the Polynomial equation especially in large dimensions.

Polynomial models have the capability to smooth noisy functions which enhances quick convergence in optimization [39]. There are some disadvantages in using Polynomials to model highly nonlinear functions because in some cases instabilities may arise by using high order Polynomials [14] .

Additional details on least-squares regression and response surface modeling can be found in the literature [31], [38], [30].

2.4.2 Kriging method (Gaussian process regression):

The origins of Kriging models are in mining and geostatistical applications and it was originally developed by the South African mining engineer called Krige [40].
Kriging model is a class of approximation techniques that show good promise for building accurate global approximation of a design space. Kriging models are also known as spatial correlation metamodeling or design and analysis of computer experiments (DACE) modeling. In this type of models, the design variables are assumed to be correlated as a function of distance during prediction. These metamodels are flexible in a sense that they can either honor the data by doing an exact interpolation or smooth the data by providing an inexact interpolation, depending on the choice of the correlation function [41]. The application of Kriging to computer experiments was introduced by Sacks et al. [26], and a summary focusing on Kriging is given by Koehler et al. [28].
Kriging model is extremely flexible due to wide range of correlation functions. They can make accurate predictions of highly nonlinear functions [27]. Due to the wide range of functions that can be used in building of Kriging models, they can approximate linear and nonlinear functions equally well [10].

Welch & Sacks recommended using Kriging models as metamodels of simulators instead of Polynomial models for three reasons [26]. First, since in the simulators there is only systematic error and no random error. Second, least squares method produces a smoothed curve through the data which may not necessarily pass through the known data points. Third, they observed poor predictions of Polynomial models in several examples.

The Kriging model expresses the response of a regression as a result of a regression model F and a random function (stochastic process):

$$y(x) = F(\beta, x) + z(x)$$

$F(\beta, x)$ is the regression model and $z(x)$ is a random function. $F(\beta, x)$ globally approximates the design space, $z(x)$ creates localized deviations so that the Kriging model interpolates the sampled data points. The β coefficients are regression parameters. The random function z is assumed to have zero mean and the following covariance between $z(w)$ and $z(x)$:

$$Cov\ [z(w), z(x)] = \delta^2 R(\theta, w, x) = \delta^2 \prod_{i=1}^{m} \exp(-\theta_i \left| w_i - x_i \right|^{p_i})$$

Where $\theta_i > 0$ and $0 < p_i \leq 2$. W and x are vectors of input variables, and δ^2 is the process variance and $R(\theta, w, x)$ is the correlation model with parameters θ. The model parameters $(\beta_i, \delta, \theta_i, p_i)$ are typically estimated by a maximum likelihood method which can be computationally intensive [42]. The covariance function depends upon the distance between the given points and the known points. For the known points the Kriging model reproduces the data. For the unknown points, the model determines the output by a linear combination of the known output values for the nearest data collection points.

The DACE toolbox provides Regression models $F(\beta, x)$ with polynomials of orders 0, 1 and 2. It is also possible to define new regression models. In many cases in the literature $F(\beta, x)$ is simply taken to be a constant term [18], [26], [28].
As Weltch and Sacks [26] we also restrict our attention to correlation functions of the form:

$$R(\theta, w, x) = \prod_{j=1}^{n} R_j(\theta, w_j - x_j)$$

There are different choices for the correlation function $R(\theta, w, x)$, as shown in Table 2-6:

Table 2-6: Different Correlation models in the Kriging model

Name	Correlation model $R(\theta, w, x)$, $d_j = w_j - x_j$
EXP	$\exp(-\theta_j \left| d_j \right|)$
EXPG	$\exp(-\theta_j \left| d_j \right|^{\theta_{n+1}}),\ 0 \langle \theta_{n+1} \langle 2$
GAUSS	$\exp(-\theta_j d^2{}_j)$
LIN	$\max \left\{ 0, 1 - \theta_j \left| d_j \right| \right\}$
SPHERICAL	$1 - 1.5\xi_j + 0.5\xi_j^3,\ \xi_j = \min \left\{ 1, \theta_j \left| d_j \right| \right\}$
CUBIC	$1 - 3\xi_j^2 + 2\xi_j^3,\ \xi_j = \min \left\{ 1, \theta_j \left| d_j \right| \right\}$

The choice of correlation function should be made by considering the phenomenon of interest, e.g., a function we want to optimize or a physical process we want to model. If the phenomenon is continuously differentiable, the correlation function will likely show a parabolic behavior near the origin, which means that the *Gaussian*, the *Cubic* or the *Spline* function should be chosen. On the other hand, for physical phenomena which show a linear behavior near the origin, and *Exp*, *Expg*, *Lin* or *Spherical* would usually perform better [43]. Some correlations tend to smooth the data, while others interpolate, see Cressie [41]. However, Gaussian correlation is the most used correlation in Kriging models.

In this work a Gaussian correlation is employed [10]:

$$\mathrm{R}(x^i, x^j) = \exp[-\sum_{k=1}^{ndv} \theta_k \left| x_k^i - x_k^j \right|^2]$$

Equation 2-16

Where n_{dv} is the number of design variables, θ_k are the unknown correlation parameters used to fit the model, and x_k^i and x_k^j are the k th components of sample points x^i and x^j, respectively. The Predicted response values y at untried values of x are given by:

$$y = \beta + r^T(x)R^{-1}(y - f\beta)$$

Equation 2-17

Where y is the column vector that contains the values of the response at each sample point. $r^T(x)$ is the correlation vector between an untried x and sample points $\{x^1, x^2, ..., x^{ns}\}$ and is given by

$$r^T(x) = \left[R(x, x^1), R(x, x^2), ..., R(x, x^{ns}) \right]$$

Equation 2-18

β is estimated as:

$$\beta = (f^T R^{-1} f)^{-1} f^T R^{-1} y$$

Equation 2-19

The maximum likelihood estimates or best guesses for the θ_k in Equation 2-16 are found by maximizing the following expression:

$$\max_{\theta>0, \theta \in R^n} -[n_s \ln(\sigma^2) + \ln|R|]/2$$

Equation 2-20

Where σ^2 and $|R|$ are both functions of θ. The best Kriging model is found by solving the k-dimensional unconstrained nonlinear optimization problem by maximizing Equation 2-20.

The major disadvantage of Kriging models is that model construction can be very time-consuming. Determining the maximum likelihood estimates of the θ parameters used to fit

the model is a K-dimensional optimization problem, which can take significant time if the sample data is large. Moreover, the correlation matrix can become singular if multiple sample points are spaced close to one another or if the sample points are generated from particular designs. Fitting problems have been observed with some full factorial designs and central composite designs when using Kriging models [44]. A well written Kriging modeling code named DACE (in MATLAB) is used for this study.

2.4.3 Artificial Neural Network:

Artificial neural network, often named neural network, is a mathematical model inspired by biological neural networks [45]. Neural networks are used for modeling complex relationships between large sets of inputs and outputs and finding patterns in data. A General introduction to ANN can be found in [46], [47]. ANN sets up a number of nodes and connections. The inputs are connected to outputs through some weights (or hidden neurons). The higher the weight for an input, the stronger will be the effect of that input. To get statistical details of ANN, see [48] or [49]. An ANN model is often represented by a diagram of nodes in different layers. At the input layer, the nodes contain inputs and at the output layer, the nodes contain outputs. Between input and output layers, there exists at least one hidden layer which connects the two. The nodes represent computational units and the connections determine the information flow between them [45]. Connections between nodes can "feed back" to previous layers, but the typical ANN for function approximation is "feedforward" [50].

Figure 2-9 shows schematic view of relating inputs to outputs in ANN. ANN is used partly in chapter 5 to find the input-output relations for some of the data.

Figure 2-9: ANN Architecture
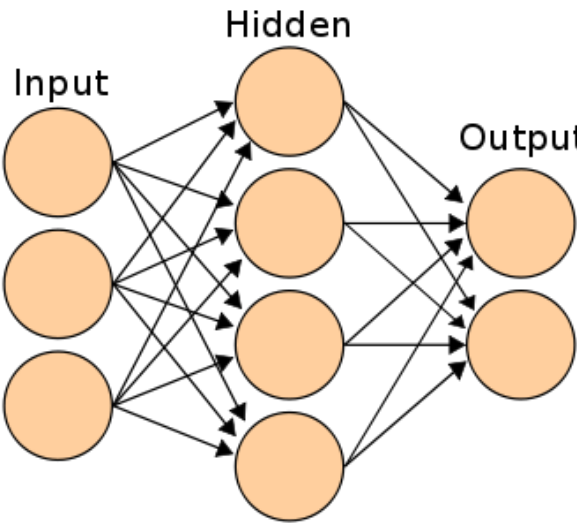
2.5 Statistical background information

In this section, some statistical information is presented. First multiple regression is discussed followed by error analysis terms.

2.5.1 Multiple regression:

The purpose of multiple regression is to predict a single variable from more than two independent variables. Multiple regression with many predictor variables is an extension of linear regression with two predictor variables.

In this thesis, since we want to correlate several inputs to one output in each metamodel, there need to use multiple regression, although the toolbox do all these procedures for us. Nevertheless it is worthwhile to briefly mention this statistical method.

The end result of multiple regression is the development of a regression equation (line of best fit) between the dependent variable and several independent variables.

$$y = \beta_0 + \beta_1 x_1 + \beta_2 x_2 + ... + \beta_n x_n \qquad \text{Equation 2-21}$$

Matrix of coefficients $(\beta's)$ can be calculated by Equation:

$$B = A.C \qquad \text{Equation 2-22}$$

Where:

B= Vector of regression coefficients

A= Matrix of sums of squares and cross products (based on mean deviations)

C= vector of some of cross products of y

$$
\overset{B}{\begin{pmatrix} \beta_1 \\ \vdots \\ \beta_k \end{pmatrix}}
=
\overset{A}{\begin{pmatrix} \sum x_1^2 & \cdots & \sum x_1 x_k \\ \vdots & \ddots & \vdots \\ \sum x_k x_1 & \cdots & \sum x_k^2 \end{pmatrix}}
.
\overset{C}{\begin{pmatrix} \sum x_1 y \\ \vdots \\ \sum x_k y \end{pmatrix}}
$$

The equation of the regressed line is:

$$y_i = \beta_0 + \beta_1 x_{i1} + \beta_2 x_{i2} + ... + \beta_n x_{in} + \varepsilon_i \qquad \text{Equation 2-23}$$

The β parameters are determined to minimize the sum of squares of residuals (error terms). The error term is the deviation between the real output and predicted output. The

regression coefficients can be thought of as weights and the term that has bigger coefficient has more influence in the regression. Further information about multiple regression and regression analysis can be found in statistical literature such as [51].

2.5.2   Error Analysis

In order to assess the accuracy of the built metamodels, statistical methods are employed. Coefficient of determination (R^2) is used as a measure to judge between fitted metamodels. The terms involved in the development of R^2 are briefly discussed here.

Sum of Squares due to Regression:

SSR is a measure of explained variations and discrepancy between the data and the estimated model. A small SSR indicates a reasonable fit to the data:

$$SSR = \sum (y - \bar{y})^2 \qquad\qquad \text{Equation 2-24}$$

Where y is the model output, $\bar{y}$ is the average simulation output and y is the true simulation output.

Sum of Squares due to Error:

SSE is the sum of squared error (residuals or deviations from the regression line) and is a measure of unexplained variations:

$$SSE = \sum (y - y)^2 \qquad\qquad \text{Equation 2-25}$$

A value closer to 0 indicates that the model has smaller random error, and that the fit will be more useful for prediction.

Total Sum of Squares:

SST is the measure of total variations in y :

$$SST = SSE + SSR = \sum (y - \bar{y})^2 \qquad\qquad \text{Equation 2-26}$$

R-Squared

The Coefficient of Determination, also known as R Squared (R2), is known as the goodness of fit of a regression. It explains how good the fit is in explaining the variation of the data. R-squared can take on any value between 0 and 1, with a value closer to 1 indicating that a greater proportion of variance is accounted for by the model. It is also called the square of the multiple correlation coefficients and is calculated by dividing the explained variation to the total variation:

$$R^2 = \frac{SSR}{SST}$$

Equation 2-27

It represents the percent of the data that is closest to the fitted line. If the regression line passes through each of the data points, then it accounts for all the variations in data and the further the line is from the points, the less it explains the variations.

3 Process Design and Modeling

In this chapter standard IRCC process with two shift reactors is discussed. There have been new designs for the shift reactors in the recent years. One of them is the Advanced ECN shift reactor which was part of the thesis description. Due to the sake of completeness of study, the focus was on the standard shift reactors only and the investigation of the ECN Advanced shift reactor is put for future studies. Details of process modeling are presented in this Chapter.

3.1 IRCC model with 2 shift reactors

The steady state simulation of the IRCC process was done in ASPEN HYSYS version 7.3. Figure 3-1 gives a brief overview of possible alternatives in the design of an IRCC with CO_2 capture.

Figure 3-1: Different configurations in an IRCC design
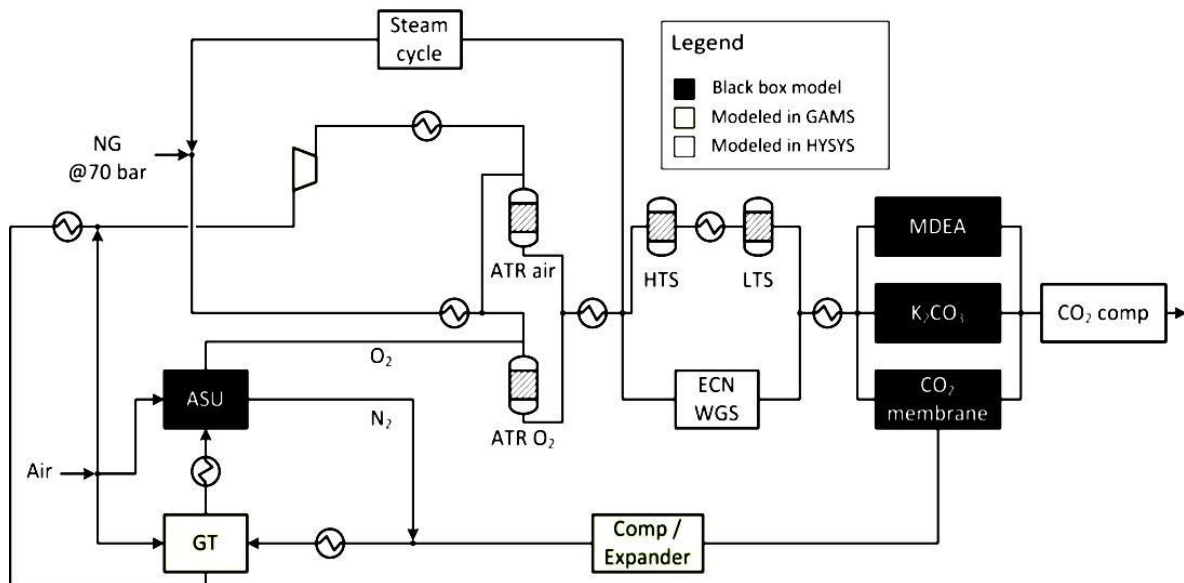
 Two different configurations were studied in which the difference was in the oxidant used in the reformer: oxygen blown ATR and air blown ATR. Each of these configurations will be discussed in the following sections. Simulations were done with standard two shift reactors only and Advanced ECN shift reactor is not covered in the thesis.

The supplied natural gas had an assumed pressure range of 15 to 35 bar and a temperature of 20°C with composition as listed in Table 3-1. The ambient air composition is given in Table 3-2.

Table 3-1: Natural Gas composition

Component	Volume fraction
CH_4 - Methane	89.00
C_2H_6 - Ethane	7.00
C_3H_8 - Propane	1.00
I-Butane	0.05
N-Butane	0.05
I-Pentane	0.005
N-Pentane	0.004
CO_2	2.00
N_2	0.89

Table 3-2: Ambient air composition

Component	Volume fraction
N_2	77.30
CO_2	0.03
H_2O	1.01
Ar	0.923
Oxygen	20.74
Molecular weight	28.854

3.1.1 IRCC process with oxygen blown reformer:

Flow sheet of the oxygen blown IRCC process is shown in Figure 3-3. Natural Gas is mixed with steam and heated to a range between 250-500°C prior to entering the pre-reformer where most of its heavy hydrocarbons are transformed to a mixture of CH_4, CO_2, H_2 and CO. The mixture is then heated up to a temperature range between 250-500°C in the reformer pre-heater. Oxygen (with purity of 95%) for the Reformer is provided by the Air Separation unit (ASU) and is compressed in a three-stage compressor train with inter-stage cooling to reach the pressure of Natural Gas. It is heated to 250°C before entering the reformer. Oxidation of methane in the reformer provides the heat for the endothermic reforming reaction (Equation 2-2). Reformer temperature is adjusted by the amount of oxygen intake. Reformer temperature changes in the range between 850-1050°C. The syngas, consisting of a mixture of primarily CO, H_2 and H_2O is cooled and sent to a two stage water gas shift (WGS) reactors where CO reacts with H_2O to form H_2 and CO_2. Since WGS reaction favors low temperature to increase CO_2 yield, one heat exchanger is placed before each WGS reactor. This provides the possibility of producing steam needed elsewhere in the process. Inlet

temperature to High Temperature Shift (HTS) and Low Temperature Shift (LTS) reactors are part of the input variables in the metamodels. The former one changes between 300-450°C and the latter one between 150-300°C. The shifted syngas from the LTS reactor is cooled to 30°C to separate the water and the syngas is then sent to the CO_2 capture unit (CCU) where CO_2 is separated from syngas using aMDEA as the solvent. Then the Hydrogen rich gas is preheated to 200°C to be used in the gas turbine based combined cycle.

Peng Robinson equation of state is used to closely represent the true behavior of the system since it is the most enhanced model in Aspen HYSYS and is applicable in a large range of temperatures and pressures [52]. Pre-reformer, HTS and LTS reactors are modeled as Equilibrium reactors. Reformer is modeled as a Gibbs reactor. It is not necessary to specify reaction stoichiometry in this type of reactor to compute the outlet composition. It works on the principle that the Gibbs free energy of the reacting system is at minimum or entropy is maximized at equilibrium conditions.

Air Separation Unit (ASU) is needed to provide oxygen to the ATR, and is modeled in HYSYS as in Figure 3-2. ASU efficiency for oxygen and nitrogen is assumed to be 95% and 90% respectively. The amount of oxygen needed for the ATR determines the amount of inlet air to ASU.

Figure 3-2: ASU modeling in the oxygen blown ATR
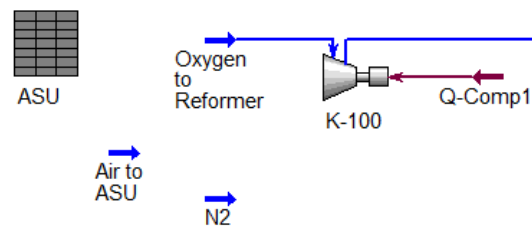
Figure 3-3: Flow sheet of the oxygen blown IRCC
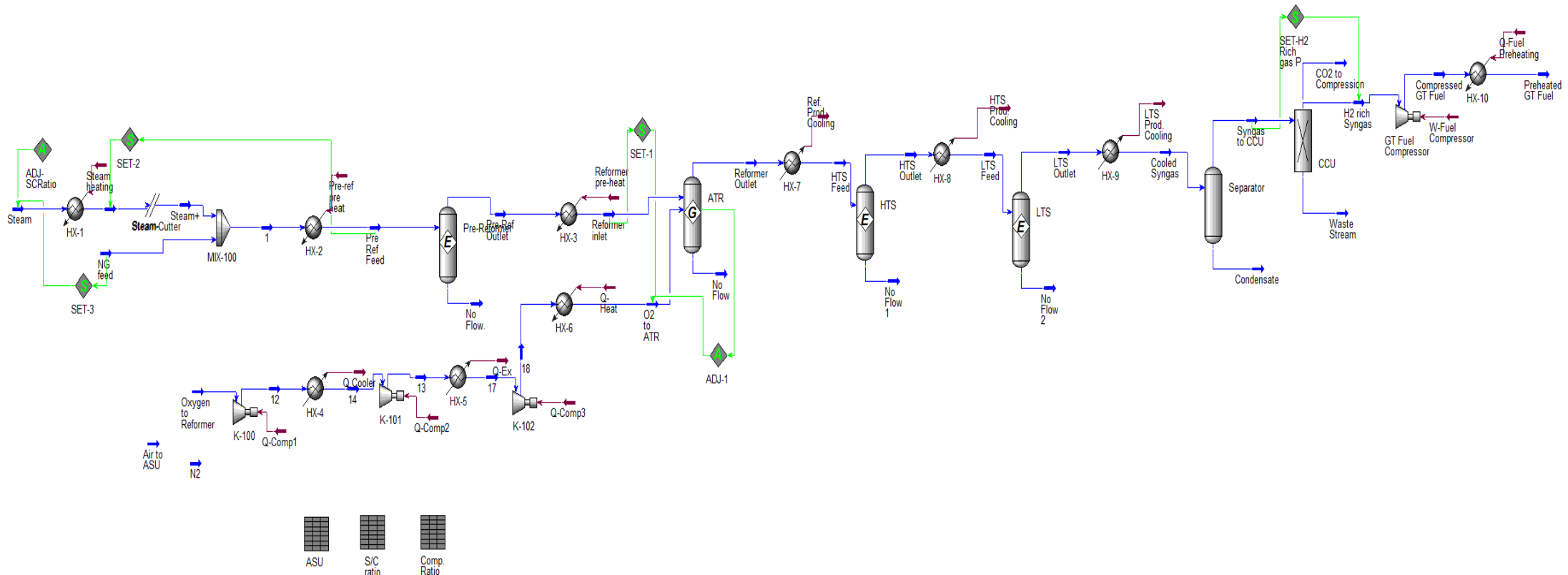
3.1.2 IRCC process with Air blown reformer:

The simulation details are the same as O₂ blown case except that ambient air is fed to the ATR and there is no need for ASU. Introducing Air with its inert components (mostly nitrogen) to ATR causes the equipment downstream of ATR to be larger and increases the amount of cooling needed after ATR. The single point of difference between air and oxygen blown IRCCs is shown in Figure 3-4.

Figure 3-4: Air blown IRCC
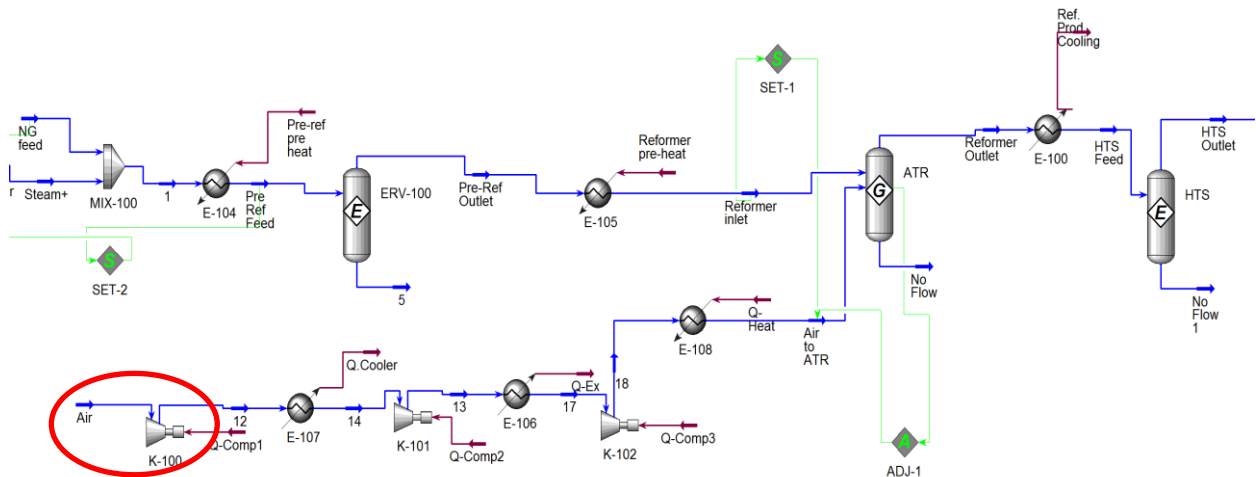
4 Identification of Operating Parameters

In order to get a better understanding of the process and the effect of different inputs on outputs, sensitivity analysis was performed. Degree of freedom (DOF) analysis was also performed to figure out how many parameters are allowed to be changed at the same time around each unit operations. These analyses are presented in this Chapter.

4.1 Sensitivity Analysis:

The relationships between pressures, temperatures, mass and energy flows in chemical and thermodynamic processes are often complex. Many of the relationships in an IRCC process are non-linear and to obtain a satisfactory level of accuracy, there is a need for non-linear optimization. In order to investigate which of the input parameters have the greatest impact on the process and worth to be involved in metamodel, sensitivity analysis was done on both of the processes (air blown and oxygen blown cases). It is a very useful tool to determine the impact of different input variables on the output of the process and therefore help to simplify the metamodel. The effect of 8 input variables were investigated on 25 output variables. The goal is to detect the input variables for the metamodeling step which yield accurate approximation models.

The input variables domain or design space was constrained by upper and lower limits. The limits were chosen to represent the area of interest in optimization. The input variables with their limits as well as output variables are listed in Table 4-1. We will go through the oxygen blown case first in each part and then if air blown case behaves differently, it is mentioned immediately afterwards.

The sensitivity analysis procedure was done as follows: **1-** A base case simulation in air and oxygen blown ATRs was established with the specifications listed in Table 4-2. **2-** Each of the input variables was changed one at a time with the rest of the input variables kept the same as in the base case. This is to see the effects of changing only one input variable at a time on the outputs. **3-** Resulting graphs were saved and reported below.

Table 4-1: Input & Output variables and their ranges

Input variables and ranges	Output variables
Pre-reformer temperature: 250°C-500°C	Steam flow
Pre-reformer pressure: 15 bar-35 bar	O_2 or Air flow
S/C ratio in Pre- Reformer inlet: 0.6-2	$xH_2/xCO_2/xCO/xCH_4/ xH_2O$ @ LTS outlet
Reformer inlet temperature: 250°C –500°C	$xH_2/xCO_2/xCO/xCH_4/ xH_2O$ @ ATR Inlet
Reformer temperature: 850°C-1050°C	$xH_2/xCO_2/xCO/xCH_4/ xH_2O$ @ ATR Outlet
O_2 temp: 185°C –500°C	Pre-reformer preheat
HTS temperature: 300°C-450°C	Reformer preheat
LTS temperature: 150°C-300°C	O_2 or Air compression work
	Reformer product cooling
	HTS outlet temp
	HTS product cooling
	LTS outlet temp
	LTS product cooling

Table 4-2: Base case specifications

	Input variables	Setting
1	Pre-reformer temperature	300°C
2	Pre-reformer pressure	20 bar
3	S/C ratio in Pre-reformer inlet	1
4	Reformer inlet temperature:	400°C
5	Reformer temperature	1000°C
6	O_2 temperature	400°C
7	HTS temperature	400°C
8	LTS temperature	250°C

4.1.1   Pre-reformer temperature: 250°C-500°C

Pre-reformer temperature is changed from 250°C to 500°C and its effect on the output variables was investigated. Concentrations at three point of the process are of great interest: ATR Inlet, ATR Outlet, and LTS Outlet. We will go through each of them:

Concentrations in the ATR inlet:

By increasing the pre-reformer inlet temperature, concentration of Methane decreases, since Methanation reaction is exothermic according to the following reaction:

$$CO + 3\text{H}_2 \Leftrightarrow CH_4 + \text{H}_2\text{O} \qquad \text{Equation 4-1}$$

Concentration of H_2 increases due to the following endothermic reactions:

$$\text{C}_2\text{H}_6 + 2\text{H}_2\text{O} \Leftrightarrow 2CO + 5\text{H}_2 \qquad \text{Equation 4-2}$$

$$\text{C}_3\text{H}_8 + 3\text{H}_2\text{O} \Leftrightarrow 3CO + 7\text{H}_2 \qquad \text{Equation 4-3}$$

$$\text{C}_4\text{H}_{10} + 4\text{H}_2\text{O} \Leftrightarrow 4CO + 9\text{H}_2 \qquad \text{Equation 4-4}$$

$$\text{C}_5\text{H}_{12} + 5\text{H}_2\text{O} \Leftrightarrow 5CO + 11\text{H}_2 \qquad \text{Equation 4-5}$$

According to Figure 4-1, a slight increase in CO_2 concentration is observed. That's due to the exothermic water-gas shift (WGS) reaction (Equation 2-4). Although it is an exothermic reaction but still it moves to the right, mainly because the effect of CO concentration on equilibrium is more than the effect of released heat of the reaction. Air blown case shows the same behavior.

Figure 4-1: Concentrations in ATR inlet
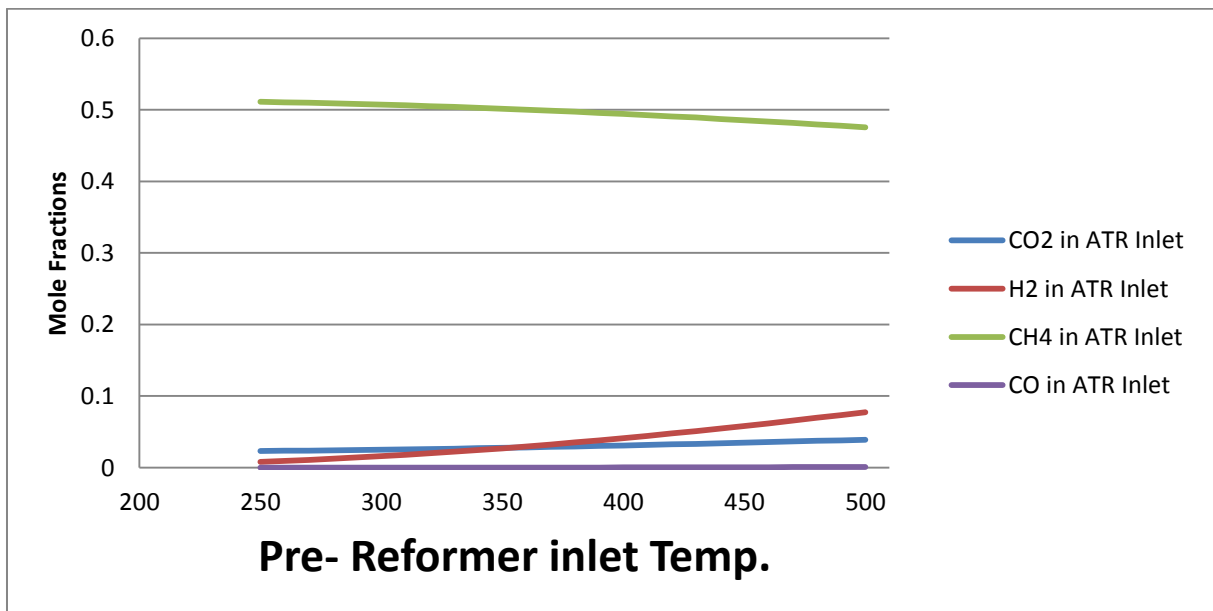
Concentrations in the ATR Outlet:

Slight increase in H_2 and CO concentrations is observed (Figure 4-2). By changing pre-reformer inlet temperature, almost the same can be seen in LTS outlet concentration (Figure 4-3). This can be the result of changing concentrations in pre-reformer outlet. The same behavior is observed in air blown case.

Figure 4-2: Concentrations in ATR outlet (O_2)
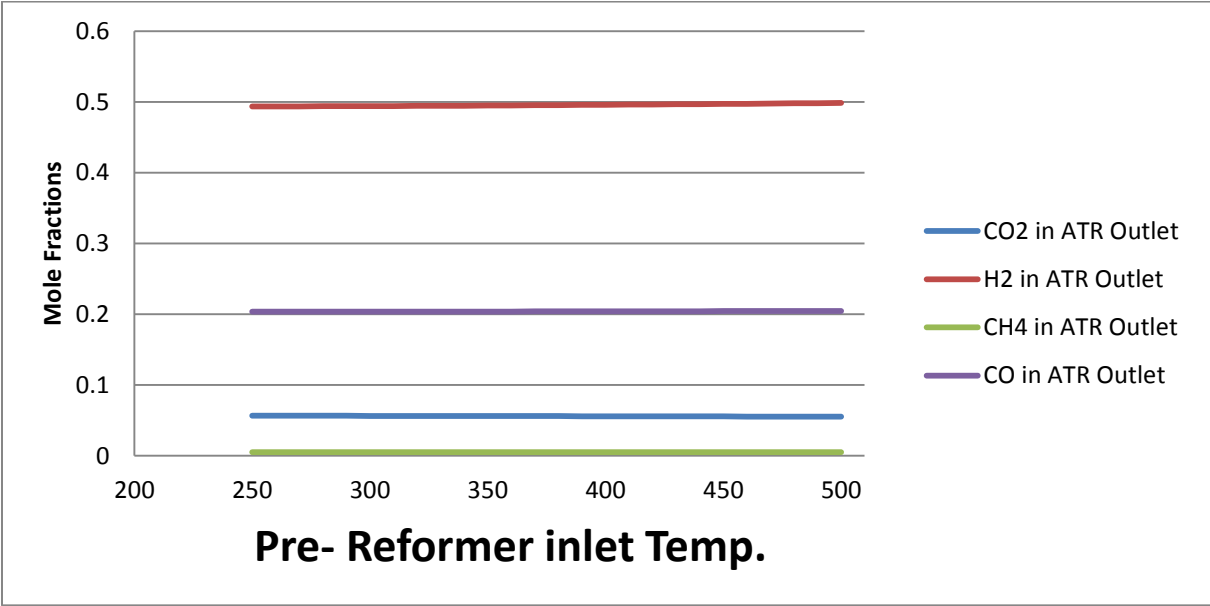
Figure 4-3: Concentrations in LTS Outlet (O_2)
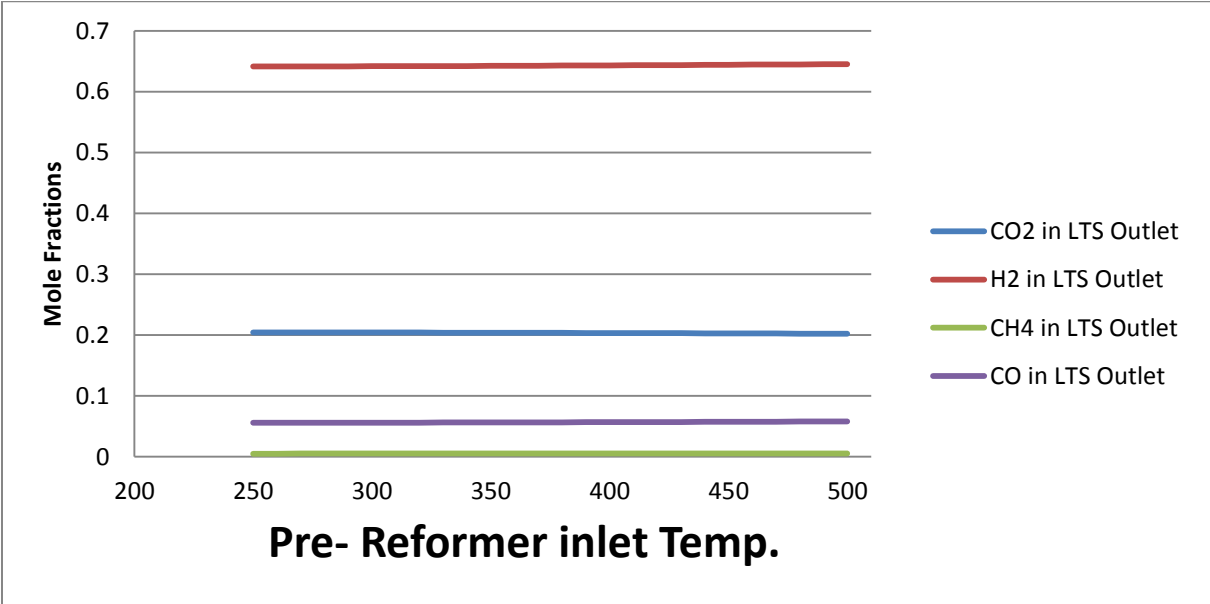
Compression work:

The effect of increasing pre-reformer inlet temperature on O_2 compression work is rather obvious, so that by increasing the inlet temperature, the amount of O_2 needed for the ATR reduces due to less need for combustion of CH_4, and so does the work of compression (Figure 4-4). The Air blown case exhibits the same behavior.

Figure 4-4: O_2 Compression work
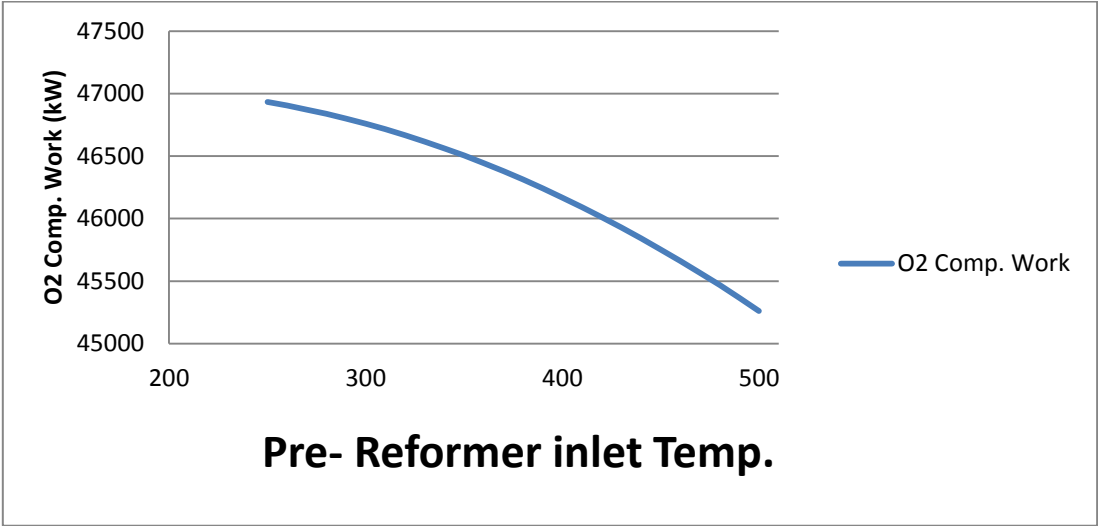
4.1.2   Reformer Inlet Temperature 245°C- 500°C:

Concentrations in ATR inlet:

In both oxygen and air blown cases, there is no change in ATR inlet concentrations by increasing reformer inlet temperature (Figure 4-5). And that is logical, since warming up a stream will not have effect on its concentrations.

Figure 4-5: Concentrations in ATR Inlet
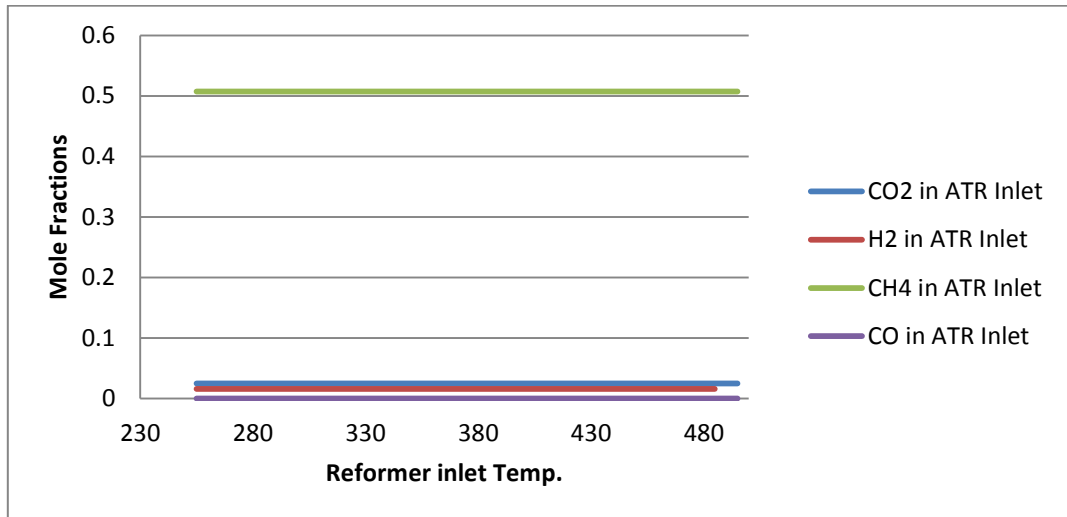
Concentrations in ATR Outlet:

Increase in H_2 and CO concentrations in ATR outlet is observed by increasing reformer inlet temperature (Figure 4-6). This can be due to more conversion of unburned methane in ATR to H_2 and CO. The same is true for the air blown case.

Figure 4-6: Concentrations in ATR Outlet
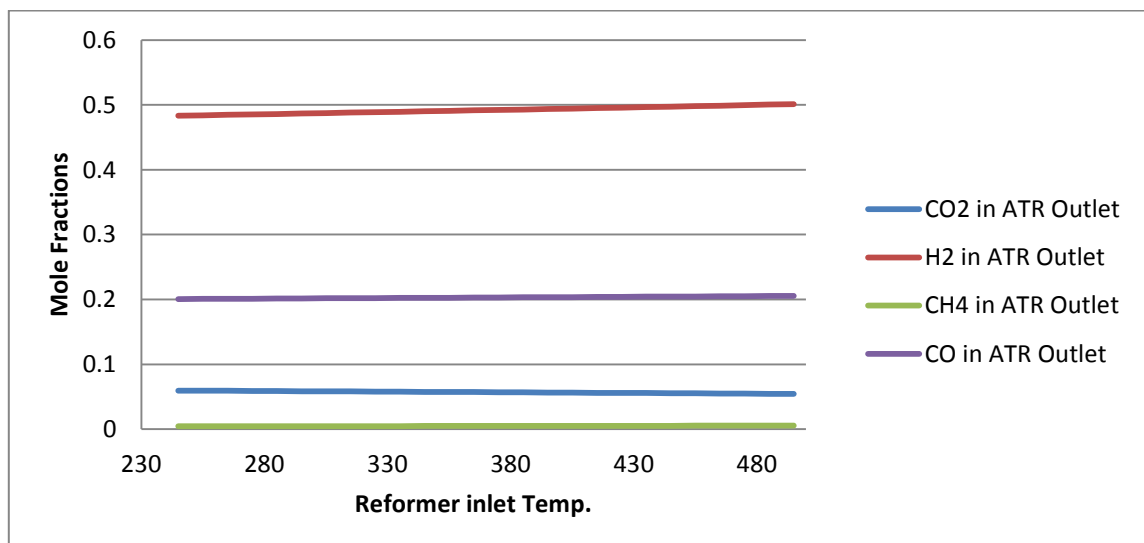
Concentrations in LTS outlet:

Increase in reformer inlet temperature causes an increase in H_2 and CO concentrations in LTS outlet stream (Figure 4-7). This is due to the fact that increase in H_2 and CO concentrations started from ATR outlet and then it propagates downstream of the system. The same is true for the air blown case (Figure 4-8).

Figure 4-7: Concentrations in LTS Outlet
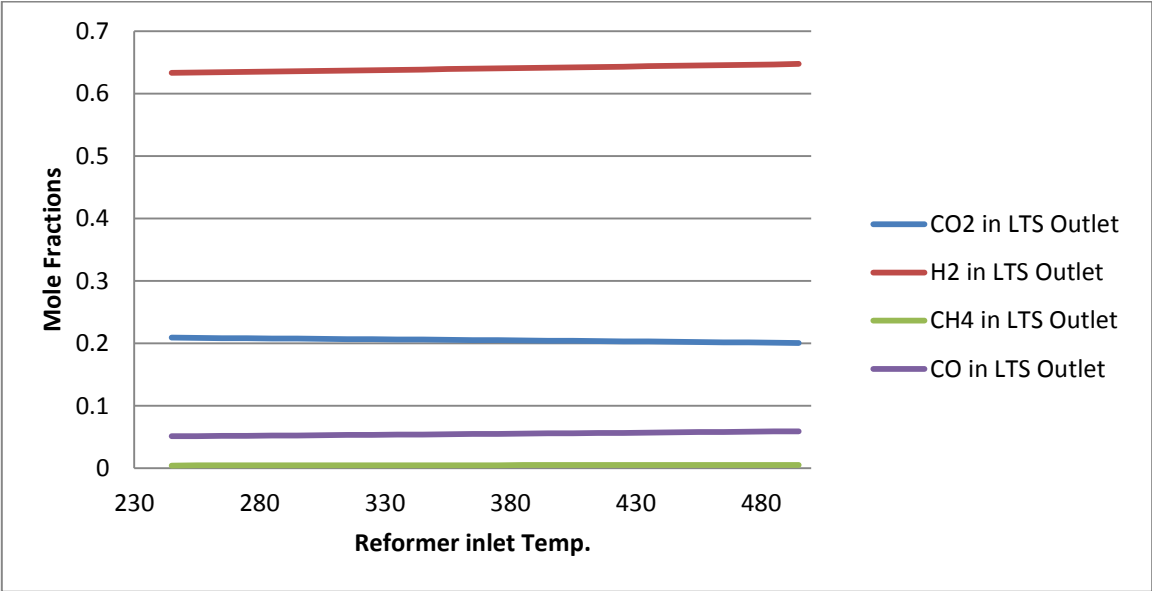
Figure 4-8: Concentrations in LTS Outlet (Air)
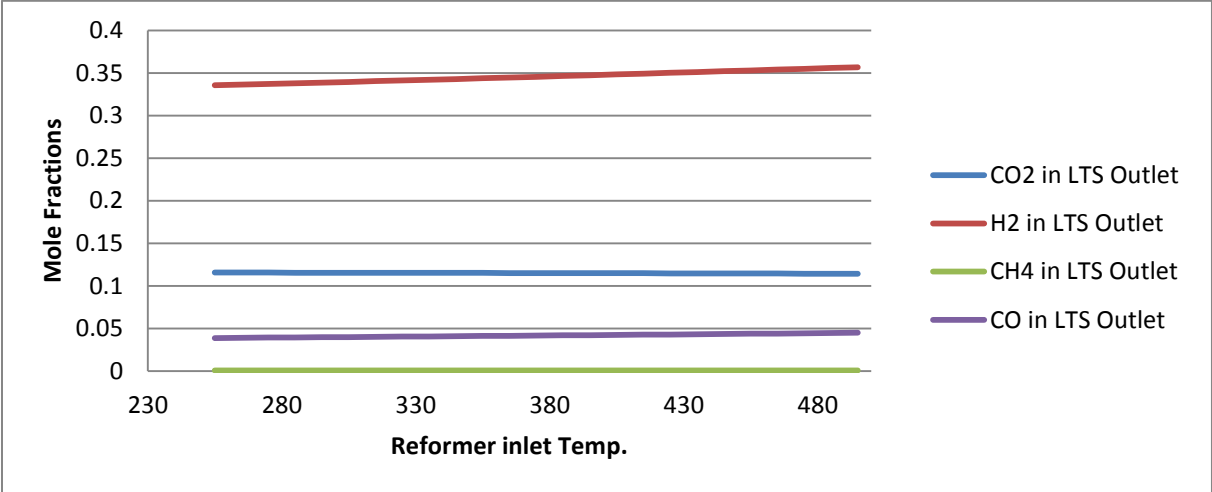
Oxygen/ steam flow and compression work:

By increasing reformer inlet temperature, there is a reduction in oxygen flow (Figure 4-9). The reason is due to less need of oxygen to keep ATR temperature high enough for the reactions to occur. The steam flow does not change because it is determined by S/C ratio and is not influenced by the reformer temperature. The S/C ratio is fixed at the beginning of the process (by use of a *Set* unit in HYSYS). The compression work is related to O_2 flow and reformer temperature. A linear relationship between temperature rise and O_2 compression work is observed (

Figure 4-10). The same trends are observed in the air blown case.

Figure 4-9: O_2 & Steam Flow
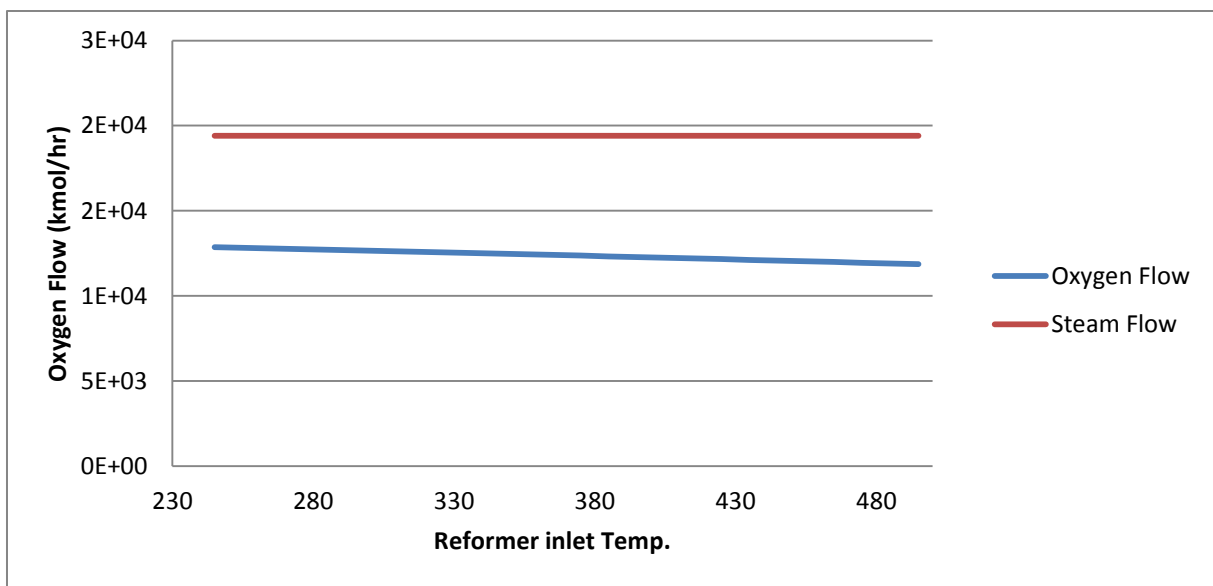
Figure 4-10: O_2 Comp. work
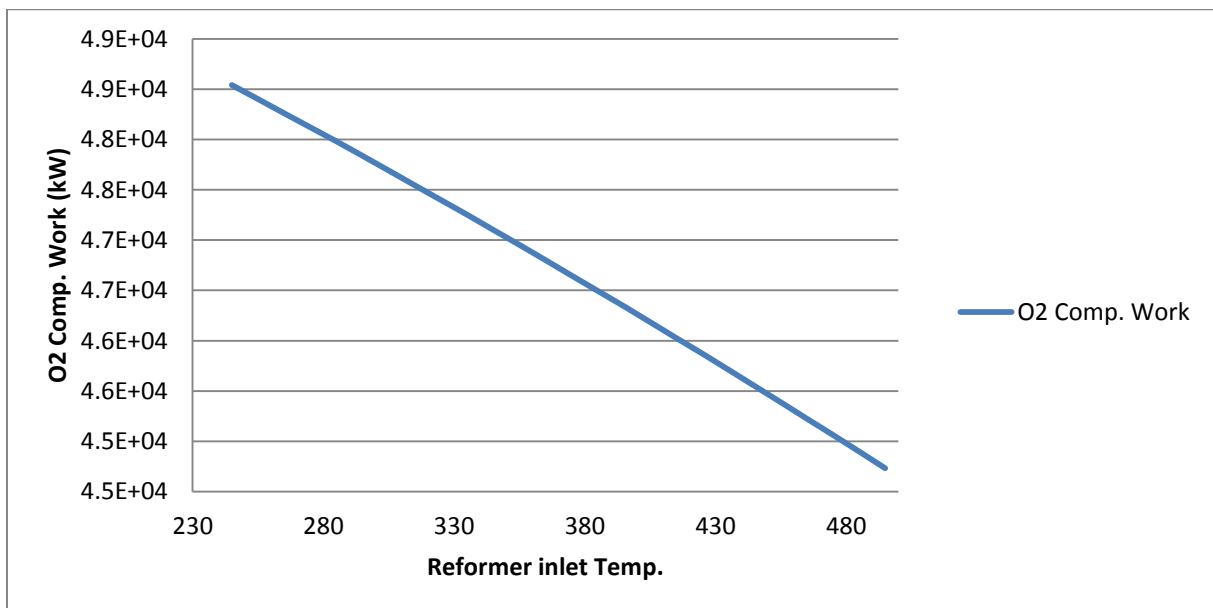
4.1.3 Reformer temperature 850°C–1050°C

Concentrations in ATR outlet:

With the sensitivity analysis conditions as given in Table 4-2, slight increase in H_2 and CO concentrations is observed in oxygen blown case (Figure 4-11). That is due to the fact that more methane is converted to H_2 and CO. In air blown case, reduction in molar concentrations of H_2, CO_2 and CH_4 concentrations is observed (Figure 4-12). We expect an increase in molar flow rate of H_2 by increasing reformer temperature and that is actually happening. If we plot molar flow rates instead of molar concentrations, increase in molar flow rate of H_2 is observed. One conclusion from this graph can be made which is it is better to work with molar flow rates instead of molar concentrations for building metamodels.

Figure 4-11: Concentrations in ATR Outlet (O_2)
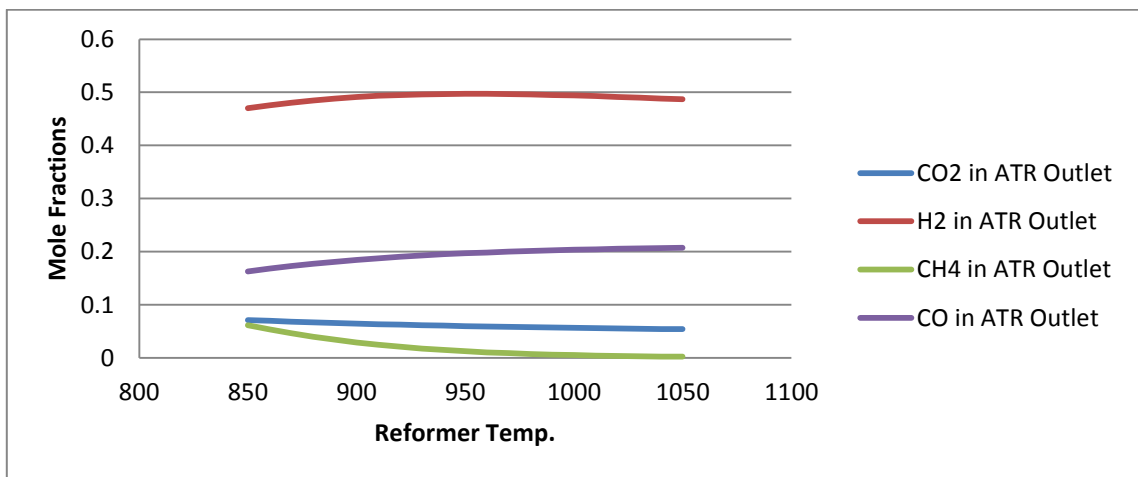
Figure 4-12: Concentrations in ATR Outlet (Air)
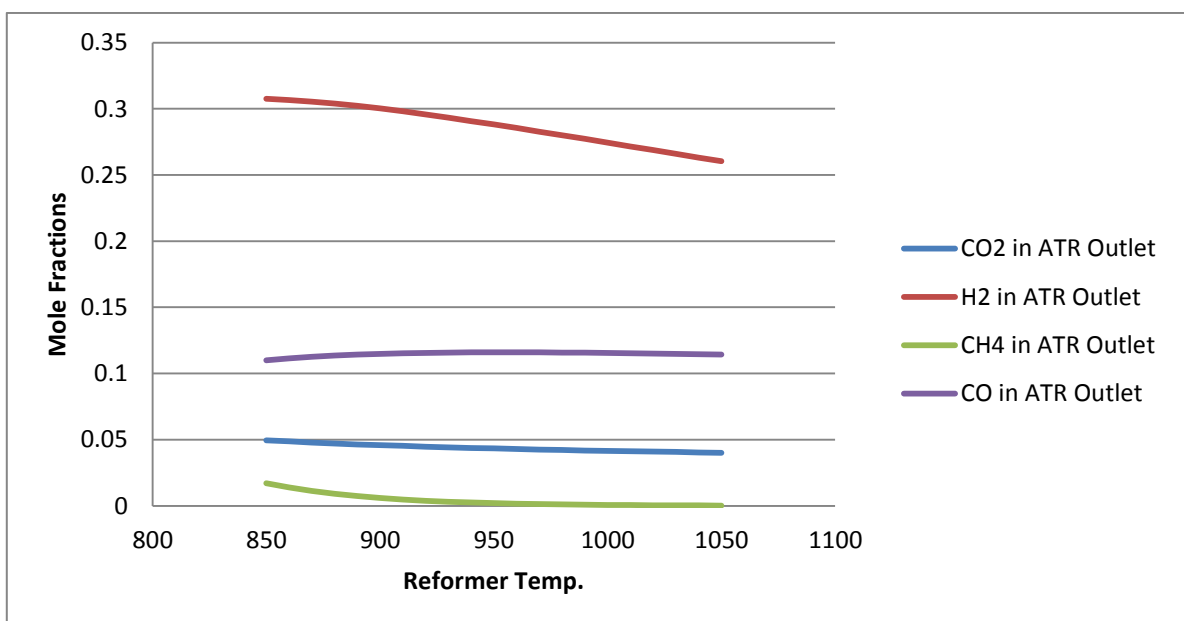
Concentrations in LTS outlet:

By increasing reformer temperature, increase in H_2 concentration is observed (Figure 4-13), that is due to the fact that more methane is converted to H_2 and CO. In air blown case, the trend is the same as ATR outlet concentrations and a reduction in H_2, CO and CH_4 concentrations is observed (Figure 4-14). This is mainly because the ATR outlet concentration effects propagate downstream of the ATR.

Figure 4-13: Concentrations in LTS Outlet (O_2)
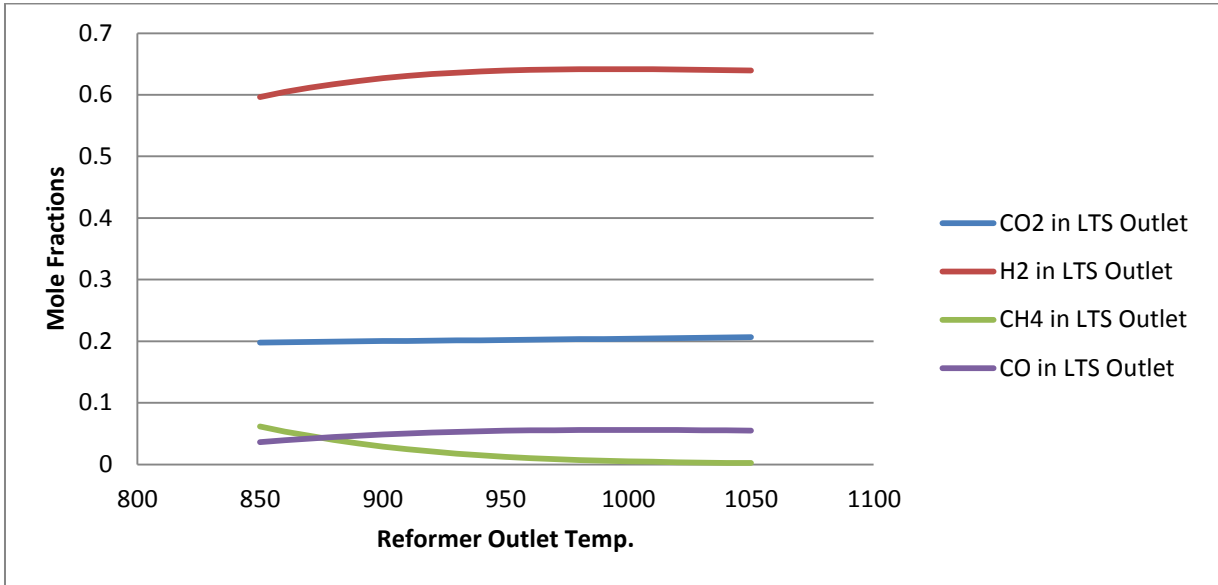
Figure 4-14: Concentrations in LTS Outlet (Air)
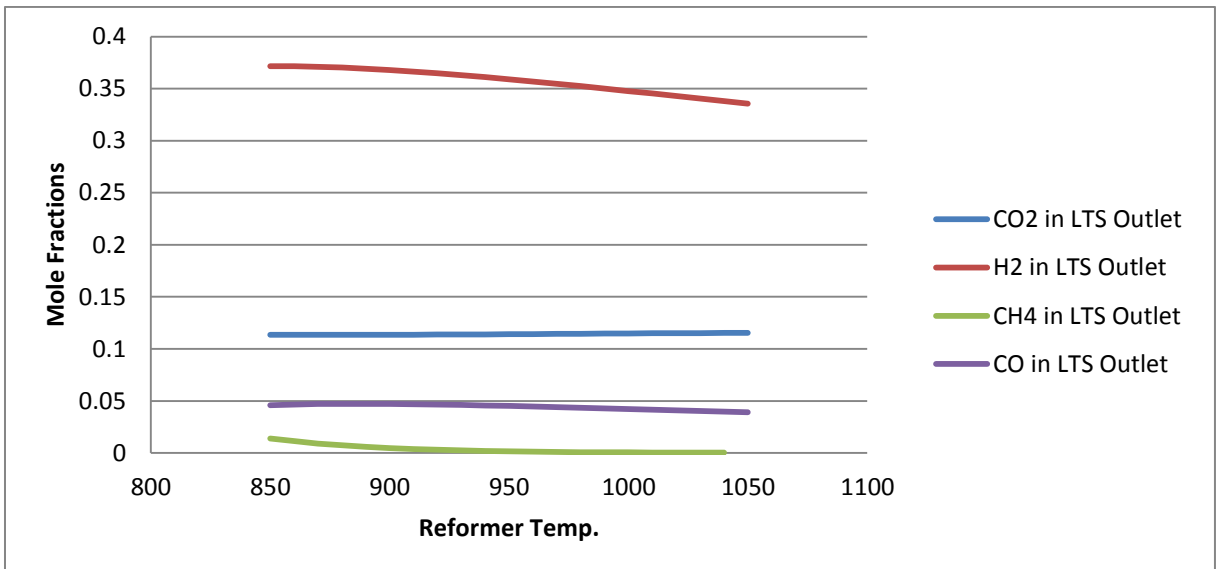
Oxygen flow and compression work:

There will be an increase in O_2 flow and compression work by increasing the reformer temperature (Figure 4-15), (Figure 4-16). This is because more oxidant is needed to keep the ATR temperature high. The increase in air flow is more than oxygen flow mainly because of large volume of nitrogen present in air flow (Figure 4-17).

Figure 4-15: O$_2$ Flow
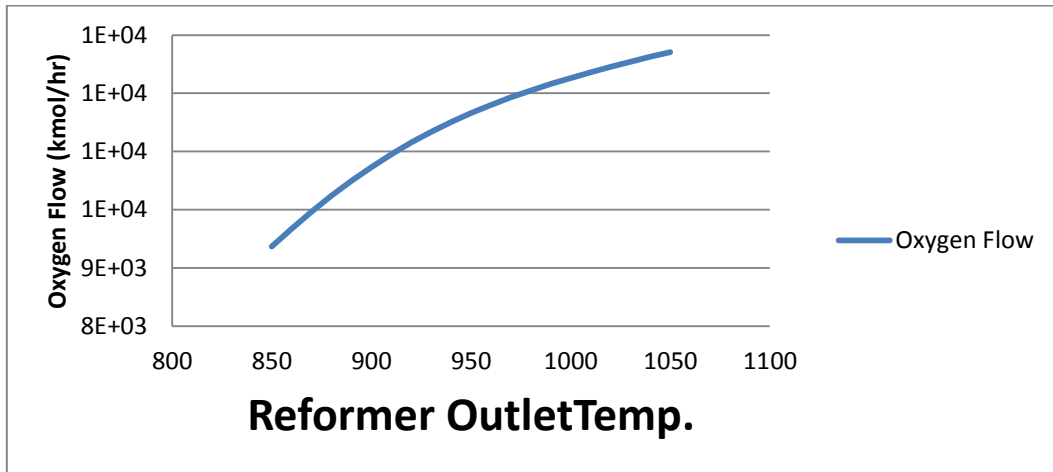
Figure 4-16: O2 Comp. Work
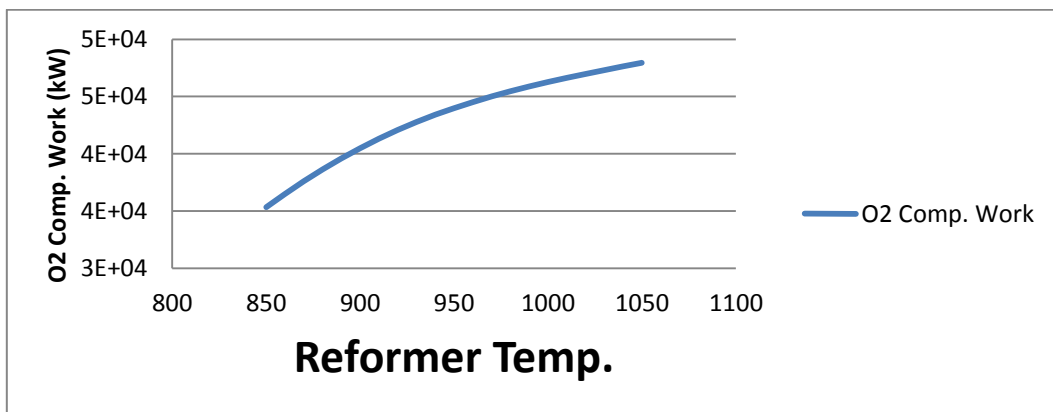
Figure 4-17: Air Flow
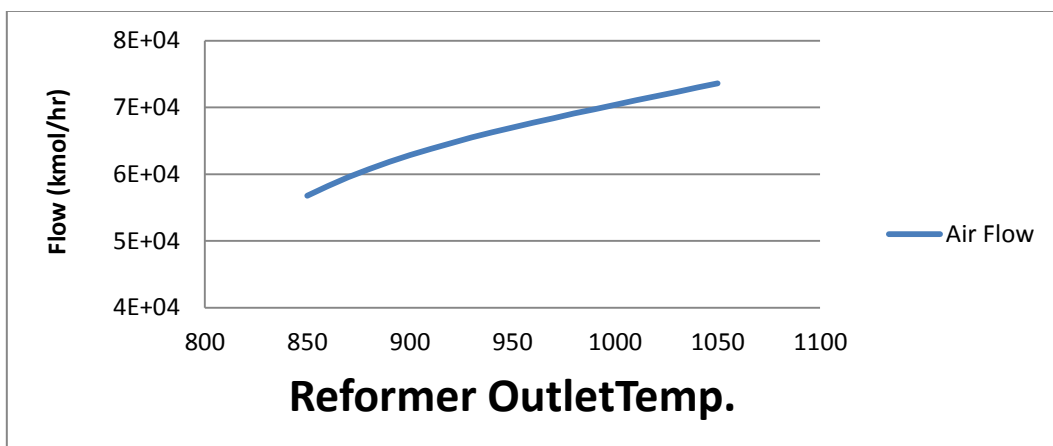
4.1.4 O$_2$ Temperature 180°C-500°C:

Concentrations in ATR outlet and LTS outlet:

In oxygen blown case, there is a slight increase in H$_2$ and CO concentrations (Figure 4-18). But in air blown case, a bigger change in H$_2$ concentartion is observed (Figure 4-19). That is on the one hand because by increasing air temperature to ATR, less air will be needed to keep reformer temperature high. Therefore, less nitrogen will enter into the reformer and concentration of H$_2$ increases. On the other hand, less CH$_4$ will be needed to burn, so it can be reformed to CO and H$_2$ in steam methane reforming reaction (Equation 2-2). The same trend is observed for LTS outlet concentrations.

Figure 4-18: Concentrations in ATR Outlet (O$_2$)
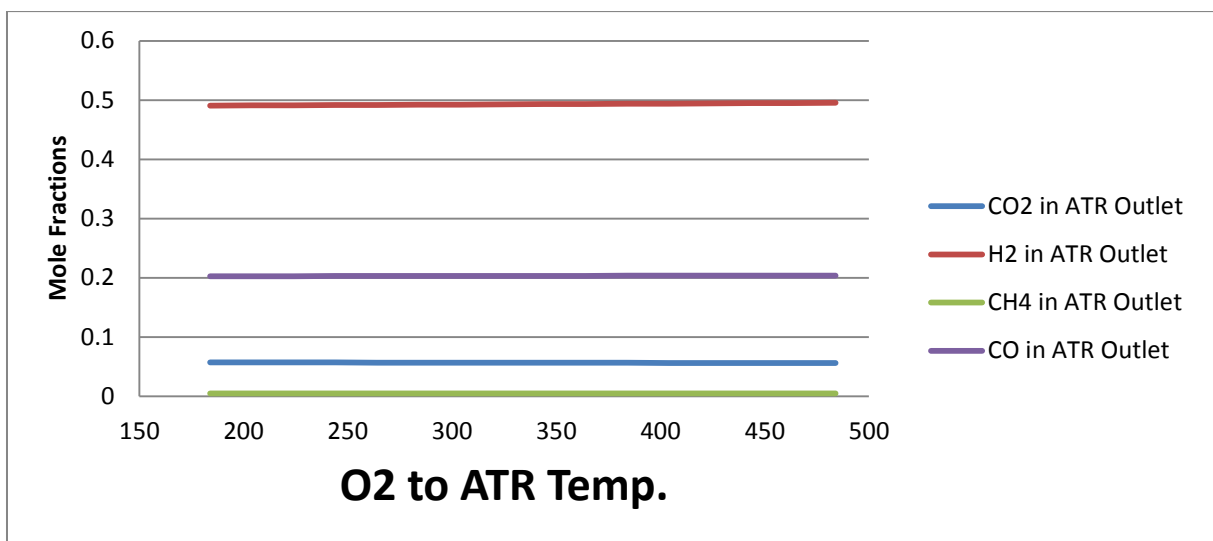
Figure 4-19: Concentrations in ATR Outlet (Air)
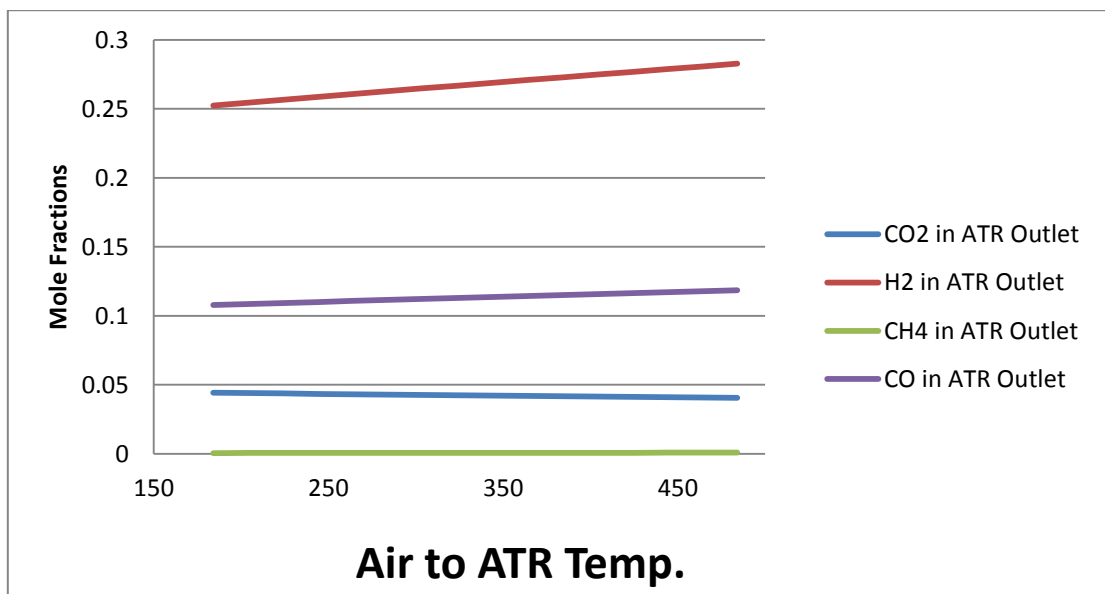
O$_2$/Air flow and compression work:

There is a decrease in oxidant flow rate by increasing its temperature to ATR (Figure 4-20). The reduction in flow rate in air blown case is more than oxygen blown case, mainly because of the large volume changes (Figure 4-21). The compression work also decreases correspondingly (Figure 4-22).

Figure 4-20: O$_2$ Flow to ATR
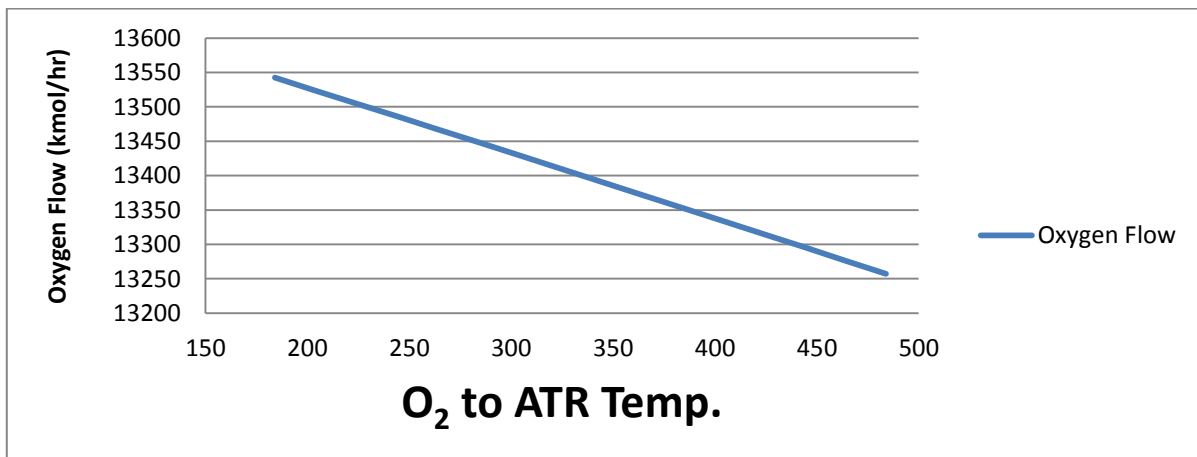
Figure 4-21: Air Flow to ATR
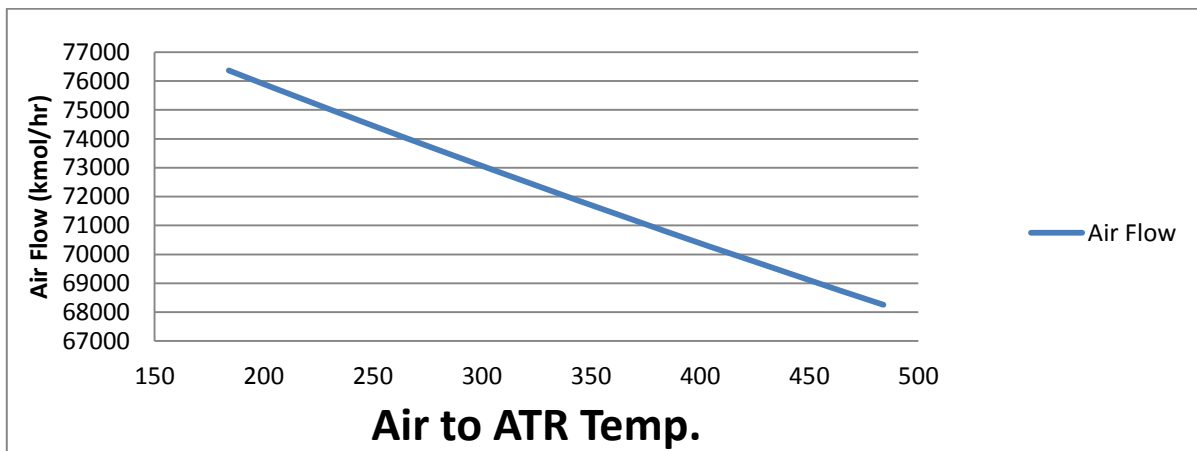
Figure 4-22: O$_2$ Comp. Work
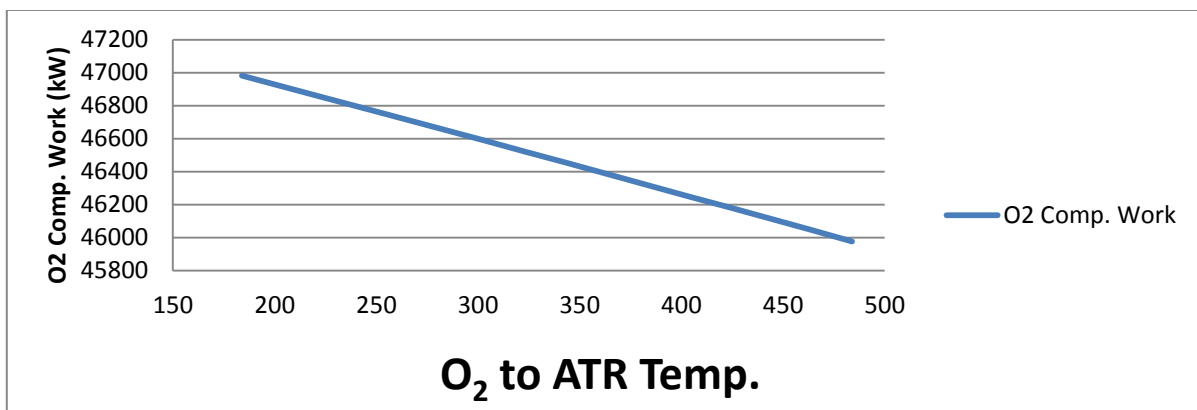
4.1.5 HTS inlet temperature 300°C- 450°C

Heating/ Cooling duty:

No changes is observed in any of the output variables upstream HTS reactor except in the heating and cooling curves. LTS and HTS product cooling increases by increasing HTS inlet temperature, but the reformer product cooling decreases (Figure 4-23). The same scenario is true with the air blown case (Figure 4-24).

Figure 4-23: Heating/ Cooling Duty (O₂)
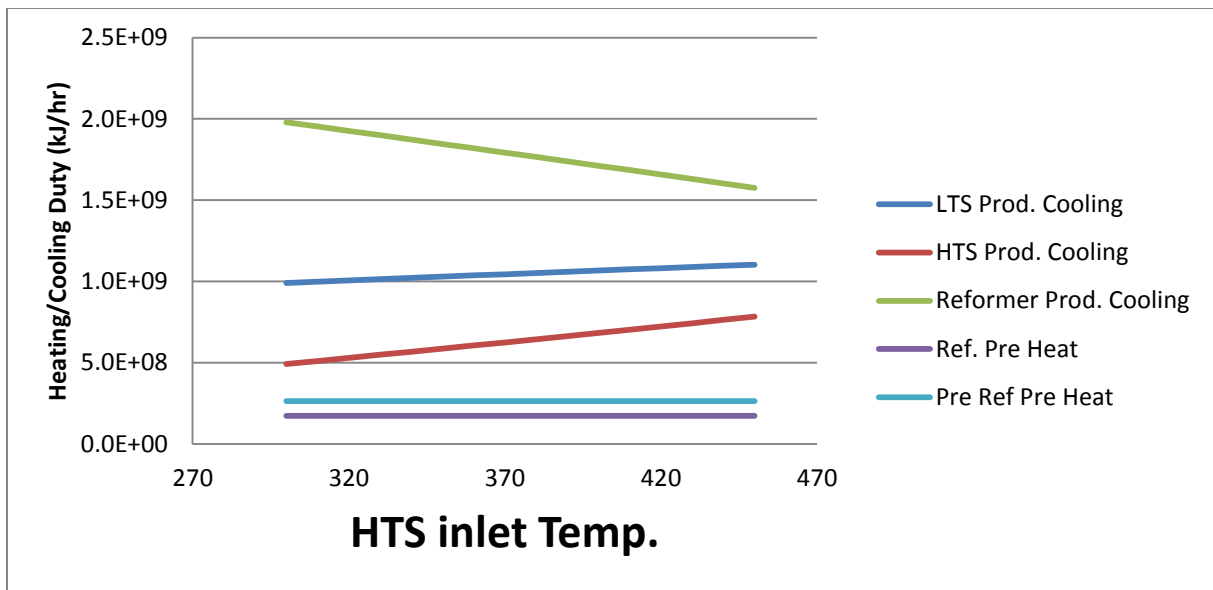
Figure 4-24: Heating/ Cooling Duty (Air)
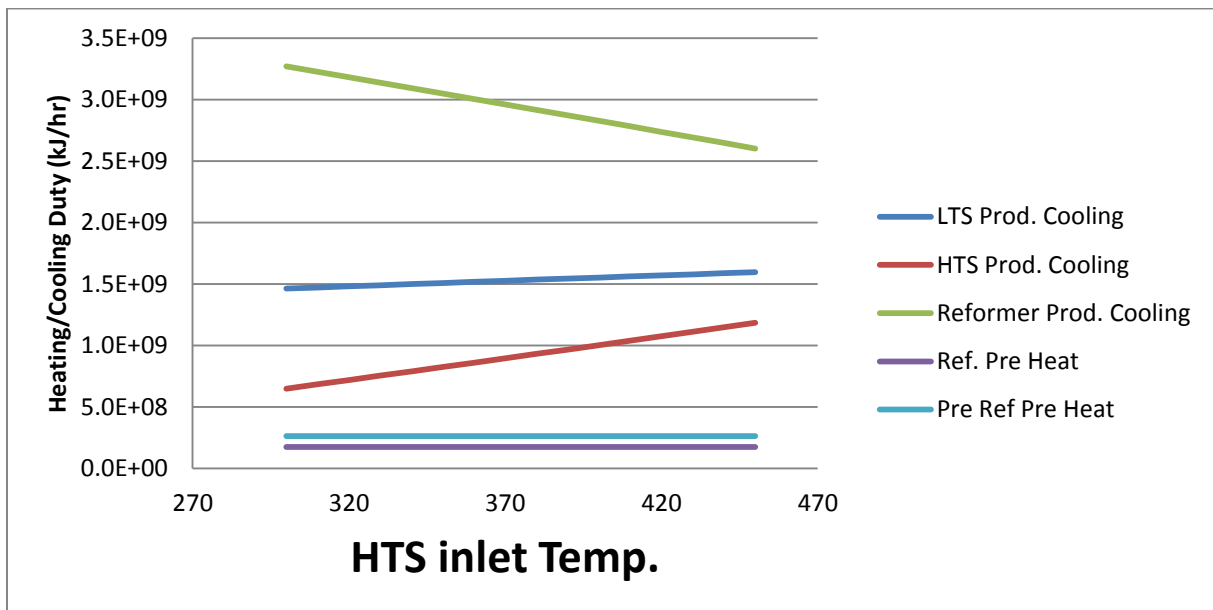
Concentrations in LTS outlet:

A slight increase in CO concentration and slight decrease in H_2 and CO_2 concentrations are observed in both oxygen and air blown cases (Figure 4-25) and (Figure 4-26). This is logical because exothermic WGS reaction (Equation 2-4) is shifted back by increasing temperature, which results in increasing CO and decreasing H_2 and CO_2 concentrations.

Figure 4-25: Concentrations in LTS Outlet (O_2)
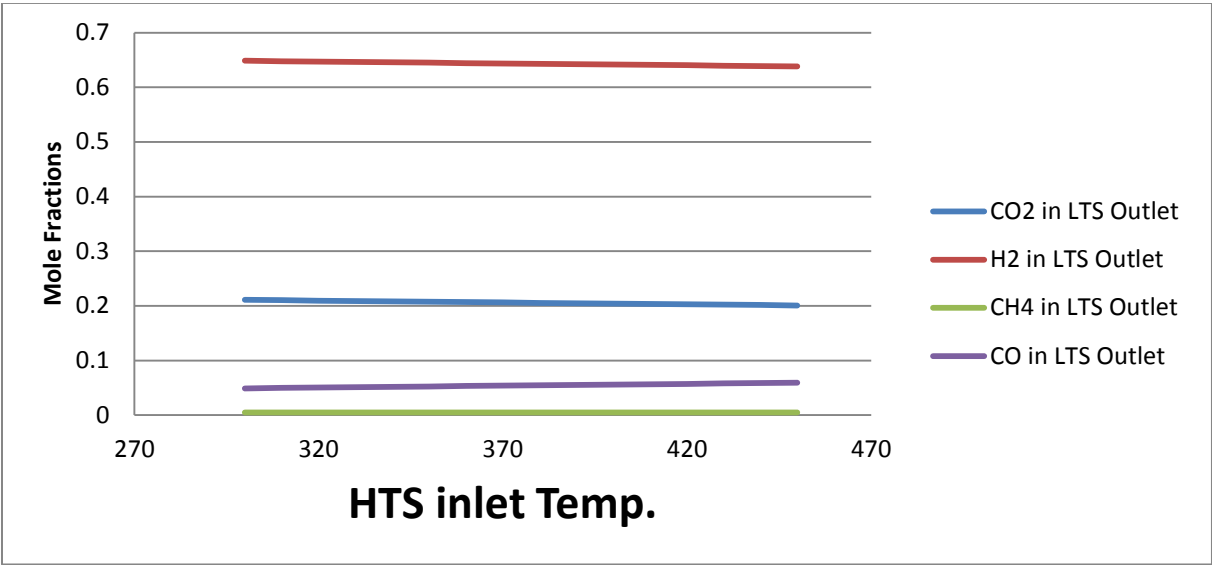
Figure 4-26: Concentrations in LTS Outlet (Air)
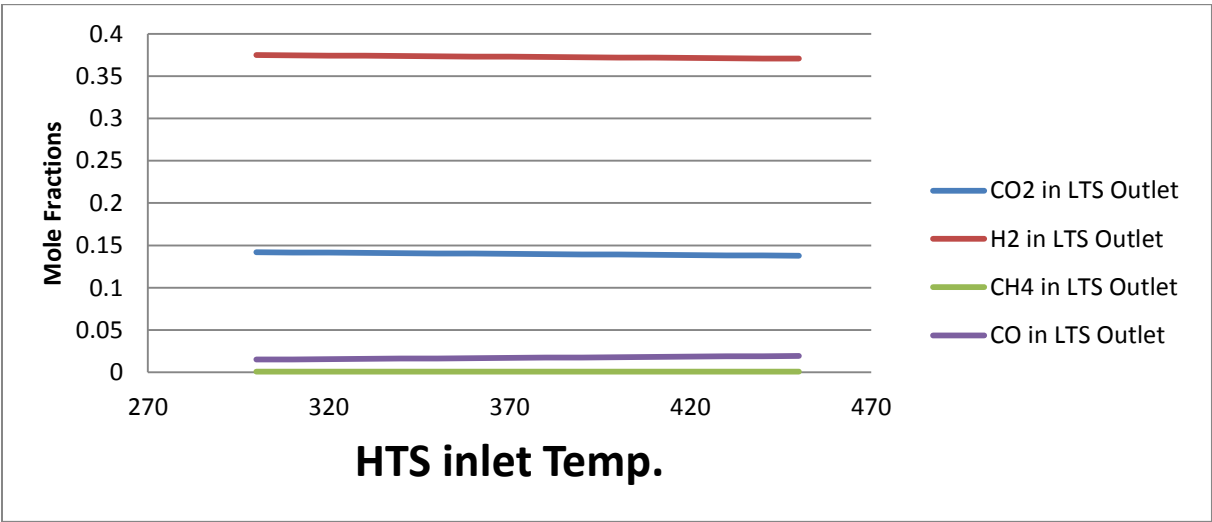
4.1.6 LTS inlet temperature 150°C- 300°C

Concentrations in LTS outlet:

When LTS inlet temperature is changed from 150°C to 300°C, reduction in H_2 and CO_2 concentrations and increase in CO concentration in both air and oxygen blown cases are observed (Figure 4-27), (Figure 4-28). This is because exothermic WGS reaction (Equation 2-4) is shifted back by increasing temperature.

Figure 4-27: Concentrations in LTS Outlet (O_2)
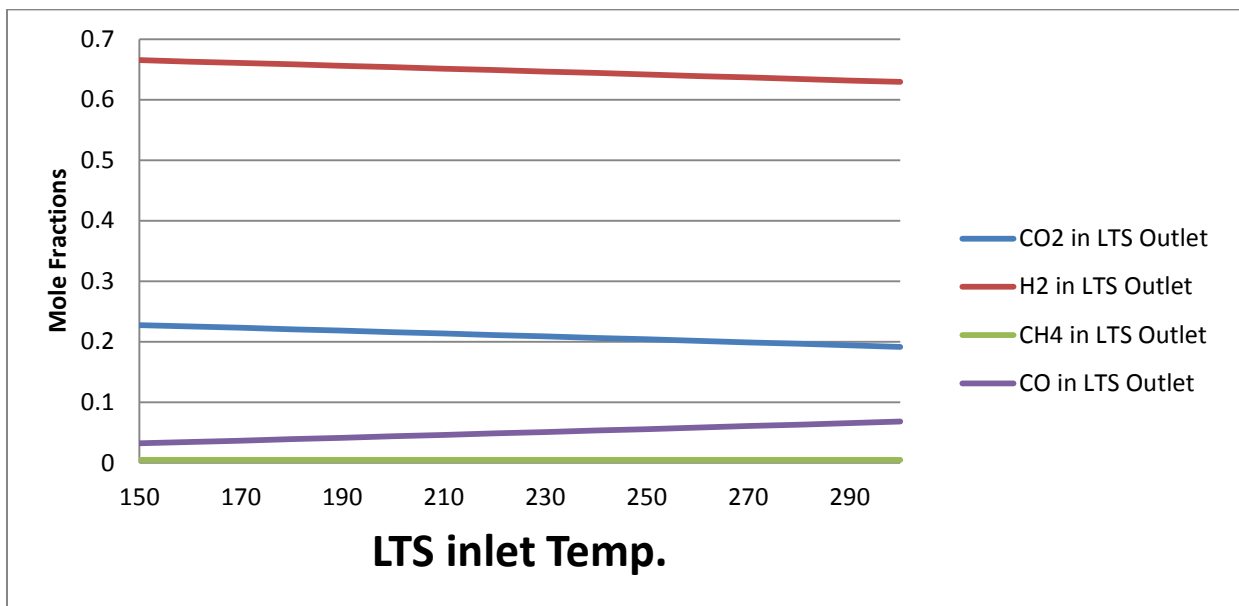
Figure 4-28: Concentrations in LTS Outlet (Air)
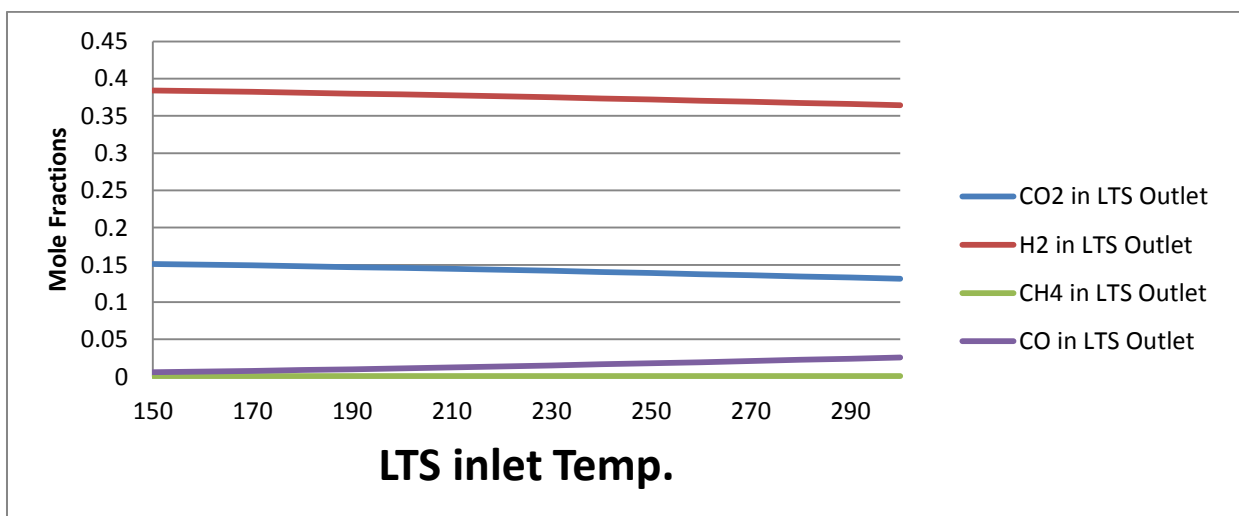
4.1.7 Pre-reformer Pressure 1500 kPa- 3500 kPa

Concentrations in ATR Inlet:

By increasing the pre-reformer pressure, a slight increase in CH_4 concentration in ATR inlet is observed (Figure 4-29). This is because a lower pressure is advantageous for the steam-methane reforming (Equation 2-2). A very small decrease in CO_2 and H_2 concentrations is observed. CO concentration is very close to zero before ATR and is not observable in a graph with this scale.

Figure 4-29: Concentrations in ATR Inlet (O$_2$)
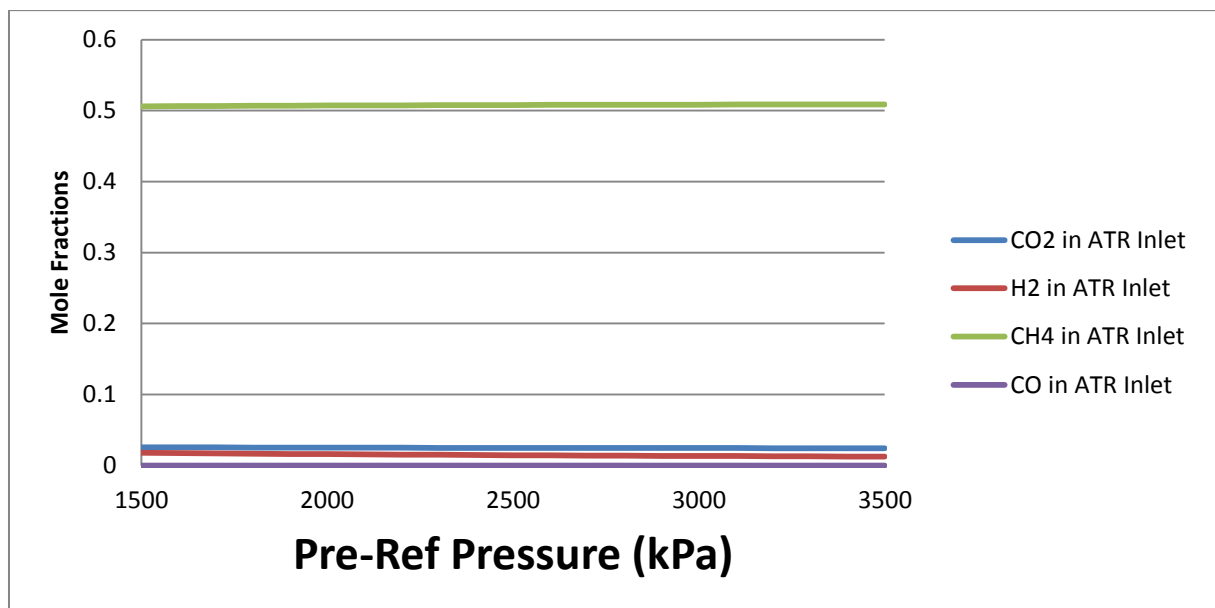
The pressure increase effect in ATR outlet concentrations is shown in Figure 4-30. Increase in CH_4 concentration and decrease in H_2 concentration is observed. This is again mainly because reverse reaction is preferred in steam-methane reforming reaction (Equation 2-2).

Figure 4-30: Concentrations in ATR Outlet (O₂)
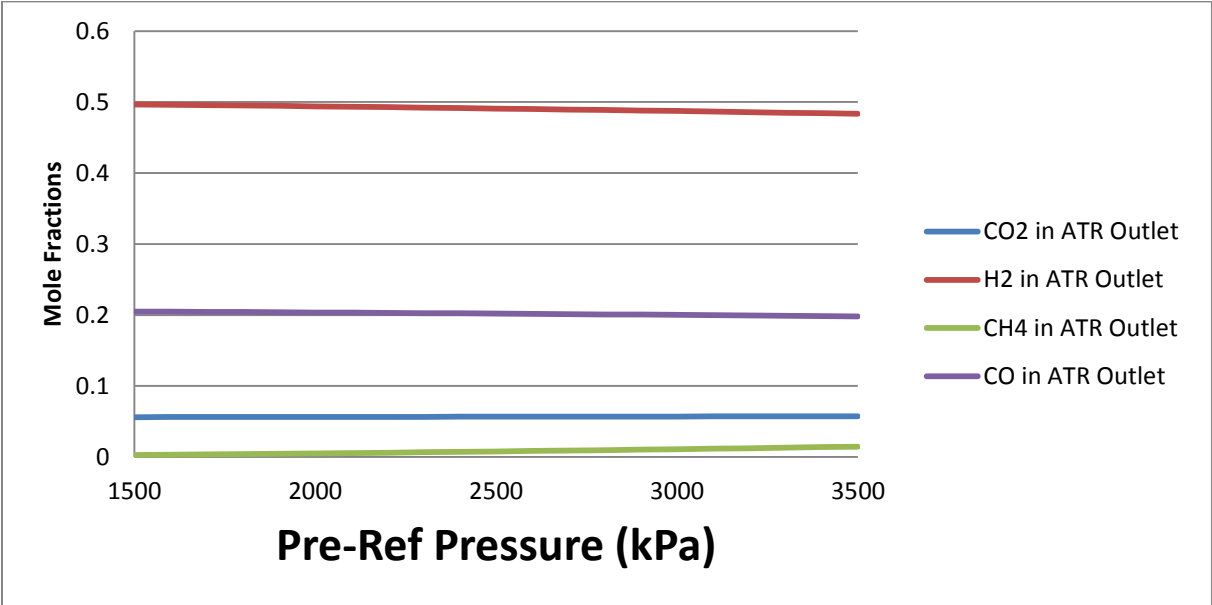
A slight decrease in H_2 and CO and increase in CH_4 concentrations is observed (Figure 4-31).

Figure 4-31: Concentrations in LTS Outlet (O₂)
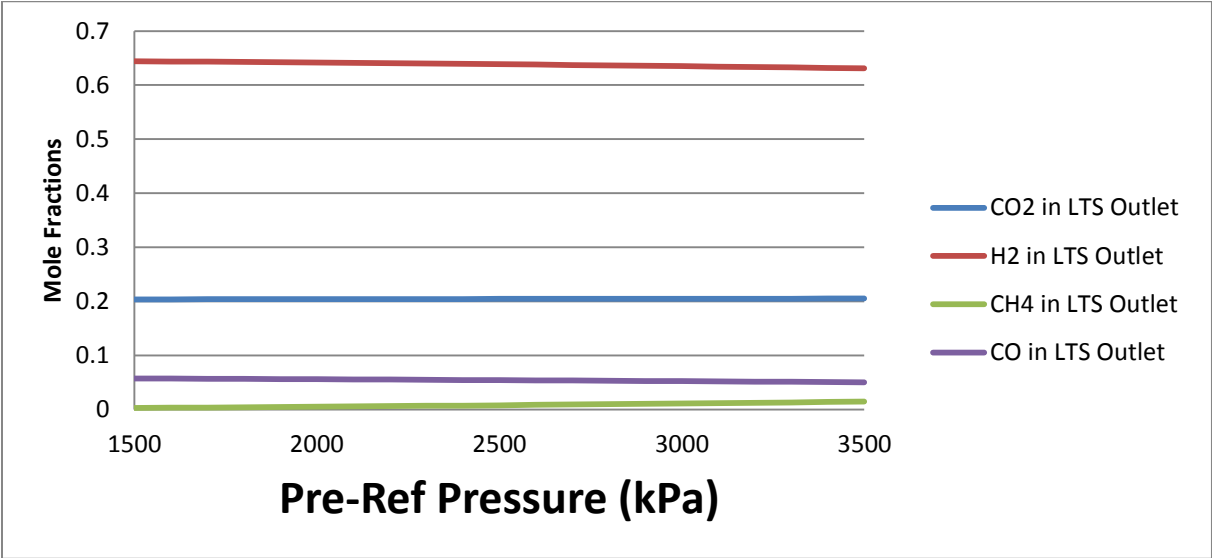
Air/O$_2$ Compression work:

The Air/O$_2$ compression work increases as the system pressure increases. The air blown case is shown in Figure 4-32.

Figure 4-32: Air Comp. Work
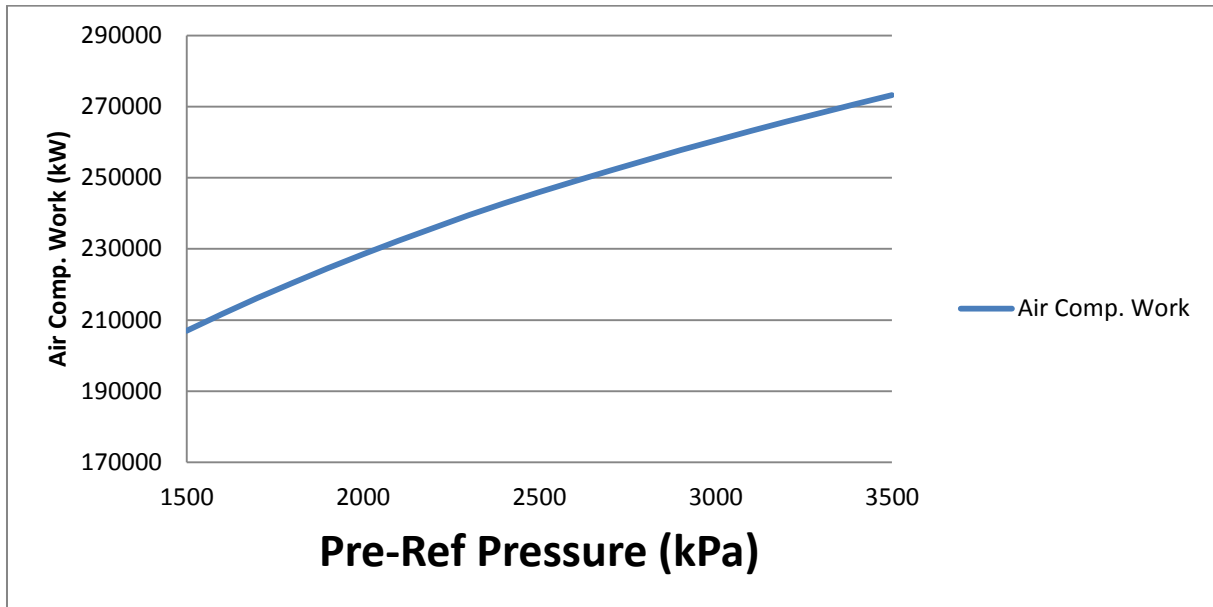
4.1.8   Steam to Carbon ratio 0.6- 2.0:

The case with S/C ratio is of great importance to us. Operations at low S/C involve the risk of soot formation in ATR and carbon formation in pre-reformer.

Concentrations in ATR Inlet:

By increasing S/C ratio in the inlet of the process, Methane concentration decreases, due to the fact that in methane reforming (Equation 2-2) forward reaction is preferred (Figure 4-33). The same is true with the air blown case (Figure 4-34).

Figure 4-33: Concentrations in ATR Inlet (O_2)
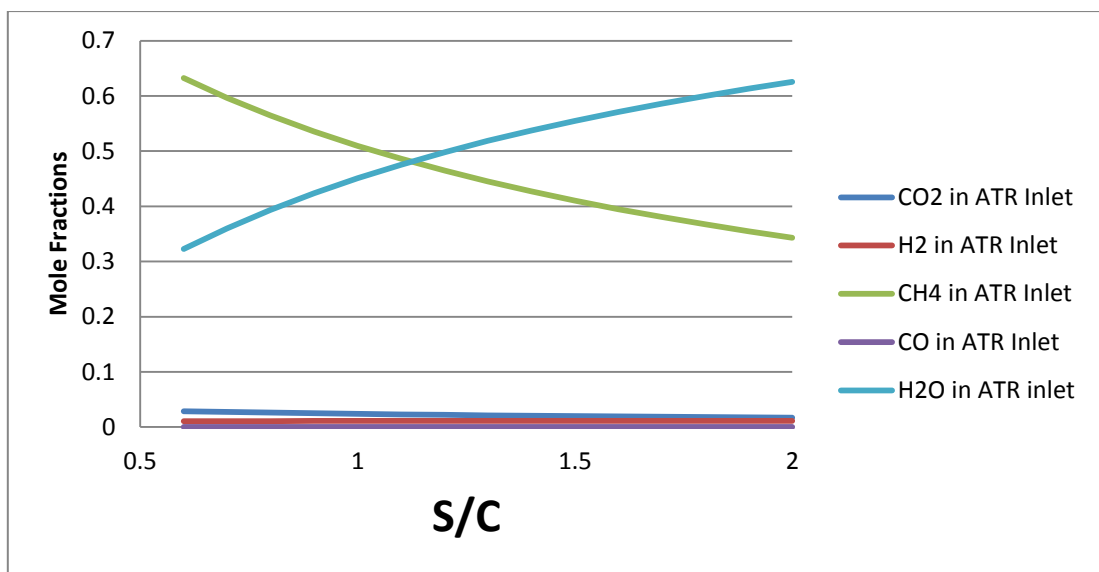
Figure 4-34: Concentrations in ATR Inlet (Air)
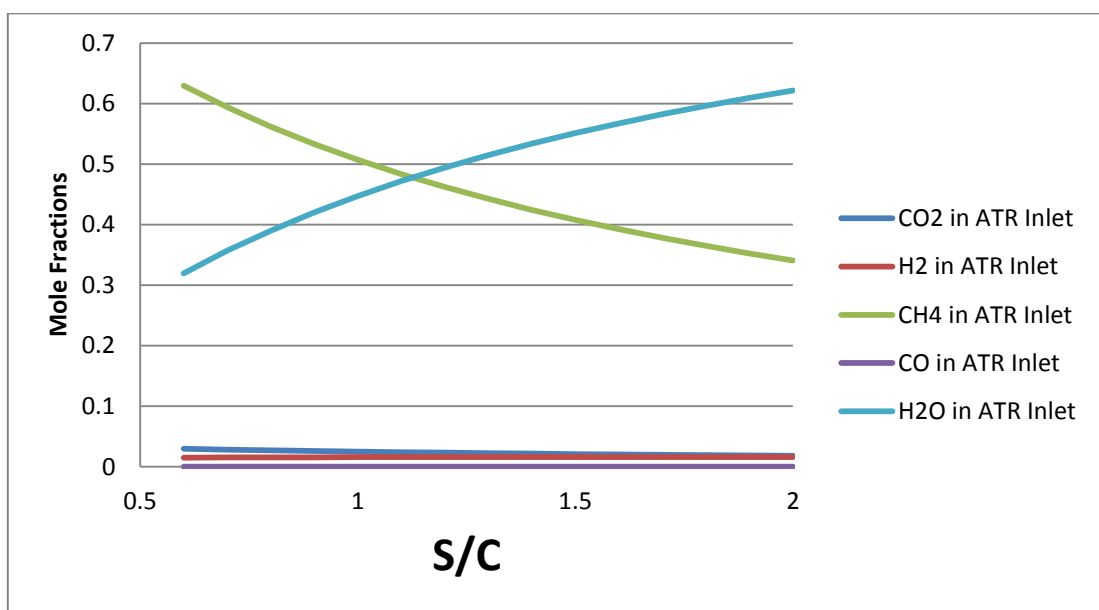
Concentrations in ATR outlet:

This part is surprising, because what we expect is to see increase in H_2 concentration because of Steam Methane Reforming reaction (Equation 2-2). According to Figure 4-35 , however, H_2 concentration decreases as S/C increases. This Figure is misleading, because in reality H_2 concentration increases but at the same time concentration of H_2O also increases which damps the effect of increasing H_2 concentration. The same behavior is observed in air blown case (Figure 4-36).

Figure 4-35: Concentrations in ATR Outlet (O₂)
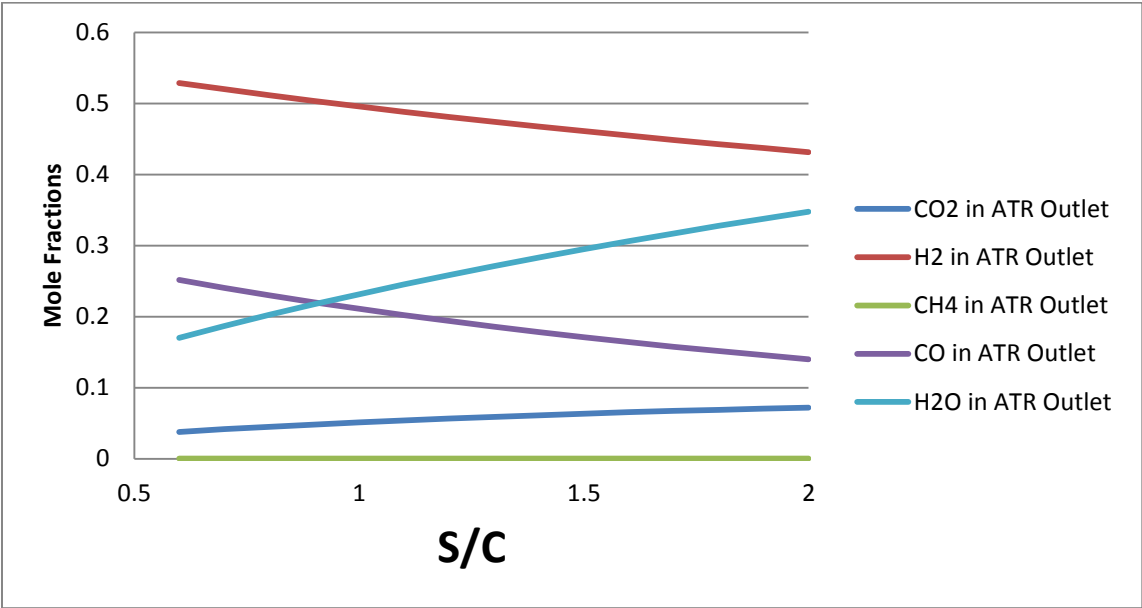
Figure 4-36: Concentrations in ATR Outlet (Air)
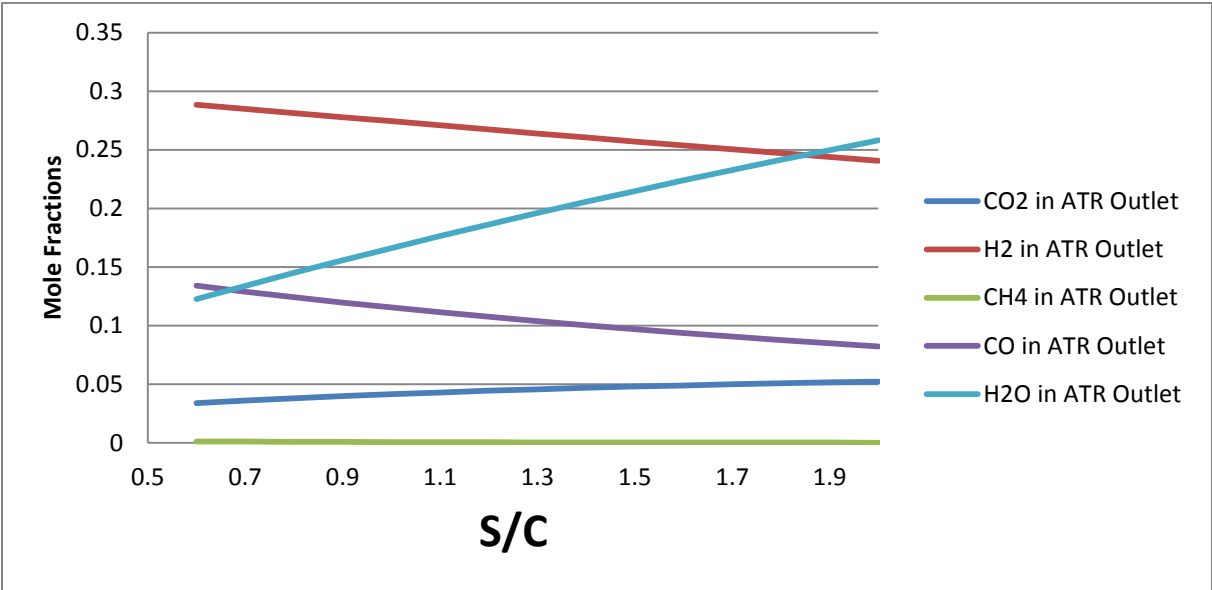
Concentrations in LTS Outlet:

Concentrations in LTS outlet follow the same trend as in the ATR outlet (Figure 4-37).

Figure 4-37: Concentrations in LTS Outlet (O$_2$)
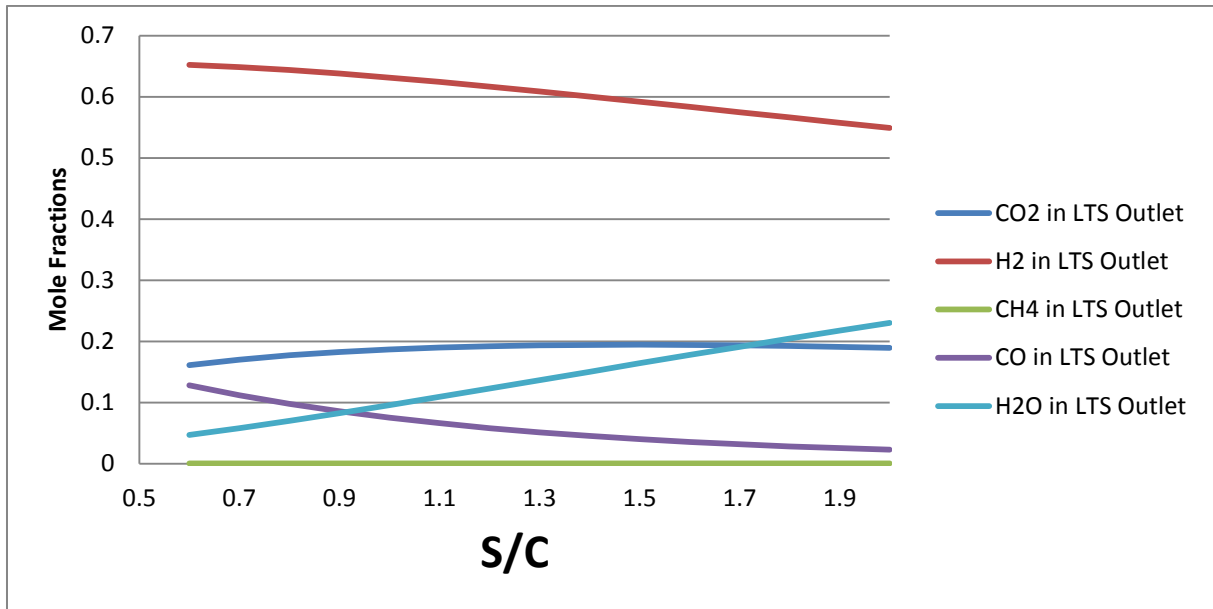
O$_2$ Compression work:

Increasing S/C ratio, causes an increase in needed oxidant in ATR, thus increases the cmpression work in both oxygen and air blown cases (Figure 4-38).

Figure 4-38: Air Compression Work
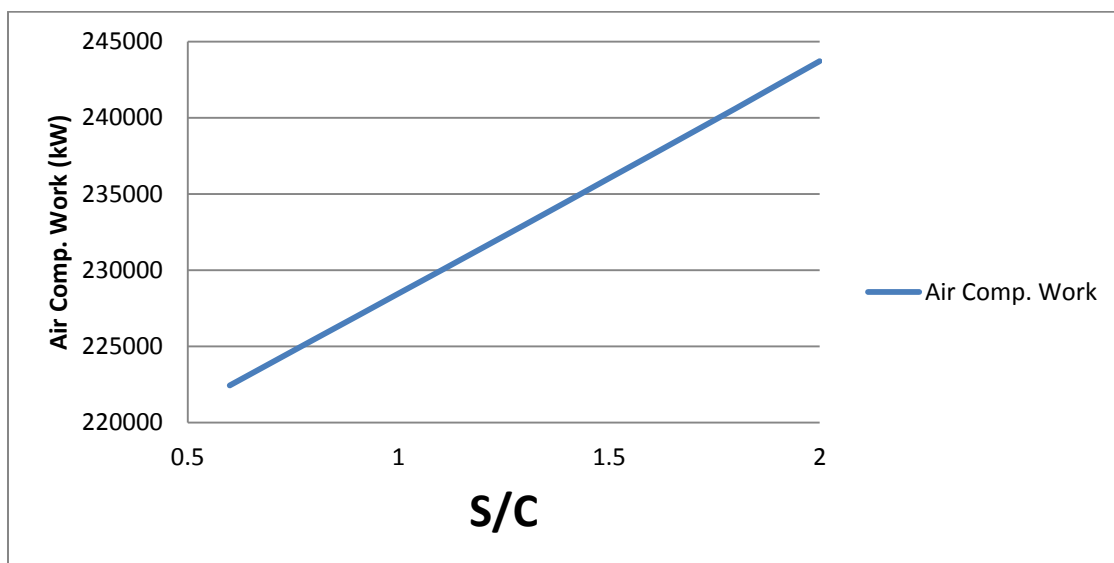
4.2 Correlation between input and output parameters

The results of the sensitivity analysis help us better understand the relationships between input and output parameters. The sensitivity analysis results are tabulated in Table 4-3. S/C ratio and reformer temperature are strongly connected to most of the outputs. In case of the polynomial model, the correlation between inputs and outputs can be understood from the regression coefficients. The higher the regression coefficient for an input, the stronger the correlation between that parameter and the output. If we take a look at regression parameters for Polynomial models in Appendix I, they reflect the results of the following Table. It is worthwhile to check the regression parameters with the results in this Table. Therefore as an example regression parameters for the 700 point Polynomial model with 7 inputs in oxygen blown ATR case are given in Table 4-4. Only regression parameters for linear terms are given. It is seen that the linear regression coefficients for S/C and ATR temperature are higher than other terms for most of the outputs which proves their strong effect on the outputs.

Table 4-3: Results of Sensitivity analysis

	Outputs	**Inputs**	
		Weakly connected	**Strongly connected**
1	Steam Flow	T preRef- T Refin- T Ref- T O_2- T HTS in- T LTS in- P preRef	S/C
2	O_2 Flow	T preRef- T Refin- T O_2- T HTS in- T LTS in- P preRef	T Ref- S/C
3	xH_2 @ LTS Outlet	T preRef- T O_2- T HTS in- P preRef- T LTS in	T Refin- T Refout- S/C
4	xCO_2 @ LTS Outlet	T preRef- T Refin- T O_2- T HTS in- P preRef- TRef- T LTS in	S/C
5	xCO@ LTS Outlet	T preRef- T Refin- T Refout- T O_2- T HTS in- T LTS in- P preRef-	S/C
6	xCH_4@ LTS Outlet	T preRef- T Refin- T Refout- T O_2- T HTS in- T LTS in- P preRef- S/C	
7	xH_2O @ LTS Outlet		S/C
8	xH_2 @ ATR Outlet	T O_2- T HTS in- T LTS in- P preRef- T preRef- T Refin	T Ref- S/C
9	xCO_2 @ ATR Outlet	T preRef- T Refin- T O_2- T HTS in- T LTS in-P preRef	T Ref- S/C
10	xCO@ ATR Outlet	T preRef- T Refin- T O_2- T HTS in- T LTS in- P preRef	T Ref- S/C
11	xCH_4@ATR Outlet	T preRef- T Refin- T Ref- T O_2- T HTS in- T LTS in- P preRef- S/C	
12	xH_2O @ ATROutlet		S/C
13	xH_2 @ ATR Inlet	T Ref- T O_2- T HTS in- T LTS in- S/C- T Refin- P preRef- T preRef	
14	xCO_2 @ ATR Inlet	T Refin- T Ref- T O_2- T HTS in- T LTS in- P preRef- S/C- T preRef	
15	xCO@ ATR Inlet	T preRef-T Refin- T Ref- T O_2- T HTS in- T LTS in- P preRef- S/C	
16	xCH_4@ATR Inlet	T preRef-T Refin- T Ref- T O_2- T HTS in- T LTS in- P preRef	S/C
17	xH_2O @ ATR Inlet		S/C
18	Q pre Ref (preheat)	T Refin-T Ref- T O_2- T HTS in- T LTS in- P preRef- S/C	T preRef
19	Q Ref (Preheat)	T Ref- T O_2- T HTS in- T LTS in- P preRef	T preRef- T Refin- S/C
20	Q Ref Prod Cooling	T preRef- T Refin- T O_2-T LTS in- P preRef	T Ref-T HTS in- S/C
21	HTS Prod Cooling	T preRef- T Refin- T Ref- T O_2- P preRef	T HTS in- T LTS in- S/C
22	LTS Prod Cooling	T preRef- T Refin- T O_2- P preRef- T Ref	T HTS in- T LTS in- S/C
23	O_2 Compression work	T HTS in- T LTS in- T preRef- T Refin	S/C - T Ref- T O_2- P preRef
24	T HTS Out	T preRef- T Refin- T O_2- T LTS in- P preRef- S/C- T Ref	T HTS in
25	T LTS Out	T preRef- T Refin- T Ref- T O_2- T HTS in- P preRef- S/C	T LTS in

			Steam Flow	O2 Flow	xCO2 @ ATR Inlet	xCO@ ATR Inlet	xH2 @ ATR Inlet	xCH4@ATR Inlet	xCO2 @ ATR Outlet
			Table 4-4: Linear regression coefficients in 700 point Polynomial model with 7 inputs in O$_2$ blown ATR						
Output Number			1	2	3	4	5	6	7
Reg. Constant	1		48.45153927	-47399.80452	0.035075819	0.001507448	0.00158732	0.865258066	0.284546128
T preref	2		0.029378587	0.71887025	-1.89E-05	-8.47E-06	-9.76E-05	6.61E-06	-9.44E-06
Pre-ref P	3		0.006082587	-4.867249561	-2.42E-07	1.17E-07	2.74E-07	-5.46E-06	1.34E-05
S/C	4		19379.37375	6454.775744	-0.016590422	0.000396888	0.004309317	-0.421364057	0.038182452
ATR inlet Temp	5		-0.046306022	-14.61993661	-2.13E-06	6.85E-07	-2.69E-07	-3.77E-05	1.95E-05
ATR T	6		-0.048536394	115.9004734	1.86E-06	-1.10E-06	-6.71E-07	2.98E-05	-0.000468086
HTS Temp	7		-0.021340753	10.27784405	5.79E-07	-1.40E-06	3.68E-06	-3.42E-05	-4.24E-05
LTS Temp.	8		-0.107353462	4.322274064	-6.66E-07	5.26E-08	1.66E-06	-2.57E-05	-1.32E-05

		xCO@ ATR Outlet	xH2 @ ATR Outlet	xCH4@ATR Outlet	xCO2 @ LTS Out	xCO@ LTS Outlet	xH2 @ LTS Outlet	xCH4@ LTS Outlet
Output Number		8	9	10	11	12	13	14
Reg. Constant	1	-0.71512218	-0.71512218	1.638823459	-0.035870075	-0.382944536	-1.1387324	1.641476831
T preref	2	-2.67E-05	-2.67E-05	6.15E-05	-2.62E-05	-1.78E-05	-0.00018428	6.07E-05
Pre-ref P	3	-7.87E-05	-7.87E-05	0.00013561	-1.58E-05	-4.86E-05	-0.000164942	0.000135963
S/C	4	-0.031375174	-0.031375174	-0.249394152	0.033659451	-0.026187962	0.097236562	-0.24910932
ATR inlet Temp	5	-0.000177445	-0.000177445	0.000343587	-1.32E-05	-0.000142161	-0.000221013	0.000344042
ATR T	6	0.002012683	0.002012683	-0.003196066	0.000557986	0.000970201	0.004021251	-0.003200096
HTS Temp	7	0.000152674	0.000152674	-0.000257367	3.29E-05	6.33E-05	0.00023191	-0.000260749
LTS Temp.	8	9.99E-05	9.99E-05	-0.000240274	-7.06E-05	0.000139913	0.000117568	-0.000245886

		Pre-Ref. Preheating	Ref. preheating	O2 Compr. work	Ref.Product Cooling	HTS Outlet Temp.	HTS Prod. Cooling	LTS Outlet Temp.	LTS Prod. Cooling
Output Number		15	16	17	18	19	20	21	22
Reg. Constant	1	-18240282.91	48827287.13	-169809.4255	-1494557694	-175.4562165	-1117133569	-489.933398	-318308351.9
T preref	2	703357.7159	-1253110.867	2.580109126	948462.1916	0.003985839	-440476.2234	0.045093829	799200.2688
Pre-ref P	3	6688.665323	7864.913472	-17.44276067	-240491.8076	-0.022033588	-165399.3396	-0.022560461	80052.97296
S/C	4	5282282.351	-51648604.88	23130.17086	306490529.5	19.75715687	245828639.4	-2.51981663	408361789.5
ATR inlet Temp	5	-4481.203095	570693.4512	-52.42878986	-1387839.399	-0.062818799	-349596.9967	-0.00713327	-134480.1528
ATR T	6	2257.545114	11521.47561	415.3164282	4437028.956	0.742350615	3283959.692	1.043042751	-710893.7787
HTS Temp	7	-942.4839698	6789.276671	36.83291163	152020.1631	0.741178553	672796.2081	0.39919889	750394.1419
LTS Temp.	8	-1765.99993	3836.109245	15.47479319	-157167.561	0.003515909	-878933.4708	0.912930294	936057.7005

4.3 Degree of freedom analysis:

Degree of freedom (DOF) analysis helps us in figuring out if a unit is correctly specified or not. It also provides insight of how many parameters are allowed to be changed at the same time around each unit operations. Degree of freedom is the number of independent variables that can be varied to specify the system or process.

In this section, degree of freedom analysis for process units is presented. We will go through different units of the process and explain their degrees of freedom.

1- Heat exchanger (HX-1):

Figure 4-39: Heat exchanger
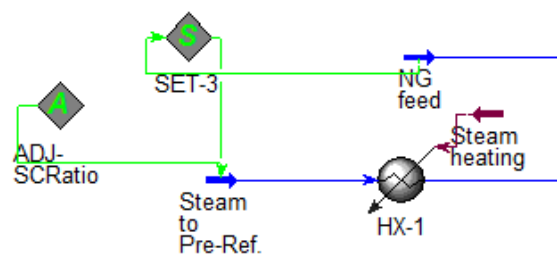
Heat exchanger (HX-1) is located at the beginning of the process and heats up the steam (Figure 4-39). A schematic view of the heat exchanger is shown below.
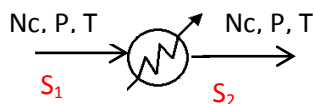
We have Nc components in the inlet and outlet of the Heat exchanger. Pressure and temperature in stream S_1 is known and specified because of steam specifications.

There are Nc mass flow equations for each of the components $f_i^{s_1} = f_i^{s_2} \quad \forall i = 1,...,nc$

With heat balance equation, the amount of heat necessary is determined: $Q = mc_p \Delta T$

We are left with only two degrees of freedom in the system, which are needed to specify the whole unit. They are pressure and temperature in stream S_2.

DOF = 2

2- Mixer (Mix-100)
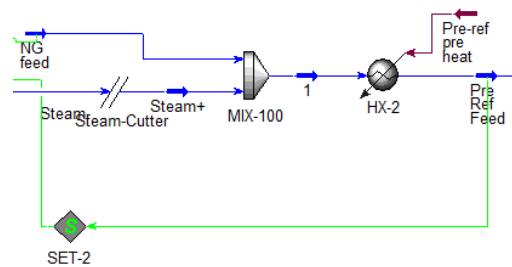
Mix-100 is mixing natural gas feed with steam and is located at the beginning of the process (Figure 4-40). A schematic view of it is shown below.
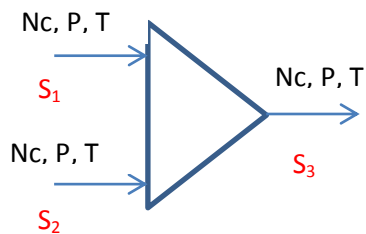
Stream S_1 is specified because the properties of natural gas are known and stream S_2 is also specified because of the HX-1. We have three unknowns at the outlet of the mixer, which can be obtained by three constraints:

1- Mass balance for each component $f_i^{S_1} + f_i^{S_2} = f_i^{S_3} \qquad \forall i = 1,...,nc$

2- $P^{S_3} = \mathrm{Min}(P^{S_1}, P^{S_2})$

3- Heat balance for streams: $H^{S_1} + H^{S_2} = H^{S_3}$

With these three equations, all the properties in outlet stream will be known and therefore there will be no degrees of freedom.

DOF = 0

3- Pre- Reformer:
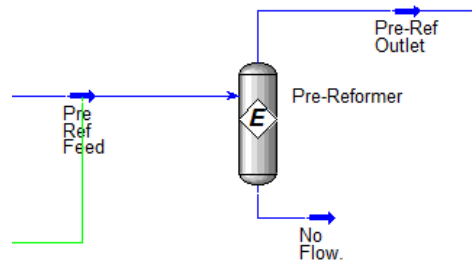
Pre-reformer feed enters the equilibrium reactor and products leave from the top (Figure 4-41). There is no flow from the bottom of the reactor. A schematic view of the pre-reformer is shown below.
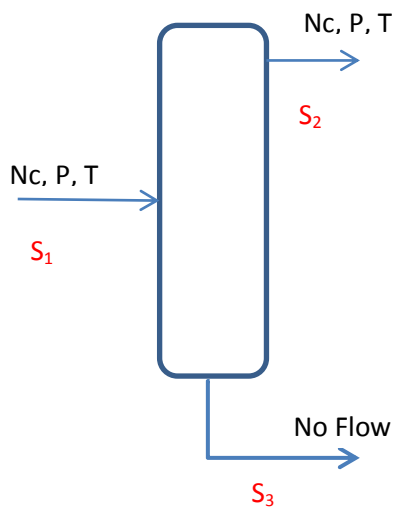
Stream S_1 which is pre-reformer feed is fully specified from downstream unit (Mix-100). There is no flow from the bottom of the reactor and therefore there is no need for any specifications. Six equilibrium reactions determine component molar flows in stream S_2. Heat balance equation determines temperature of S_2. One degree of freedom is left and that is Pressure of S_2. In the simulation it is specified that $\Delta P_{Pre-Reformer} = 0$

DOF = 1

4- Compressor (K-100):

Figure 4-42: Compressor
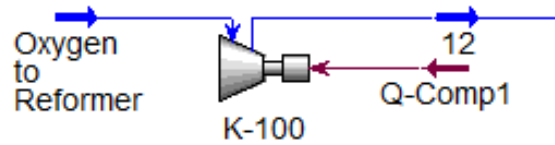
There are three compressors in the process to increase air or oxygen pressure to the required level before the reformer (Figure 4-42). The inlet stream specifications are completely known because of the known properties of air or oxygen. There is no change in flow composition during compression, therefore the outlet composition is known. The pressure and temperature in the outlet stream will be determined by specifying either of them according to the following relations:

$$\frac{P_{S_2}}{P_{S_1}} = \text{pressure ratio}$$

$$\frac{P_{S_2}}{P_{S_1}} = (\frac{T_{S_2}}{T_{S1}})^{\frac{n}{n-1}}$$

Compression work : $W = H_{S_2} - H_{S_1}$

Therefore there is one degree of freedom in which we can either specify the temperature or pressure in the outlet stream:

DOF = 1

Nc, P, T

S_1

Nc, P, T

S_2

57
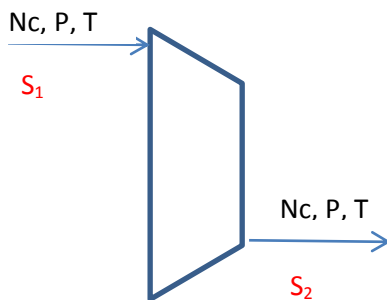
5- Reformer (ATR):

Figure 4-43: Reformer
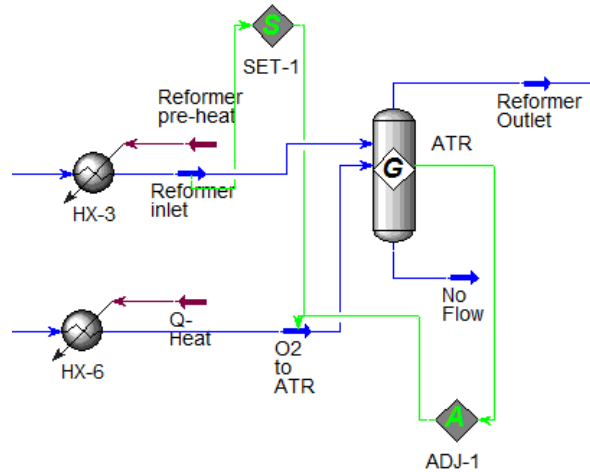
Gibbs reactor is used as the reformer (Figure 4-43) and it calculates equilibrium concentrations based on minimizing the Gibbs free energy (at a specified temperature and pressure) or maximizing entropy (at a specified pressure and heat duty). Schematic view of the reformer is shown below.
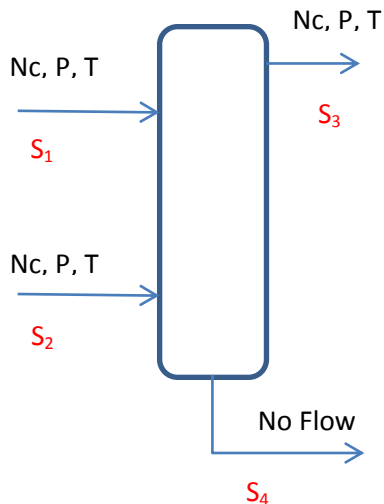
All the properties of stream S_1 is known. Nc component molar flows, pressure and temperature in stream S_3 are to be determined. Two scenarios can be considered in ATR analysis:

Fisrt: The case where all the parameters of the input streams (S_1 and S_2) are known. The pressure in S_3 is specified by specifying the pressure drop in the ATR. $P_{S_3} = P_{S_1} - 1 \ (bar)$

Heat balance equation determines the temperature in S_3.
And finally mass balance equations determine the outlet molar flows.

$$\sum_{nc} \dot{m}_{in}{}^{S_1} + \sum_{nc} \dot{m}_{in}{}^{S_2} = \sum_{nc} \dot{m}_{out}{}^{S_3}$$

By specifying the pressure drop in ATR all the outputs are known and therefore there is one degree of freedom:

DOF = 1

Second: If molar flow of stream S_2 is not determined, but instead the temperature and pressure of S_3 are specified. Then the ATR calculates the molar flow rate in stream S_2 so that it satisfies the outlet temperature and pressure in S_3. Again the same equations as in the first case apply here. By specifying the pressure drop in ATR all the outputs are known and therefore there is one degree of freedom:

DOF = 1

6- HTS and LTS reactors:

Figure 4-44: HTS and LTS reactors
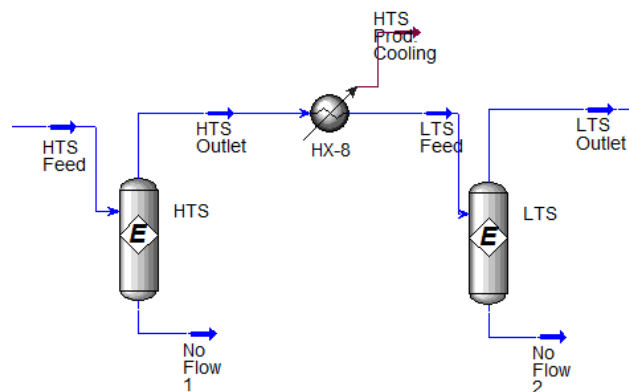
The case with HTS and LTS reactors (Figure 4-44) are exactly the same as the pre-reformer and they have one degree of freedom with which pressure drop can be specified in these two reactors.

DOF = 1

5 Metamodel Building

In this chapter the metamodel building step and their results are presented. As mentioned earlier, effort was made to compare two types of metamodels: Polynomial vs. Kriging. The Polynomial model was considered due to its historical usage in the statistical literature. The Kriging model was considered next because of its popularity for interpolating output from computer simulations.

The IRCC process from an optimization point of view is very complex and computationally expensive. There is a need for techniques that consider computational efficiency and show promise for application to large scale flow sheet optimization problems. Surrogate models show the potential to surpass these difficulties in optimization software. The process parameters that initially were considered to be important as the inputs in the metamodel building step are given in Table 5-1.

The part of the IRCC process for which metamodeling was performed is shown in Figure 5-1.

Figure 5-1: Flow sheet for metamodeling part of the process
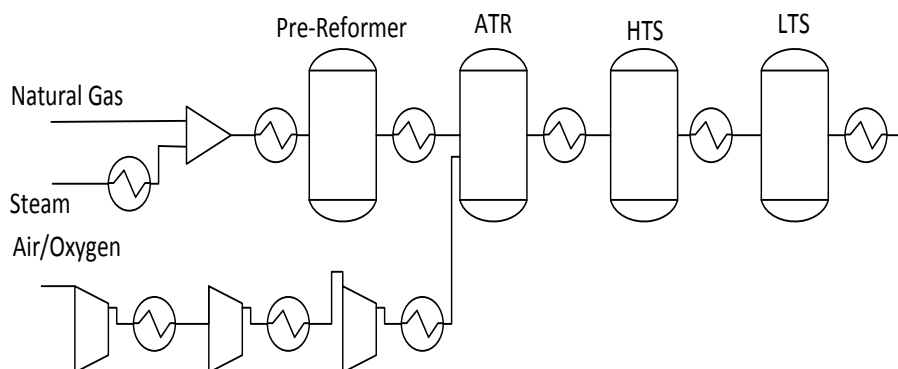
Table 5-1: Input variables and their ranges

Input No.	Input variables	Range
1	Pre-reformer temperature	250°C-500°C
2	Pre-reformer pressure	15 bar-35 bar
3	S/C ratio in Pre-reformer inlet	0.6-2
4	Reformer temperature	250°C– 500°C
5	Reformer outlet temperature	850°C-1050°C
6	O_2/Air temperature	185°C – 500°C
7	HTS temperature	300°C-450°C
8	LTS temperature	150°C-300°C

Twenty-two outputs were considered important as they provide essential figures in the optimization of an IRCC plant. These variables are listed in Table 5-2.

As mentioned earlier, simulations were done in ASPEN HYSYS software. For the sake of comparison and seeing the effect of number of runs on the accuracy of the model, several simulation runs were taken. For ease of performing data analysis and easy communication with HYSYS, Aspen Simulation Workbook (ASW) in Excel was used as a tool to make simulation runs. It is a powerful add-in tool that allows HYSYS to link process models to an Excel workbook. It allows the user to set up a number of different scenario runs for a simulation in Excel. The user can decide on a number of variables, which they want to vary and enter these in Excel. Excel feeds these values to HYSYS and runs the simulation for each of the scenarios. The user can define which output values they want HYSYS to feed to Excel. Thus, the simulation is run from Excel and Excel becomes the controlling program. This tool is very useful to do parametric studies without the need of user intervention.

Metamodels were made for each of the outputs, which means 22 polynomial models and 22 Kriging models in each simulation case.

Table 5-2: Output variables

	Variable		Variable
1	Steam flow	**12**	xCO@ LTS outlet
2	O_2 flow	**13**	xH_2 @ LTS outlet
3	xCO_2 @ ATR inlet	**14**	xCH_4@ LTS outlet
4	xCO@ ATR inlet	**15**	Pre-reformer preheating
5	xH_2 @ ATR inlet	**16**	Reformer preheating
6	xCH_4@ATR inlet	**17**	O_2 compression work
7	xCO_2 @ ATR outlet	**18**	Reformer product cooling
8	xCO@ ATR outlet	**19**	HTS outlet temperatue
9	xH_2 @ ATR outlet	**20**	HTS product cooling
10	xCH_4@ATR outlet	**21**	LTS outlet temperature
11	xCO_2 @ LTS outlet	**22**	LTS product cooling

Each of the inputs was scaled to the range (-0.5, 0.5) according to equations given in Table 5-3 . Then MATLAB program was used to generate the LHS samples in the range (-0.5,0.5). The samples were then descaled to their real values and entered into Excel. By use of Aspen Simulation Work book in Excel, the simulation cases were run. HYSYS results were automatically exported to Excel sheets. Now we have the results of the simulations in excel sheets, ready to be processed. The schematic view of this process is given in Figure 5-2.

Table 5-3: Scaling of input variables

Input Number	Variable name	Range of input	Scaling Equation
1	Pre-reformer temperature	250°C-500°C	$\dfrac{T_{\text{PreRef}} - 375}{250}$
2	Pre-reformer pressure	15 bar-35 bar	$\dfrac{P - 25}{20}$
3	S/C ratio	0.6-2	$\dfrac{S/C - 1.3}{1.4}$
4	Reformer temperature	250°C– 500°C	$\dfrac{T_{Ref} - 375}{250}$
5	Reformer outlet temperature	850°C-1050°C	$\dfrac{T_{\text{Refout}} - 950}{200}$
6	O₂/Air temperature	185°C– 500°C	$\dfrac{T_{O2/Air} - 342.5}{315}$
7	HTS temperature	300°C-450°C	$\dfrac{T_{HTS} - 375}{150}$
8	LTS temperature	150°C-300°C	$\dfrac{T_{LTS} - 225}{150}$

Figure 5-2: Structure of data handling and software interaction

MATLAB (LHS Samples) → Excel (Aspen Simulation Work book) → Simulation Results → MATLAB (Regression)

Input to Run Scenarios

Simulation Results

HYSYS
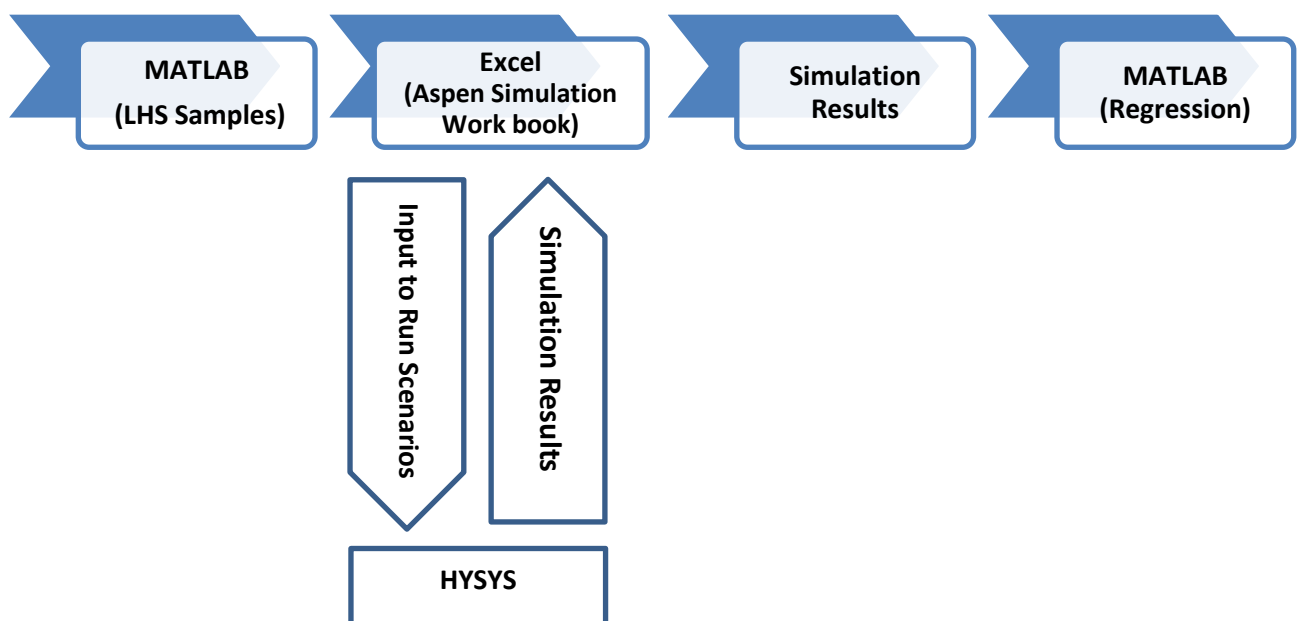
Figure 5-3 shows the overall work that has been done in metamodel building. A total of 30 cases for oxygen blown and air blown ATRs were investigated. In each of the 30 cases, 22 Kriging metamodels and 22 Polynomial metamodels were built which means for each of the 22 outputs, one Kriging and one polynomial model was made. The number of cases considered for the air blown and oxygen blown ATRs are given in (Table 5-4).The reason for having few cases considered in the air blown ATR is the smooth behavior of the metamodels fit, whereas in oxygen blown cases there are some irregularities in fit which will be discussed later in section 5.3.

Figure 5-3: Overall work in metamodel building
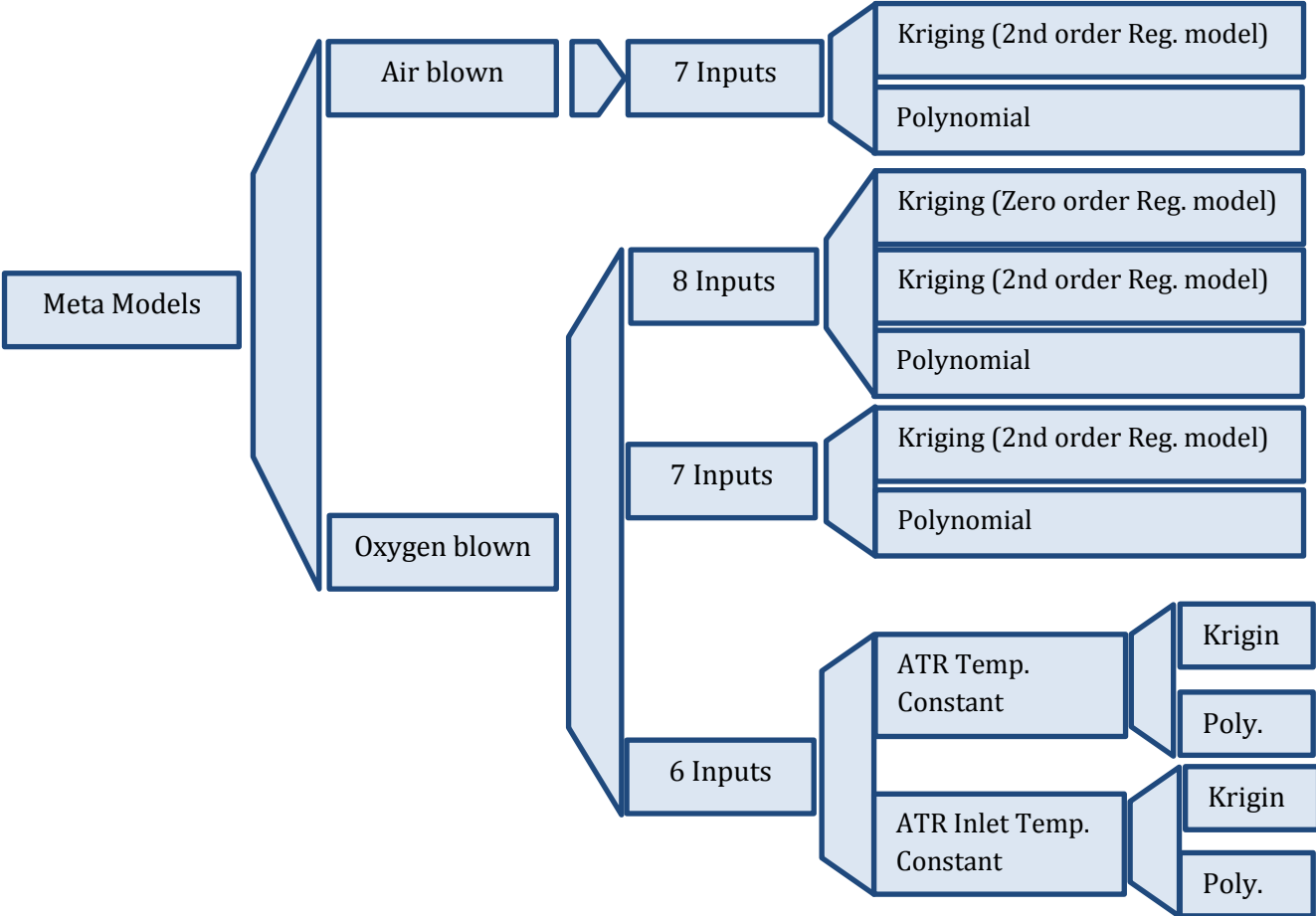
Table 5-4: Number of cases considered based on ATR and model types

Type of ATR	Model Type	No. of cases cosidered
Oxygen blown	Kriging	14
	Polynomial	12
Air blown	Kriging	2
	Polynomial	2

Number of cases considered based on the number of sample points and ATR type is given in Table 5-5.

Table 5-5: Number of cases considered based on ATR and Sample size

Cases considered		
Sample Size	ATR Type	No. of Cases
600	O_2	2
700	Air	2
	O_2	9
800	O_2	2
900	Air	2
	O_2	9
1000	O_2	2
1100	O_2	2
Sum		30

For Metamodel building step, it was decided to use MATLAB programs available in the literature written specifically for this purpose. This was due to the fact that these programs are reliable and trustable enough for our study.

For making Polynomial models Surrogate toolbox in MATLAB [53] was used. It is a general-purpose library of multidimensional function approximation and optimization methods. The capabilities of this toolbox are given in Table 5-6. It is capable of making polynomial models from multidimensional inputs for a single dimension output.

Table 5-6: Surrogate toolbox capabilities [53]

Experimental Designs	Full factorial and variants of the Latin hypercube designs
Surrogates	Gaussian process, Kriging, polynomial response surface, radial basis neural network and linear Shepard
Error Analysis and cross validation	Class error analysis (R^2, root mean square error and others), leave-one-out and k-fold cross-validation.
Surrogate based optimization	Global sensitivity analysis, conservative surrogates (via safety margin), contour estimation, and variants of the efficient global optimization (EGO) algorithm.

Kriging models were made by use of DACE toolbox written in MATLAB [43]. DACE stands for Design and Analysis of Computer Experiments. It is a well written program specifically to generate Kriging models made in Technical University of Denmark (DTU). It is capable of producing Kriging metamodel from high dimensional inputs and outputs.

It is worthwhile to mention that the computer models addressed here are deterministic, and lack random error, i.e., repeated runs for the same inputs gives the same response from the model.

Metamodels need to be evaluated and their accuracy be validated before they can be used in optimization software. For the validation step, 200 LHS sample points for oxygen blown ATR and 200 LHS sample points for air blown ATR were made and they were fed into the HYSYS. Then the results of these simulations were compared to the metamodel results for the same 200 points. Then as described in Chapter 2, SSE, SSR, SST and finally coefficient of determination (R^2) were calculated for each metamodel. The comparison between metamodels is based on R^2.

The procedure used in developing metamodel in this thesis is as follows:

1) Choosing the input and output parameters that yield accurate metamodels: as is done in Chapter 4
2) Use of LHS experimental design method to pick the inputs to the simulation
3) Running the simulation case at selected inputs via Aspen Simulation Workbook

4) Use of DACE and Surrogate toolboxes for regression and fitting metamodels to the data
5) Model validation via 200 validation points
6) Calculation of R^2 as a measure of goodness of fit

In section 5.1 Oxygen blown cases is considered and in fact most of the metamodeling focus is on this type of ATR, because of the unusual behavior of metamodel fit to the data. Kriging and Polynomial model results are given in section 5.1.1 and 5.1.2, respectively. Air blown ATR case is presented in section 5.2. A general overview of the presentation of the results is given in Figure 5-4 and Figure 5-5. The numbers in the right hand side of the diagrams are number of simulation runs which metamodels were made for. For example in oxygen blown and for the 7 input case, six different sample sizes were used in metamodel building: 600, 700, 800, 900, 1000 and 1100. This is to investigate the effect of sample size on the goodness of fit of the model. For each of these sample sizes, 22 Kriging and 22 Polynomial metamodels were made, one for each of the 22 outputs.

Figure 5-4: Overview of presentation of results
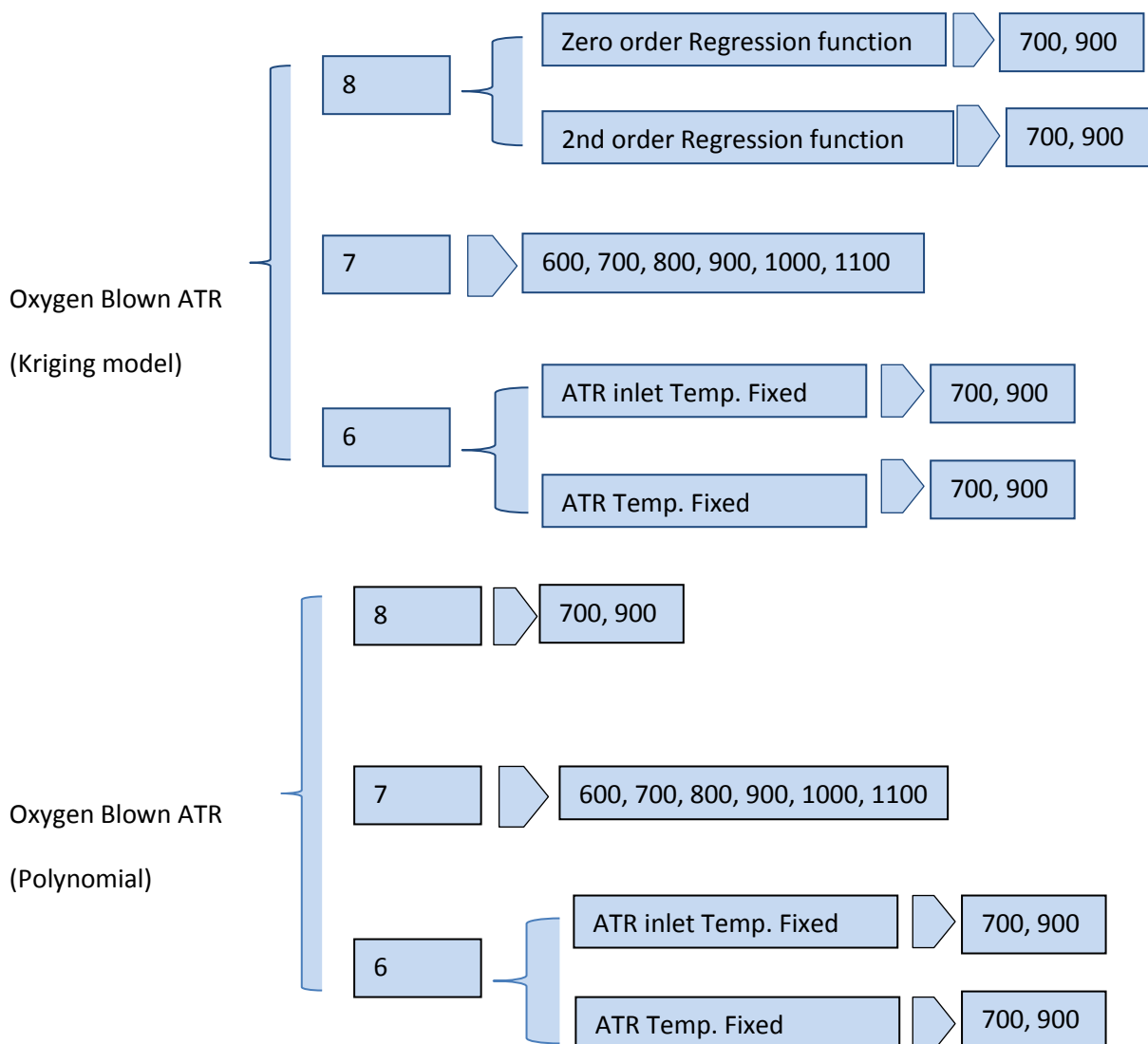
Figure 5-5: Continue of overview of presentation of results
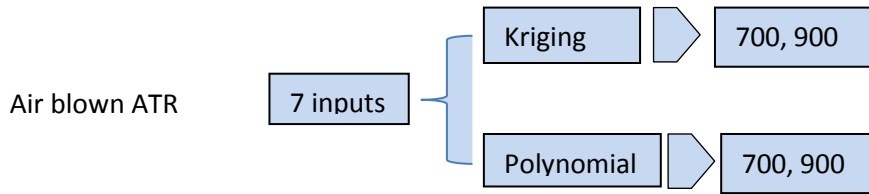
5.1 Oxygen Blown ATR

26 cases were considered for the oxygen blown ATR. The presentation of the results is based on the number of inputs used in metamodel building. Kriging model results are presented first followed by results from Polynomial models.

The work started with building metamodel for the oxygen blown case. The results in this case were not so interesting because some of the outputs were not fit satisfactorily. The reason for bad fit was thought to be because of over specifying around ATR. It was concluded to relax the constraints around the ATR, because already 4 variables were changing at the same time around it: 1- reformer temperature, 2- reformer outlet temperature, 3- temperature of oxygen to ATR, and 4- reformer pressure. By removing the temperature of oxygen to ATR from the list of the inputs and fixing it to 250°C, the constraints were reduced. The results in the oxygen blown cases with 7 inputs showed improvement comparing to 8 input cases. This conclusion was used in the air blown case to start to build metamodels with 7 inputs. The air blown case showed much smoother results and much better fit unlike the oxygen blown case, although the only difference in the simulation of air blown and oxygen blown is addition of ASU to the oxygen blown case. Further to improve the goodness of metamodel fit, another constraint was removed from ATR which means working with 6 inputs. As a first step, ATR temperature was fixed to 1000°C and metamodels were made. The results showed decrease in Coefficient of Determination (R^2) and therefore the fit became even worse than in 7 input case. Another idea that improved the fit of the metamodel was to fix the temperature of the inlet feed stream to ATR. In this case R^2 had the highest number among all other metamodels in O_2 blown case. Thus, the best fit in oxygen blown case was with 6 input and inlet temperature to ATR fixed.

5.1.1 Kriging Metamodels
The DACE toolbox was used to make the Kriging metamodels. The toolbox provides regression models with polynomials of orders 0, 1 and 2. The user can also supply a new regression model in the form of a function. More details are provided in the user manual of the toolbox [43].

The results are presented according to the number of inputs used. Metamodel results with 8, 7 and 6 inputs are given in the following sections.

Using 8 input variables:

8 inputs → Zero order Regression function → 700, 900

8 inputs → 2nd order Regression function → 700, 900
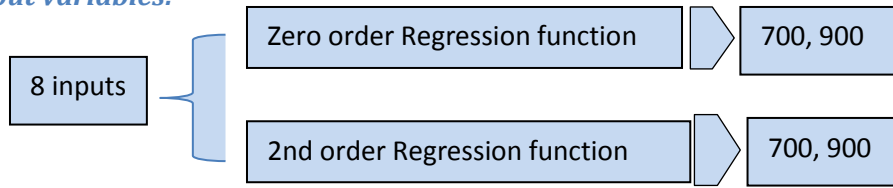
The first metamodels were made for O_2 blown ATR with 8 inputs. For each of the outputs a Kriging model was built and then R^2 was calculated by use of statistical measures as described in chapter 2. As an example, tabulated results for 900 point model are presented here. Figure 5-6 shows calculated Theta parameters for 8 inputs. Figure 5-7 shows calculated Beta parameters in Kriging models. Figure 5-8 gives the variance calculated for each of outputs. Figure 5-9 shows statistical measures used to calculate R^2. The rest of the regression results for all the metamodels are given in Appendix I which accompanies the thesis.

Figure 5-6: Theta parameters for one sample size (22 Metamodels)

	Θ_1	Θ_2	Θ_3	Θ_4	Θ_5	Θ_6	Θ_7	Θ_8
O2 blown- 900 point Kriging model	2.5	0.947323	2.5	1.65	1.09	2.18	0.625	8.71

Figure 5-7: Beta parameters in Kriging models for one sample size

22 Outputs

O2- 900-2nd order- Kriging- Betas

Beta parameters (Kriging model)

y^1	2	3	4	5	6	7	8	9	10	11	12	13	14	15	16	17	18	19	20	21	22
-3.57E-05	0.248649	-0.20811	-0.52601	-0.14972	-0.15283	0.072062	0.032707	0.165397	-0.38755	0.706741	-0.27038	0.307781	-0.38905	-0.03846	-0.04371	0.248417	0.0611	0.117424	0.03807	0.195064	0.001962
8.67E-06	-0.07862	0.790348	0.812883	0.979452	-0.11636	-0.0417	0.012664	0.054764	0.002127	-0.04335	0.02019	0.040205	0.002243	0.998488	-0.57473	-0.07858	-0.01118	-0.00432	0.001826	-0.00623	-0.0209
6.70E-07	-0.15223	-0.11177	-0.06323	-0.13622	0.015953	0.043333	-0.11183	-0.25898	0.284355	-0.21337	0.284785	0.047109	-0.0275	-0.15568	0.013644	-0.02831	-0.0081	-0.06504	0.007624		
1.000004	0.329749	-0.55157	-0.26159	0.021952	-0.98577	0.84007	-0.89656	-0.90261	-0.33839	0.127873	-0.83982	-0.85908	-0.3379	0.013771	0.068724	0.329564	0.546858	-0.05513	0.438222	-0.23782	0.925933
-1.03E-05	-0.26848	-0.00128	0.01029	-0.00046	-0.00089	-0.16818	0.047129	0.165368	0.024553	-0.1378	0.055233	0.126961	0.024433	-7.48E-05	0.791502	-0.26835	0.001763	-0.00325	-0.01472	0.015244	-0.05544
2.85E-05	0.743861	0.000686	0.005035	6.75E-05	0.001344	-0.44839	0.368316	0.11542	-0.65928	0.250562	0.160804	0.274833	-0.65946	5.25E-05	-4.68E-05	0.743448	0.622211	0.199407	0.167352	0.095168	0.071985
-2.11E-05	-0.06493	1.48E-05	-0.00342	0.000215	-0.0005	-0.03724	0.008114	0.033313	0.011665	-0.03922	0.012637	0.02221	0.011498	0.000186	-0.00014	-0.0649	0.000997	-0.00216	-0.00907	0.005606	-0.00922
1.25E-05	-0.00143	0.000551	-0.00987	-0.00018	0.000662	-0.00079	-0.00238	-0.00893	0.009469	-0.17521	0.077638	-0.05986	0.009223	8.26E-05	0.000346	-0.00143	-0.40531	0.968031	0.517293	0.214268	0.089367
-9.69E-06	0.010551	-0.00044	0.001333	-0.00064	0.000301	-0.00711	0.005312	-0.0024	-0.00966	-0.67553	0.31726	-0.20242	-0.01016	5.76E-06	-2.24E-05	0.010543	0.010735	0.002488	-0.69727	0.892235	0.364315
-1.76E-05	-0.00919	0.111141	0.406588	0.149984	-0.01909	-0.00639	0.003537	0.011968	-0.00732	-0.00103	0.001803	0.009844	-0.00743	0.040473	0.017872	-0.00919	0.001988	0.000518	-0.00071	0.000689	-0.0024
-2.59E-05	-0.00763	-0.04576	-0.05043	-0.05681	0.006773	0.006227	-0.00762	-0.01331	0.016941	0.005379	-0.00865	-0.00916	0.017039	-0.00372	-0.01638	-0.00758	-0.00379	0.00168	0.009213	-0.01372	-0.00524
-3.55E-06	-0.01956	0.021534	-0.2579	0.008872	0.008585	0.005328	-0.0037	0.004165	0.004876	0.024262	-0.01234	0.010607	0.0508	-0.00311	-0.07457	-0.01955	-0.00737	0.001799	0.010471	-0.00645	-0.01091
4.25E-05	0.003642	0.001181	-0.01045	0.000669	0.000397	-0.0058	0.001004	-0.00722	0.006466	-0.00167	-0.00022	-0.0044	0.006684	5.75E-05	0.002547	0.003646	0.008803	0.0216	0.002258	-0.00142	0.001129
-7.15E-06	-0.03718	0.000929	-0.00874	0.000865	-0.00023	0.026463	-0.01822	-0.00027	0.029421	-0.014	-0.0058	-0.01138	0.029415	4.00E-05	-7.56E-05	-0.03717	-0.03583	-0.01177	-0.01111	-0.00173	-0.00289
-6.47E-06	-0.00567	0.001062	-0.01159	0.000867	-0.00017	0.001754	-0.00341	-0.00541	0.009659	-0.00162	-0.00322	-0.00547	0.009593	-4.14E-06	0.000141	-0.00566	-0.00352	-0.00131	-0.00471	0.003322	0.00223
-7.11E-06	-0.01945	-0.00024	-0.00899	-0.00017	-0.00065	0.012553	-0.01085	-0.00666	0.021108	0.001389	-0.00963	-0.00835	0.02106	-1.19E-08	-0.00028	-0.01944	-0.01401	-0.00415	-0.00412	-0.00389	-0.00195
1.11E-05	0.018628	-0.00064	0.01173	-0.00043	0.000226	-0.01244	0.008233	-0.00272	-0.01091	-0.00292	0.005784	-0.00068	-0.011	-0.00014	-0.00055	0.018622	0.018997	0.004661	-0.006	0.012738	0.008371
8.20E-07	-0.02644	0.014509	0.012524	0.018293	-0.00276	0.017477	-0.01189	0.005529	0.016558	-0.0168	0.001387	-0.00383	0.016764	0.000562	0.00397	-0.02631	-0.02902	-0.01072	0.002213	-0.01314	-0.01103
1.75E-05	0.053121	-0.00104	0.028342	0.001178	-0.00208	-0.03387	0.036247	0.048038	-0.09562	-0.06039	0.064107	0.03152	-0.09493	0.003613	-0.00455	0.052974	0.021586	-0.00357	0.029071	-0.02559	-0.00865
2.93E-05	-0.00882	0.00071	0.0018	0.000517	0.000511	0.000329	-0.00247	0.00012	0.006695	-0.00524	-0.00142	-0.0025	0.006504	-0.00016	0.003406	-0.00873	-0.00608	-0.00111	-0.00535	0.003205	0.001516
-1.25E-05	0.12119	0.001218	-0.00409	-0.00017	0.002418	-0.03916	0.079746	0.147748	-0.19317	0.0429	0.060491	0.13147	-0.19372	-0.00013	0.000389	0.12086	0.025265	0.020777	0.015948	0.027626	0.002092
-3.32E-06	-0.00098	-0.00092	0.007209	-0.00025	-0.00078	0.001058	-0.00279	-0.00763	0.000927	0.005828	-0.00733	-0.00591	0.008951	4.65E-06	-0.00011	-0.00095	0.003222	0.001828	-0.00539	0.00421	0.003766
1.09E-05	-0.00293	4.54E-05	0.000258	-5.50E-06	0.0001	0.004234	-0.00209	0.000956	0.003628	0.007744	-0.00667	-0.00025	0.003187	5.89E-05	0.000422	-0.00292	-0.00252	0.006369	0.005995	-0.01384	-0.00443
-3.05E-05	-0.00484	0.00063	-0.00175	0.000276	0.000556	0.000629	-0.00323	-0.00718	0.01317	0.002853	-0.00889	-0.00873	0.009688	0.000129	0.000266	-0.00484	-2.17E-05	-0.00141	-0.0257	0.033012	0.013519
1.78E-05	-0.05751	0.082422	0.095867	-0.01808	0.173268	-0.14477	0.082846	0.007963	0.117238	-0.59415	0.326303	-0.13089	0.11763	-0.00225	-0.00277	-0.05749	-0.0261	-0.08337	-0.04286	-0.10199	0.025298
-2.36E-06	-0.00615	0.001003	0.007442	0.000695	0.001047	-0.01801	0.017064	0.022456	-0.03766	0.069987	-0.01971	0.041433	-0.03786	0.000325	0.112414	-0.00614	0.020337	0.018283	0.009583	0.01799	-0.00873
2.69E-05	-0.09237	-0.00026	0.004509	-0.00042	0.000457	0.028174	-0.0786	-0.16825	0.261642	0.064256	-0.12065	-0.11966	0.260977	2.59E-05	-0.00042	-0.09232	0.029902	-0.00166	-0.01848	0.00491	0.012026
-1.54E-05	-0.00218	-3.25E-05	0.007532	-8.50E-05	0.000498	0.006487	0.000514	0.008209	-0.00736	0.021923	-0.00809	0.009994	-0.00758	-0.0018	-0.00029	-0.00218	-0.00719	0.002571	-0.00323	0.008949	-0.00042
-3.20E-06	0.007538	-0.00067	0.010084	-0.00017	-0.00033	-0.00301	0.003196	0.001847	-0.00798	0.043954	-0.01987	0.013119	-0.00841	-2.17E-05	-0.00048	0.007538	-0.04148	0.021579	0.071715	-0.00616	0.005492
1.14E-05	0.000175	0.000831	-0.01288	0.000319	0.000211	0.000146	0.000812	0.004464	-0.0047	0.140601	-0.0695	0.04022	-0.00548	0.000104	0.000364	0.000172	-0.0009	-0.00294	-0.10657	0.087047	0.055681
8.78E-06	-0.00879	0.000689	0.001044	-8.67E-05	0.001363	-0.00636	-0.00019	-0.00328	0.010999	-0.01094	0.000689	-0.00584	0.010704	-3.22E-06	0.018072	-0.00878	0.002467	-0.00017	-0.00584	0.001472	0.002393
-1.24E-05	0.023428	0.000224	-0.00183	2.39E-05	0.000241	-0.00198	0.01092	0.01415	-0.02572	0.01448	0.006771	0.01605	-0.0256	-3.12E-05	0.000143	0.023423	0.011027	0.000349	0.007837	0.001246	-0.00117
3.31E-07	0.002864	0.000854	-0.00283	0.000109	0.001127	-0.00028	-0.00048	-0.00501	0.00307	-0.00668	0.002535	-0.00561	0.003101	-6.57E-05	-5.53E-05	0.002856	0.004542	-0.0008	-0.00018	-0.00238	0.00108
4.99E-07	0.005823	0.000123	-0.00367	-0.00035	0.000545	-0.0033	0.002727	9.39E-05	-0.00346	0.005062	0.00088	0.003647	-0.00325	0.000106	-0.00013	0.005816	0.007056	0.000444	0.004282	-0.00148	-0.00227
-8.78E-06	-0.00806	0.000954	-0.0093	0.000629	0.000136	0.002499	-0.00153	0.0508	-0.00133	-0.03181	0.013944	-0.00632	-0.00129	1.37E-05	0.000251	-0.00805	-0.01091	-0.00357	-0.00279	-0.0066	-0.00097
1.50E-05	-0.14437	9.95E-05	0.000513	-0.00088	0.068027	-0.10944	-0.19695	0.253804	-0.05464	-0.08268	-0.18199	0.254007	-9.39E-05	0.000129	-0.14429	-0.002	-0.02877	-0.03069	-0.0341	0.00645	
-1.64E-05	-0.00994	0.00113	-0.00332	0.000633	0.000764	0.000317	-0.00185	-0.00096	0.006358	0.002081	-0.00089	0.002156	0.006775	-0.00011	-6.22E-05	-0.00993	-0.00261	-0.00208	0.00877	-0.00765	-0.00758
1.08E-05	0.010111	-0.00097	0.004611	-0.00058	-0.0005	-0.00517	0.00507	0.002625	-0.01451	-0.00628	0.009149	0.003457	-0.01409	-0.0001	3.50E-05	0.01011	0.001626	-0.00539	0.012094	-0.00288	0.000455
-1.50E-05	0.014057	-0.00031	-0.00699	0.000744	-0.00206	-0.00622	0.002972	-0.00817	-0.00345	-0.00053	0.005216	-0.00084	-0.0028	0.000177	-2.63E-05	0.014046	0.019394	0.005717	0.005106	-0.01548	0.000839
5.22E-06	0.011062	0.000824	-0.0034	-0.00036	0.001775	-0.00843	0.007837	0.006294	-0.01579	-0.00316	0.008523	0.006652	-0.01569	7.59E-06	0.000372	0.011043	0.007903	0.000915	0.004635	-0.00116	-0.00065
-1.44E-06	0.039356	-0.00026	-0.00439	-0.0003	-0.00022	-0.02206	0.019533	0.008543	-0.03902	0.02202	0.006814	-0.03868	2.24E-05	-0.00019	0.039336	0.031836	0.010583	0.012611	0.005299	0.000786	
-1.66E-05	0.010124	-3.63E-05	-0.00205	0.000623	-0.00113	0.005724	0.010018	-0.01818	0.00106	0.008268	0.009814	-0.01784	-8.62E-05	4.26E-05	0.010118	0.003355	0.001321	0.009448	-0.01152	-0.00432	
1.71E-05	-0.00688	-0.00038	-0.00215	0.000547	-0.00161	0.007848	-0.00301	0.007304	-0.00029	0.00867	-0.00281	0.008046	8.81E-05	-0.00012	-1.61E-05	-0.00687	-0.01418	0.005014	0.013388	-0.01135	-0.00845
1.46E-06	0.001376	0.000246	0.001969	-0.00055	0.00137	-0.00297	0.0094	-0.00249	0.001145	-0.02768	0.015779	-0.00645	0.001716	8.66E-05	0.000282	0.001378	0.003893	-0.00048	0.00072	-0.00206	-4.16E-05
-9.31E-06	-0.00129	0.000323	0.008699	-0.00012	0.001217	-0.00257	0.001619	0.002376	0.001255	-0.03351	0.020221	-0.00379	0.001849	-5.00E-05	-0.00044	-0.00129	-0.00205	-0.00098	0.020704	-0.03391	-0.01204

Figure 5-8: Calculated variance for outputs

22 Outputs

Sigma 2 (Variance)

Outputs	1	2	3	4	5	6	7	8	9	10	11	12	13	14	15	16	17	18	19	20	21	22
Sigma 2 (Variance)	10.9451357	281421.4	8.15E-09	1.64E-09	6.82E-08	3.58E-06	5.84E-06	4.14E-05	2.72E-05	8.59E-05	9.43E-06	1.44E-05	6.34E-05	8.59E-05	3.84E+10	1.7E+12	3611679	1.22E+16	13.85018	7.58E+14	21.38597	7.61E+14

Figure 5-9: Statistical measures to calculate R^2

22 Outputs

Statistical measures

O2 blown- Kriging- 8input-2nd order regression function (900)																						
Out put No.	1	2	3	4	5	6	7	8	9	10	11	12	13	14	15	16	17	18	19	20	21	22
SSE	2089.682	82460426	2.33548E-06	4.68E-07	1.81E-05	0.000772	0.001583	0.013995	0.011409	0.033012	0.001383	0.006113	0.020795	0.033016	4.98E+12	2.89E+14	1.06E+09	2.79E+18	3145.41	1.17E+17	3419.575	8.71E+16
SSR	1.23E+10	2.74E+08	0.005703695	1.13E-05	0.077332	1.33935	0.016777	0.168172	0.164503	0.086144	0.024288	0.110897	0.274931	0.086183	1.41E+18	8.03E+18	3.52E+09	1.74E+19	198753.8	7.07E+18	263094.3	2.57E+19
SST	1.23E+10	3.57E+08	0.00570603	1.18E-05	0.07735	1.340122	0.01836	0.182167	0.175912	0.119156	0.025672	0.117011	0.295726	0.119199	1.41E+18	8.03E+18	4.58E+09	2.02E+19	201899.2	7.19E+18	266513.9	2.58E+19
R2 (2nd order-8 Inputs)	1	0.76882	0.999590701	0.960328	0.999766	0.999424	0.913789	0.923172	0.935144	0.722952	0.946122	0.947754	0.929683	0.723019	0.999996	0.999964	0.769044	0.862096	0.984421	0.983714	0.987169	0.99662

As described in Chapter 2, different regression functions can be used in creating Kriging models. Two types of regression functions were used to investigate which one provides better fit: Zero order and second order Polynomial. As Figure 5-10 shows, 2nd order regression function gives better fit to the data. So, this type of regression function was used for all the Kriging models.

Figure 5-10: O_2- Kriging Zero order Vs. 2nd Order (900)
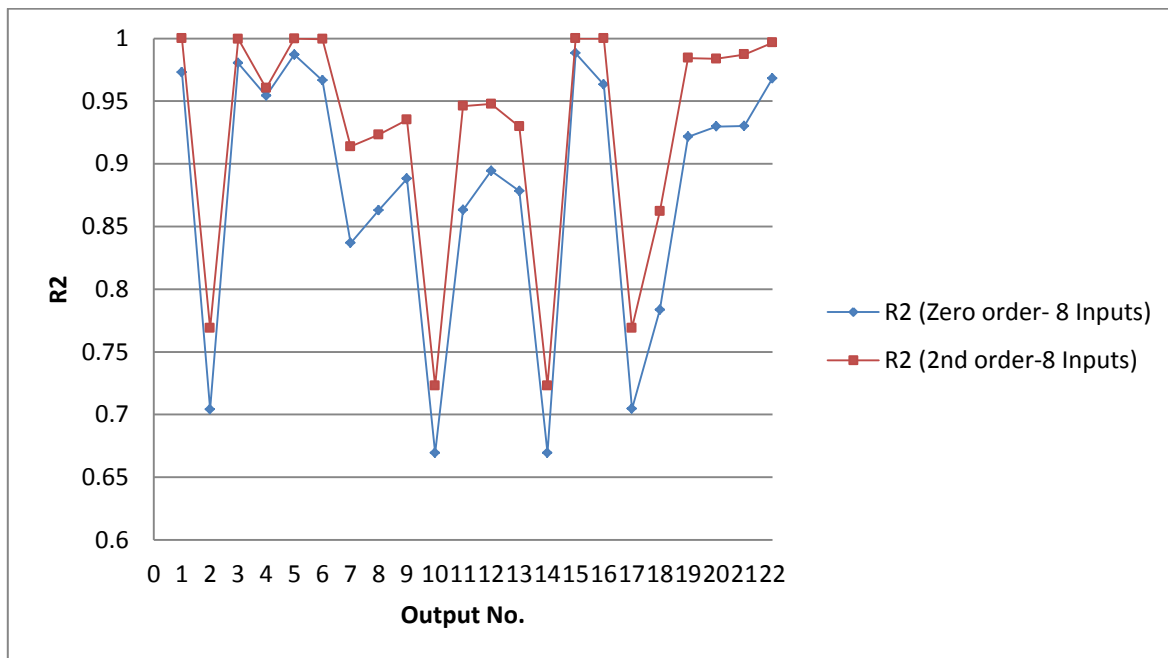
The 900 point model result is shown in Figure 5-11. R^2 above 0.95 is considered to be a good fit and it means that the model takes into account 95 % of the variations in data. As is shown in the Figure 5-11, some of the output variables with poor performance than others in terms of being fit with the metamodel and are listed in Table 5-7. The same behavior is observed in the Polynomial model. Possible reasons for bad behavior of these outputs are given in section 5.3.

Figure 5-11: O_2- Kriging 900 point model
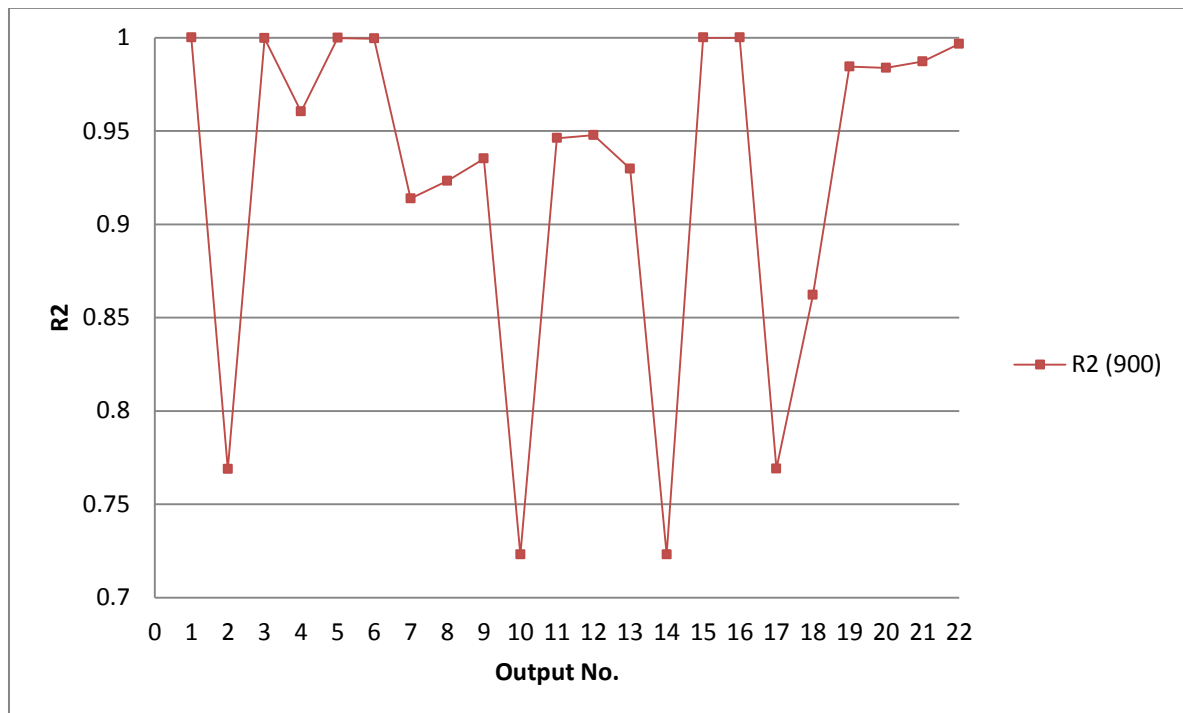
Table 5-7: Outputs with poor performance in metamodel

Output No.	Variable
2	Oxygen to reformer (O_2 flow)
10	CH_4 concentration in ATR outlet
14	CH_4 concentration in LTS outlet
17	Oxygen compression work
18	Reformer product cooling

In order to see the effect of increasing the sample points in model building step for Kriging model, 700 and 900 point models are compared in Figure 5-12. Slight improvement to the fit especially for the misbehaving outputs is observed.

Figure 5-12: O_2- Kriging- 700 vs. 900 point model
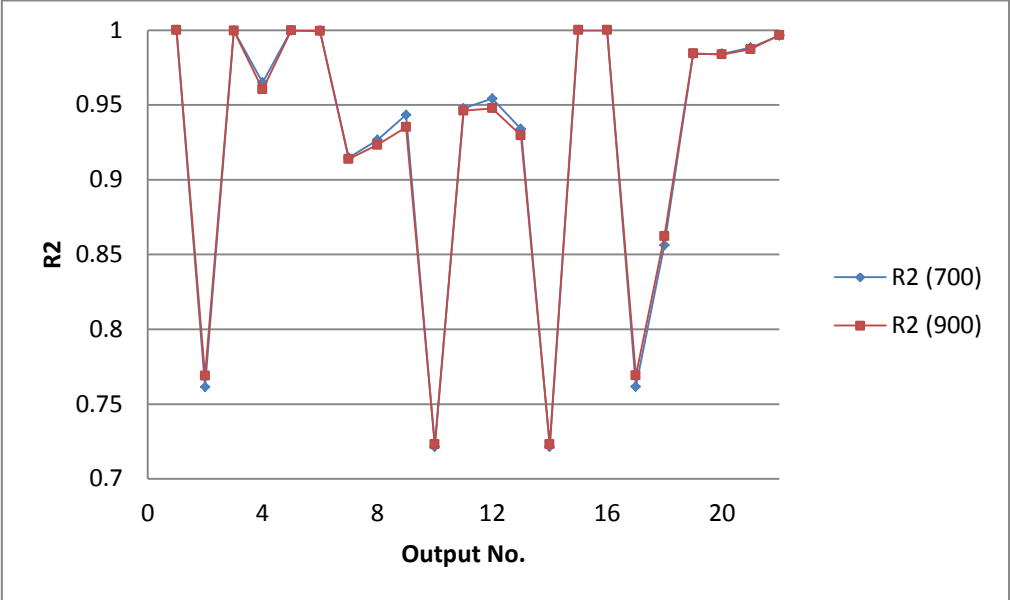
When the unexpected behavior of metamodel in fitting the data was observed, it opened new doors to search for the possible improvements to the fit. The constraints around the ATR were: O_2 temperature to ATR, Reformer temperature, Reformer inlet temp and pressure of the system. In order to ease the constraints to improve the fit, O_2 temperature was decided to be fixed to 250°C. So the number of inputs reduced to 7.

Reducing the inputs from 8 to 7, improved the metamodel fit. For comparison, 900 point model is shown in Figure 5-13.

Figure 5-13: O_2- Kriging- 7 vs. 8 Inputs (900)
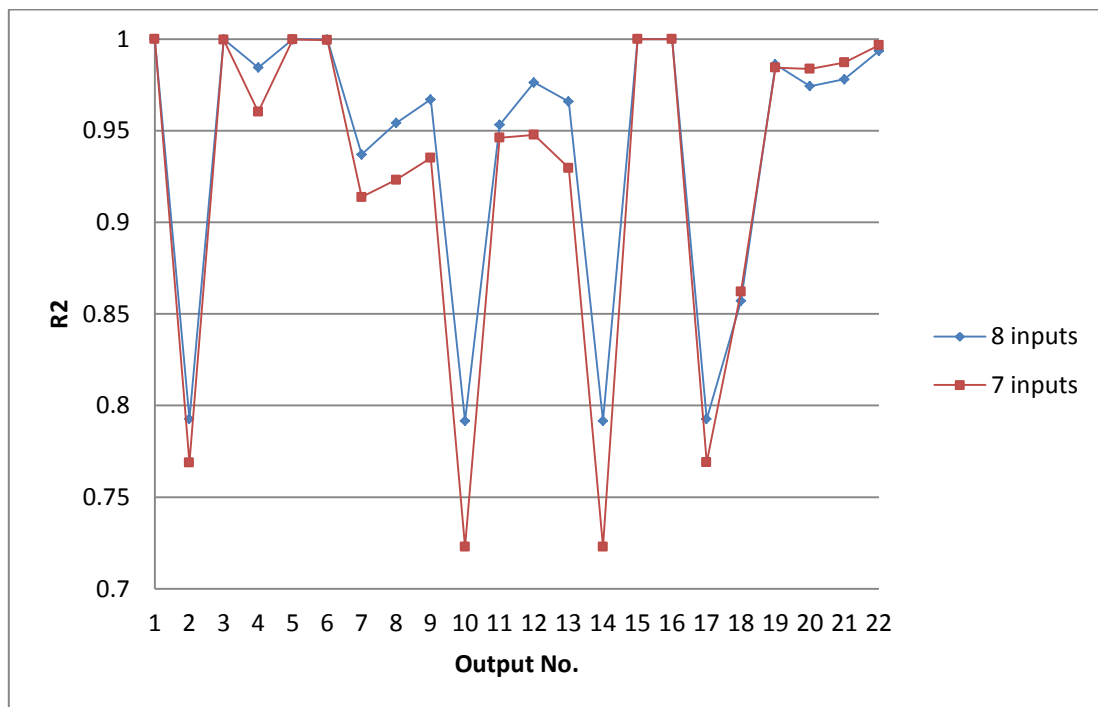
In order to investigate the effect of sample size, metamodels were made for six different sample sizes.

| Oxygen Blown ATR (Kriging model) | 7 inputs | 600, 700, 800, 900, 1000, 1100 |
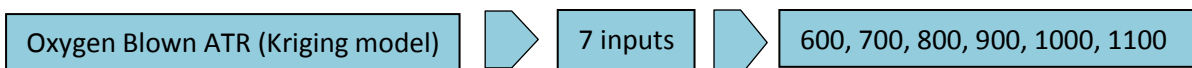
The results of the built Kriging models for these sample sizes are shown in Figure 5-14. The models demonstrate almost similar behavior and not a special pattern can be discerned from the graph.

Figure 5-14: O_2- Kriging-(600,700,800,900,1000, 1100)
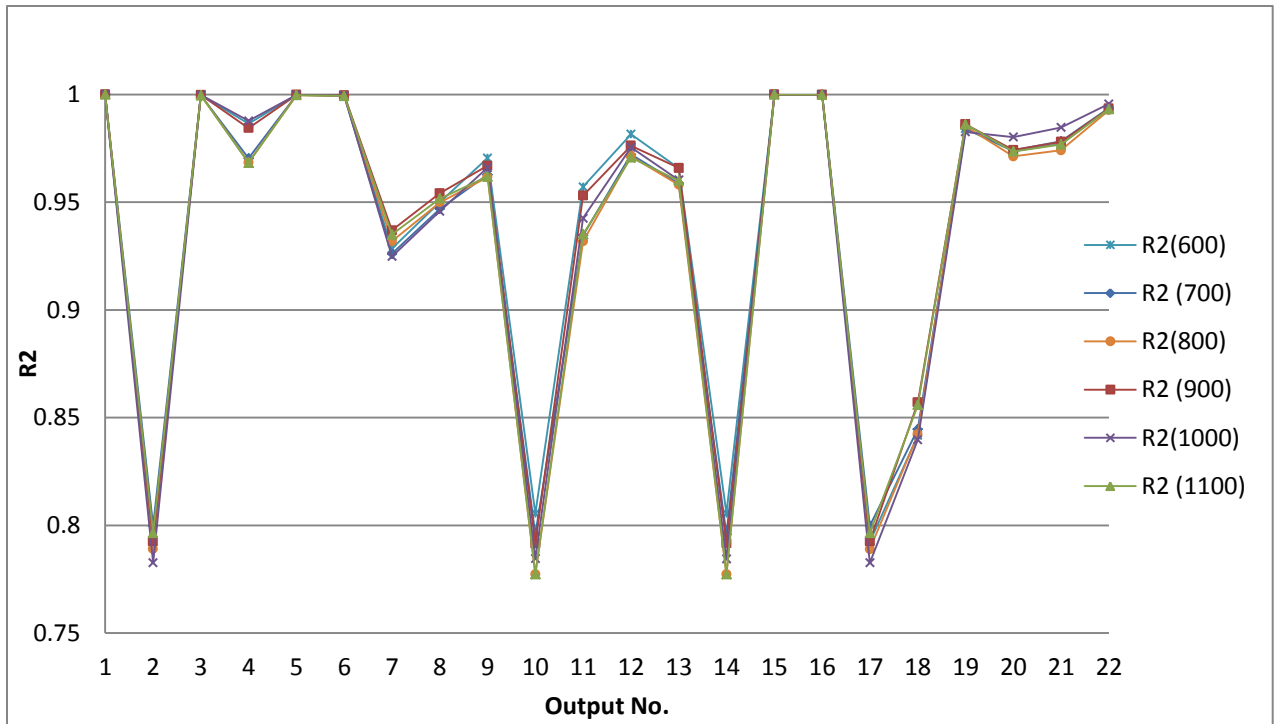
For each of the sample sizes, R^2 average was made according to the following equation:

$$R^2{}_{average} = \frac{\sum_{i=1}^{22} R_i{}^2}{22}$$

Equation 5-1

Figure 5-15 shows R^2 average for the 6 different sample sizes. No discernible pattern can be observed although one expects improvement to the metamodel fit by increasing the sample size. Average R^2 for all the sample sizes are close to each other and differ only in parts of thousands, as the vertical axis of the figure shows. Several researchers also observed the same behaviors towards increasing the sample size. Simpson et al. [27] while comparing Experimental design and metamodel types observed discrepancies among some of their sample sizes. They suggested that the reason is due to over fitting of the function because of its smooth behavior and if it was more nonlinear, taking more points would increase R^2. Laurenceau and Sagaut [54] also observed fluctuations in error of the metamodels by increasing sample sizes.

Figure 5-15: R^2 average O_2 Blown case (Kriging Model)
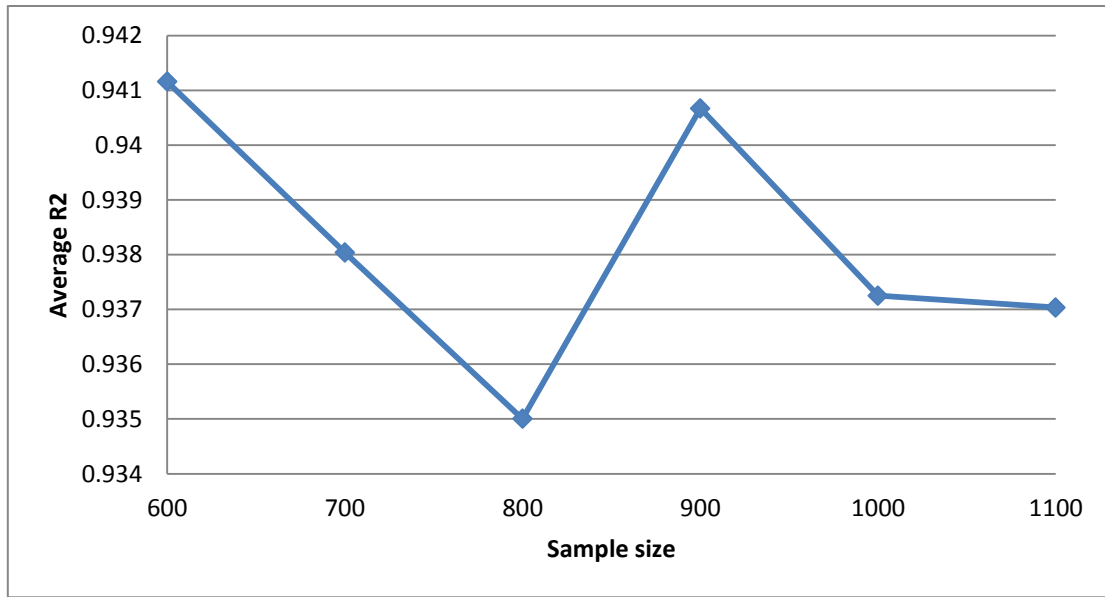
Using 6 input variables:
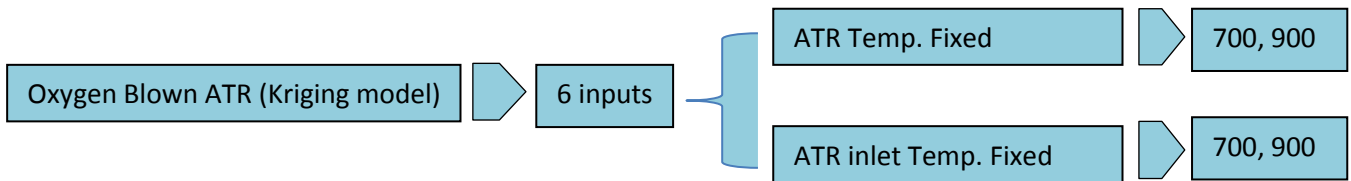
Improvements observed by moving from 8 to 7 inputs, gave this idea that by reducing the number of constraints around ATR, the metamodel fit increases. It is worthwhile to further reduce the number of constraints around ATR. As a first try, ATR temperature was fixed to 1000°C and metamodels were built for two sample sizes, 700 and 900 points. Figure 5-16 shows the results for these two cases. The results of keeping ATR temperature constant show deterioration in metamodel fit.

Figure 5-16: O$_2$- Kriging- 700 vs. 900 point model- 6 inputs with ATR Temp. Fixed
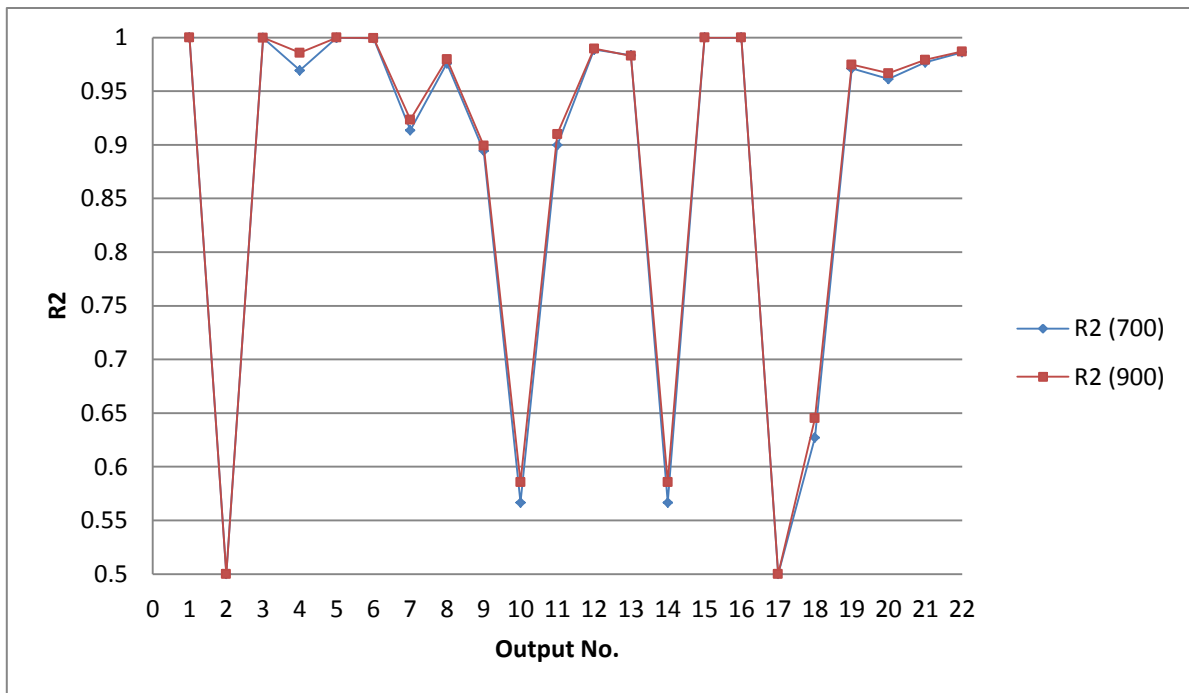
For the sake of comparison, the results with 6 inputs with ATR temperature fixed and 7 inputs for 900 point model is given in Figure 5-17. It shows how poor the metamodel fit becomes.

Figure 5-17: O$_2$- Kriging- 6 (ATR Temp. Fixed) vs.7 Inputs (900)
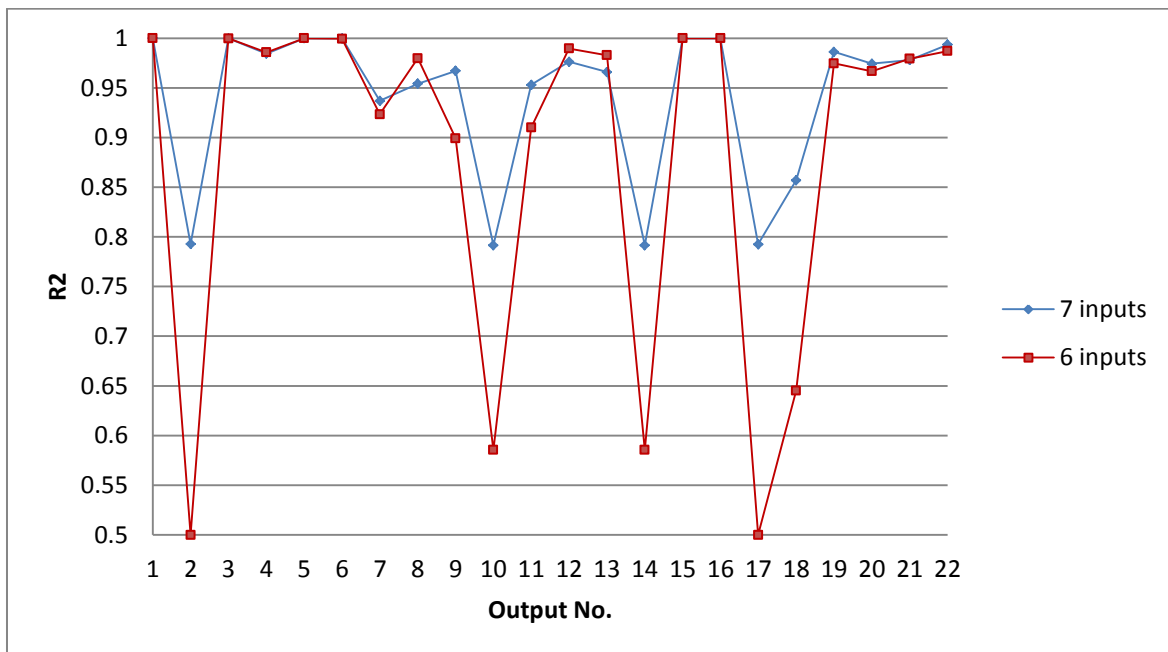
To further investigate which of the constraints around the ATR is causing the misbehavior of metamodel, it was decided to keep ATR inlet temperature constant instead of ATR

temperature. ATR inlet temperature was fixed to 450°C and then metamodels were built for 700 and 900 points. The metamodel fit improved a lot as is shown in Figure 5-18. In fact the best metamodel fit for oxygen blown ATR is in this case. It can be concluded that one cause for bad behavior of metamodel fit is ATR inlet temperature.

Figure 5-18: O_2- Kriging- 6 (ATR Inlet Temp. Fixed) vs.7 Inputs (900)
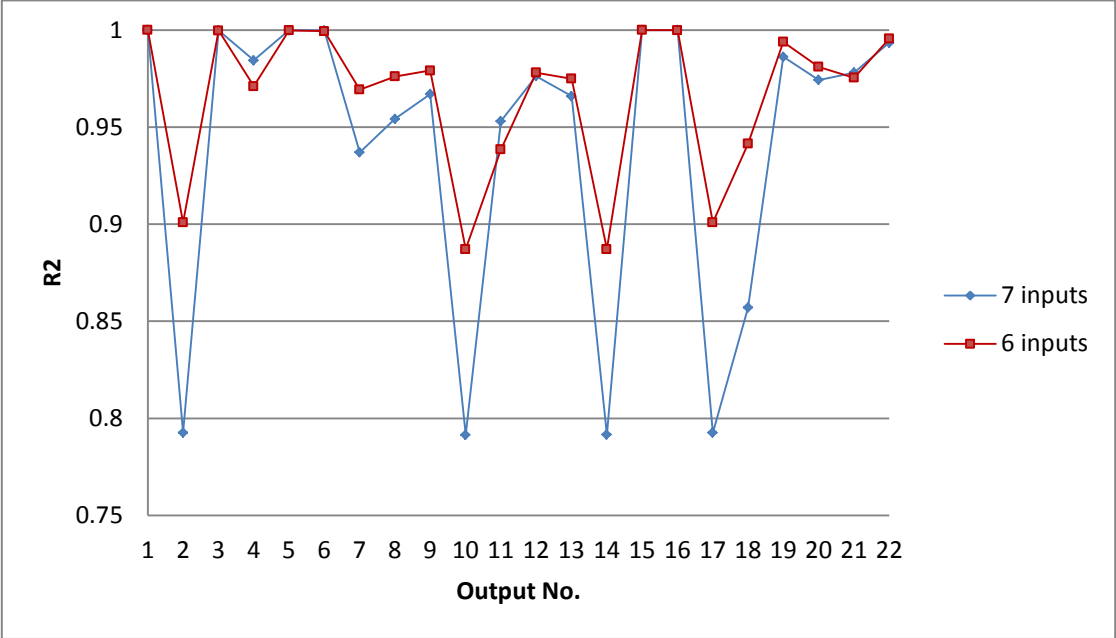
5.1.2 Polynomial Metamodel

Polynomial models were made by use of Surrogate toolbox in MATLAB [53]. As Figure 5-19 shows, the results are presented according to the number of inputs in metamodel.

Figure 5-19: Overview of presentation of results
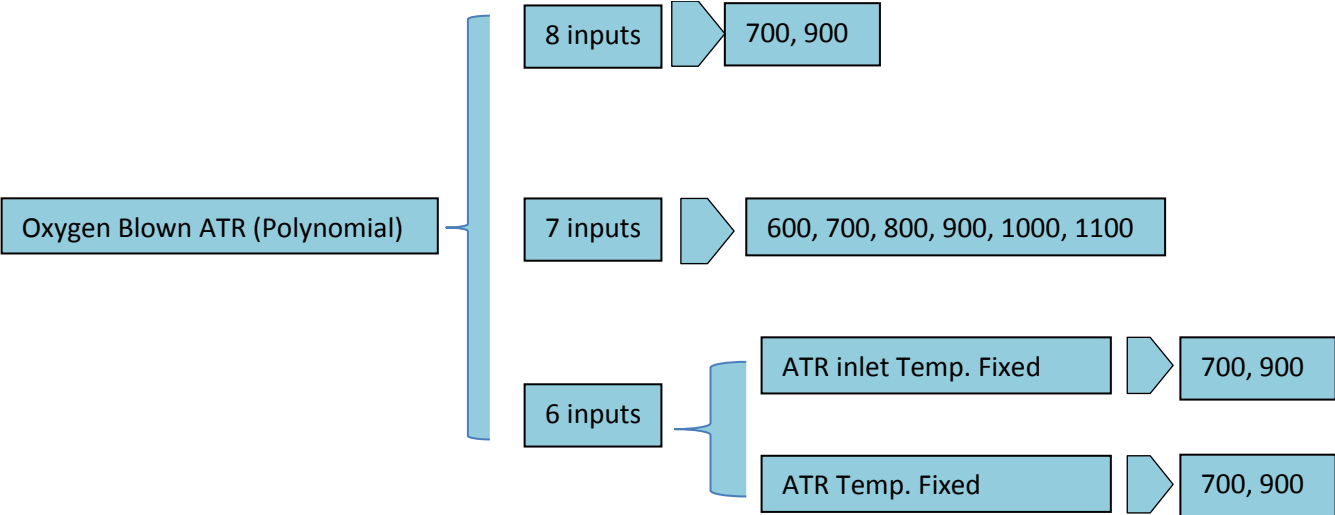
The magnitude of the coefficients in Polynomial metamodels indicate the importance of the corresponding term and the bigger effect it has on the output of the model.

Using 8 input variables:

Oxygen Blown ATR (Polynomial) → 8 inputs → 700, 900
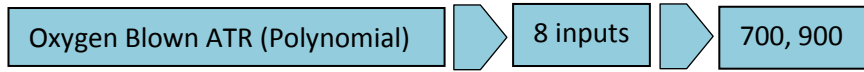
Two polynomial metamodels were made for the 8 input case. The second order polynomial models have $k = \dfrac{(n+1)(n+2)}{2}$ coefficients for n input variables. As an example, tabulated regression results and Beta parameters for 900 point model are presented in Figure 5-20 and Figure 5-21. The rest of the regression results for all the metamodels are given in Appendix I which

Figure 5-20: Statistical measures to calculate R2

Statistical measures — 22 Outputs

O2 blown-Polynomial model (8 inputs) 900

Output No.	1	2	3	4	5	6	7	8	9	10	11	12	13	14	15	16	17	18	19	20	21	22
SSE	2033.693	80963474		2.49932E-06	5.14E-07	1.96E-05	0.0000835	0.001558	0.013634	0.010679	0.031522	0.001428	0.005938	0.020053	0.031524	5.44E+12	3.22E+14	1.04E+09	2.73E+18	3102.415	1.18E+17	3397.146	8.68E+16
SSR	1.23E+10	2.73E+08	0.005704265	1.14E-05	0.077363	1.33941	0.016799	0.16819	0.164168	0.083846	0.024559	0.111778	0.273668	0.083885	1.41E+18	8.03E+18	3.51E+09	1.74E+19	199032.6	7.09E+18	262113.8	2.57E+19
SST	1.23E+10	3.54E+08	0.005706765	1.19E-05	0.077383	1.340245	0.018357	0.181824	0.174848	0.115368	0.025987	0.117716	0.29372	0.115409	1.41E+18	8.03E+18	4.55E+09	2.01E+19	202135.1	7.21E+18	265511	2.58E+19
R2=SSR/SST	1	0.771221	0.999562042	0.956744	0.999747	0.999377	0.915151	0.925016	0.938921	0.726772	0.94506	0.949555	0.931728	0.726848	0.999996	0.99996	0.77144	0.864437	0.984652	0.983643	0.9872205	0.99663

Figure 5-21: Regression parameters in Polynomial models

Regression Coefficients — 22 Outputs

900 point- 8 inputs

|	1	2	3	4	5	6	7	8	9	10	11	12	13	14	15	16	17	18	19	20	21	22
1	23.02687287	-45785.89761	0.036461522	0.00029188	0.007751625	0.838078533	0.281665994	-0.733771507	-0.95298035	1.705360532	0.087366813	-0.51944168	-1.11476997	1.709197655	-22823513	56467928.1	-164018.9811	-559058426.6	-119.0099293	-8.7E+08	-392.8606452	-426778002.5
2	0.02469536	13.44364227	-2.00E-05	-7.31E-06	-0.000103181	3.70E-05	-6.27E-05	0.000155959	4.48E-05	-0.000203296	1.44E-05	8.25E-05	0.000127852	-0.000202981	698933.8289	-1238214.797	48.15565662	2340391.557	0.081534402	449194.7	0.02848224	331802.5101
3	0.03085897	-4.218364541	-1.98E-07	1.69E-08	-4.55E-06	9.46E-06	-7.09E-05	-0.00014128	0.000127864	-9.88E-06	-4.83E-05	-0.000155318	0.000128426	7489.685737	3210.371991	-15.11751349	-74833.85626	-0.01687042	-91902	-0.023312275	42872.54076	
4	19388.1348	6485.544264	-0.016678327	0.000113998	0.004456355	-0.42950876	0.03740019	-0.030369298	0.10180947	-0.255012582	0.042145603	-0.03093989	0.113391245	-0.254300888	6141682.662	-38751403.55	23242.38804	344233771.8	19.39979605	3.24E+08	-3.340609108	330072013.2
5	-0.020490929	-8.874094214	-2.81E-06	5.10E-07	-2.45E-06	-4.33E-05	1.67E-06	-7.77E-05	-3.27E-05	0.000119454	-4.39E-05	-3.04E-05	-7.52E-05	0.000119638	1082.924552	573567.7367	-31.82699219	-1163885.843	-0.042729886	-287299	-0.00959423	-105136.9853
6	-0.041540745	114.5530563	-7.61E-07	9.66E-07	-7.32E-06	4.52E-05	-0.000460557	0.00026791	0.00329048	-0.003391033	0.000341011	0.001242093	0.004052773	-0.003395734	5762.268985	-16863.30047	410.4737398	2790588.486	0.637832331	3265994	0.792456394	-929435.5761
7	0.93470831	-4.567056516	-1.86E-06	3.65E-07	-2.84E-06	-2.05E-05	1.97E-05	-6.17E-05	-2.40E-05	8.83E-05	-3.26E-05	-2.34E-05	-9.93E-05	8.60E-05	2914.833268	249.1070572	-16.36529761	-920728.5048	-0.02434782	-547424	0.031370232	399365.8931
8	-0.092823876	-4.606350661	3.18E-06	9.92E-09	2.56E-06	6.11E-05	-1.36E-06	-5.52E-05	-0.0001252	0.00016731	-9.89E-05	-0.000290182	0.000159658	5155.041433	6227.287016	-16.51614674	-1063581.85	0.640154248	-925147	0.485349619	2015030.705	
9	0.08289895	-7.836609765	-9.88E-07	4.24E-07	-5.49E-06	1.83E-05	4.35E-05	-7.36E-05	6.30E-05	5.91E-05	-9.33E-05	1.10E-05	-0.0001594015	5.04E-05	-6451.481279	1568.720976	-28.0742522	-2429696.555	-0.048769665	-2171085	0.948823194	1723327.554
10	-2.87E-05	-0.002037092	1.21E-07	1.95E-08	5.67E-07	-2.96E-07	-1.30E-08	2.15E-08	-2.97E-08	-1.68E-10	7.19E-08	-1.68E-10	6.03E-08	-3.01E-08	648.596139	670.7127544	-0.007303423	186.3353878	5.40E-06	-14.7791	6.19E-06	-154.8488364
11	-4.73E-06	-0.00019628	-6.23E-09	-3.01E-10	-2.69E-08	1.30E-08	1.36E-09	-5.25E-09	-9.32E-09	8.26E-09	1.47E-09	-4.84E-09	-8.33E-09	8.32E-09	-7.451707737	-77.07680838	-0.000699068	-20.13278576	-1.15E-06	39.6579	-1.29E-05	-61.83147086
12	-0.000662126	-0.802824158	4.18E-06	-2.20E-06	5.97E-06	2.37E-05	1.56E-06	-3.42E-06	4.04E-06	3.26E-06	9.87E-06	-1.05E-05	1.45E-05	3.41E-06	-8877.26663	-500556.6078	-2.8760344	-64976.32157	0.002411782	67293.32	-0.008284616	-131000.3885
13	6.10E-05	0.000597877	1.36E-09	-5.09E-10	2.65E-09	7.08E-09	-1.02E-08	2.39E-09	-4.49E-08	3.39E-08	-4.65E-09	-2.78E-09	-3.86E-08	3.40E-08	0.70775734	96.3022409	0.002146664	471.8698527	1.22E-05	74.56964	-1.29E-05	66.2691985
14	-1.12E-05	-0.011065445	1.30E-09	-5.52E-10	4.27E-09	-5.43E-09	6.20E-08	-1.31E-07	2.50E-09	1.49E-07	-3.62E-08	-3.42E-08	-9.78E-08	1.49E-07	0.860185258	3.795095526	-0.039647421	-2577.822288	-9.03E-05	-468.143	-1.39E-05	-252.4018284
15	-7.11E-06	-0.001116637	9.39E-10	-4.46E-10	2.65E-09	-2.01E-09	2.62E-09	-1.65E-08	-2.56E-08	3.37E-08	-2.59E-09	-1.30E-08	-3.35E-08	3.35E-08	-0.045816339	5.290165458	-0.003995772	-161.5278535	-6.58E-06	-129.379	1.93E-05	119.4722103
16	-1.68E-05	-0.007742918	-6.08E-10	-6.45E-10	-1.27E-09	-1.83E-08	3.91E-08	-1.05E-07	-6.12E-08	1.46E-07	6.94E-09	-7.62E-08	-9.87E-08	1.46E-07	-0.04682193	-19.56865486	-0.02773961	-1343.811524	-4.16E-05	-229.648	-4.46E-05	-226.8409499
17	3.06E-05	0.008210838	-1.28E-09	9.92E-10	-3.31E-09	7.62E-09	-4.23E-08	8.88E-08	-2.40E-08	-8.75E-08	-1.36E-08	5.29E-08	-7.23E-09	-8.82E-08	-3.645217495	-35.66659556	0.02942266	1981.953625	5.14E-05	-319.601	0.000147794	963.0517994
18	-2.14E-09	-9.01E-05	2.47E-10	9.80E-12	1.08E-09	-6.42E-10	4.76E-10	-9.82E-10	5.33E-10	9.38E-10	-5.75E-10	1.65E-10	-3.77E-10	9.51E-10	0.13816754	2.309601024	-0.00321356	-24.21720541	-9.82E-07	1.244967	-1.41E-06	-11.08192822
19	0.000624474	0.287199678	-2.60E-08	3.12E-08	9.80E-08	-7.08E-07	-1.43E-06	4.78E-06	6.10E-06	-9.00E-06	-3.02E-06	6.80E-06	5.22E-06	-8.94E-06	1289.961685	-3831.70296	1.02662391	27849.17074	-0.00050734	22172.71	-0.00412834	-12728.8778
20	5.47E-06	-0.000310511	8.64E-11	1.37E-11	1.91E-10	1.13E-09	3.11E-10	-2.48E-09	-3.42E-10	4.43E-09	-1.78E-09	-9.42E-10	-1.34E-09	4.33E-09	-0.343741998	15.89837507	-0.001130907	-52.79913004	-1.22E-06	-25.1769	2.51E-06	12.08078179
21	-3.23E-06	0.004490529	2.02E-10	-3.22E-11	-2.28E-10	5.76E-09	-1.11E-08	7.24E-08	1.30E-07	-1.25E-07	1.49E-08	4.40E-08	1.52E-07	-1.26E-07	-0.318220955	2.88823865	0.016051908	209.189162	1.96E-05	83.8063	3.13E-05	18.72405682
22	-5.44E-07	-3.78E-05	-1.19E-10	3.97E-11	-1.41E-10	-1.28E-09	2.76E-10	-1.68E-09	-3.83E-09	3.73E-09	1.17E-09	-3.28E-09	-4.09E-09	3.60E-09	0.021691668	-0.489948286	-0.00011328	12.73896829	9.70E-07	-18.8244	2.90E-06	24.1653051
23	3.31E-06	-0.000122243	2.89E-11	-9.32E-12	2.87E-11	3.50E-10	1.58E-09	-2.23E-09	1.49E-09	2.64E-09	3.63E-09	-6.33E-09	1.89E-10	2.26E-09	0.206378701	3.299628585	-0.00043732	-26.25692121	8.49E-06	42.78578	-2.03E-05	-60.79139214
24	-9.48E-06	-0.000215975	1.77E-10	-2.65E-11	3.04E-10	1.90E-09	1.14E-10	-3.58E-09	-8.19E-09	8.31E-09	1.41E-09	-8.50E-09	-1.29E-08	7.78E-09	0.44132619	2.226274328	-0.00077358	5.077966715	-1.78E-06	-179.964	4.90E-05	186.2803323
25	0.711794812	-453.8118945	0.002855758	0.000145816	-0.002185131	0.065517561	-0.008772439	0.015540665	0.001333	0.019937279	-0.042107853	0.049263611	-0.031159068	0.015590962	-1144178.615	-3333088.739	-1626.163219	-49473935.58	-16.62334201	-4.8E+07	-23.69348315	55267264.16
26	-0.001215377	-0.291572677	2.10E-07	6.62E-08	5.03E-07	3.10E-06	-6.06E-06	1.79E-05	2.31E-05	-2.81E-05	2.76E-05	-1.65E-05	5.55E-05	-2.83E-05	-683.7902991	754678.7552	-1.044612444	20361.3.6245	0.020153329	58977.51	0.023549652	-107586.5789
27	0.009274043	-4.966867871	-5.64E-08	5.06E-08	-3.50E-07	1.75E-06	1.18E-05	-0.000103442	-0.00021286	0.00024587	3.18E-05	-0.00012723	-0.000190035	0.000204917	81.21630354	-3859.156278	-17.79508017	398143.0106	-0.002157954	-139166	0.007310294	180335.1452
28	-0.03328866	-0.091672183	1.59E-09	-4.96E-08	-5.88E-08	1.31E-06	1.80E-06	3.45E-07	6.71E-06	-4.28E-06	6.62E-06	-5.16E-06	1.04E-05	-4.41E-06	-424.0054481	1422.360395	-0.129580711	-62870.05763	0.002048835	-145344.5	0.008667121	-6307.293535
29	-0.000989171	0.509941211	-2.18E-07	1.37E-07	-2.39E-07	-1.32E-06	-1.56E-06	5.54E-06	3.98E-06	-1.01E-05	2.92E-05	-2.80E-05	3.02E-05	-1.06E-05	-58.81495921	5168.832669	1.827745725	-732576.9748	0.039804774	744256.7	-0.013342271	106223.4137
30	0.004881135	-0.074529489	3.01E-07	-2.08E-07	2.53E-07	1.95E-06	3.41E-07	5.37E-07	6.89E-06	-4.15E-06	9.32E-05	-9.87E-05	8.94E-05	-5.07E-06	557.3575494	4562.808551	-0.267760157	-30102.00875	-0.006013748	-1096694	0.187636633	1112117.194
31	1.28E-05	-0.002022855	7.09E-10	7.88E-11	-2.99E-10	2.05E-08	-1.26E-08	-3.63E-11	-2.89E-08	4.49E-08	-2.25E-08	2.51E-09	-4.11E-08	4.37E-08	-0.08625973	679.3627531	-0.007244293	172.9498004	3.95E-08	-191.442	1.19E-05	158.0336383
32	-2.34E-05	0.006734569	4.26E-10	-1.46E-10	2.15E-10	6.30E-09	-2.86E-09	7.92E-08	1.05E-07	-1.34E-07	3.60E-08	4.30E-08	1.48E-07	-1.33E-07	-0.56274571	8208.249173	0.024134247	696.5975737	2.40E-05	316.9857	8.62E-06	-103.6969613
33	1.75E-06	0.000256921	8.22E-10	-1.01E-10	5.22E-10	1.48E-08	6.56E-10	-5.80E-09	-2.53E-08	1.61E-08	-1.21E-08	7.42E-09	-3.73E-08	1.62E-08	-0.949196866	-1.832336184	0.00091633	160.1484733	-5.61E-06	-11.3655	-1.45E-05	49.63467682
34	1.90E-06	0.002218998	2.44E-10	-3.15E-10	-2.24E-09	1.45E-08	-9.67E-09	2.45E-08	-9.56E-10	-2.05E-08	1.63E-08	7.57E-09	-1.98E-08	-1.92E-08	2.994965194	-7.03950199	0.007942153	663.2544551	2.88E-06	246.6406	-2.28E-05	-260.6508419
35	-1.96E-05	-0.003910188	1.79E-09	-7.75E-10	4.05E-09	3.74E-09	7.41E-09	-1.21E-08	5.30E-08	-1.48E-08	-1.20E-07	1.15E-07	-7.61E-08	-1.46E-08	0.551800806	17.75214335	-0.001106781	-1048.190209	-3.74E-05	-167.235	-8.00E-05	-98.05291266
36	3.13E-05	-0.054636436	1.60E-10	-3.26E-10	3.25E-09	-2.26E-08	2.03E-07	-1.01E-06	-1.74E-06	1.67E-06	-1.88E-07	-6.31E-07	1.46E-07	1.67E-06	-2.430369801	7.430726901	-0.195734974	-168.8955085	-0.000279004	-1688.44	-0.000382951	709.9991136
37	-2.17E-05	-0.002474879	1.25E-09	-1.42E-10	2.69E-09	1.08E-08	1.17E-09	-1.12E-08	-2.69E-09	2.56E-08	4.10E-09	-3.78E-09	1.72E-08	2.73E-08	-1.690347792	2.049198105	0.018510753	171.82707	-7.13E-05	876.8633	-5.40E-05	-506.9398772
38	3.56E-05	0.005164341	-2.13E-09	4.29E-10	-4.54E-09	-1.54E-08	-2.03E-08	6.42E-08	3.71E-08	-1.31E-07	-3.06E-08	9.34E-08	5.75E-08	-1.27E-07	-3.515558196	2.914085982	0.020102974	171.060605	-7.13E-06	876.8633	-4.45E-05	60.7677995
39	-4.79E-05	0.005871967	-8.16E-10	-7.08E-10	-5.84E-08	-1.82E-08	2.17E-08	-9.81E-08	-1.28E-08	-4.90E-09	-4.08E-08	-7.21E-09	6.28E-07	6.280189009	-1.231018718	2081.060605	0.021029774	172.9498009	-8.16E-05	301.4663	-0.000295096	109.5970145
40	5.11E-06	0.001896469	5.59E-10	-8.82E-11	-9.44E-10	1.87E-08	-1.13E-08	3.17E-08	2.22E-08	-4.42E-08	-5.41E-09	2.76E-08	3.10E-08	-4.39E-08	-0.125086287	8.347059417	0.006787293	335.3445174	4.57E-06	103.8153	-5.44E-06	-16.17114374
41	-1.63E-06	0.012140086	-2.70E-10	-1.28E-09	-3.50E-09	-5.35E-08	1.47E-07	6.18E-08	-2.09E-07	6.20E-08	4.13E-08	-2.07E-07	0.597510435	-8.48769363	0.043494901	2553.375319	8.37E-05	553.4265	4.99E-05	69.7565394		
42	-3.06E-05	0.003140265	-7.99E-12	-1.50E-10	3.17E-09	-2.29E-08	-6.17E-09	4.57E-08	8.48E-08	-1.06E-07	-7.24E-09	5.70E-08	1.00E-07	-1.04E-07	-1.791766006	3.126743226	0.0112484	177.8899576	8.51E-06	401.1058	-5.78E-06	-379.1996212
43	7.86E-05	-0.004217366	-1.01E-09	-3.17E-10	6.67E-09	-7.23E-08	4.02E-08	-4.65E-08	1.13E-07	-9.55E-09	5.47E-08	-3.72E-08	1.67E-07	-5.19E-09	-5.65204826	-3.203367704	-0.015105247	-2195.45591	9.04E-05	1282.845	-0.00022384	-1554.065989
44	6.75E-06	0.00152649	5.13E-10	2.81E-10	-5.91E-09	5.47E-08	-1.81E-08	2.31E-08	-3.33E-08	1.49E-08	-1.64E-07	2.05E-07	-1.20E-07	6.97E-09	3.831012532	28.15342198	0.054473472	725.8402305	-2.81E-06	112.8038	-4.59E-05	-17.93138456
45	-3.95E-05	-0.0007816	1.06E-09	1.05E-09	-1.09E-09	5.13E-08	-1.47E-08	2.71E-08	3.26E-08	1.49E-08	-2.09E-07	2.64E-07	-8.97E-08	2.14E-08	-2.245697225	-38.35524612	-0.002816728	-288.0538697	-1.54E-05	1869.028	-0.000661057	-2111.933503

The results for 700 Vs. 900 model points are given in Figure 5-22. Both models show almost the same behavior and increasing the sample size did not have any considerable effect on metamodel fit. As with Kriging models, Polynomial models show the same behavior towards outputs number 2, 10, 14, 17 and 18 which show the worst behavior in the fitted model. The possible reasons for this behavior are presented in section 5.3.
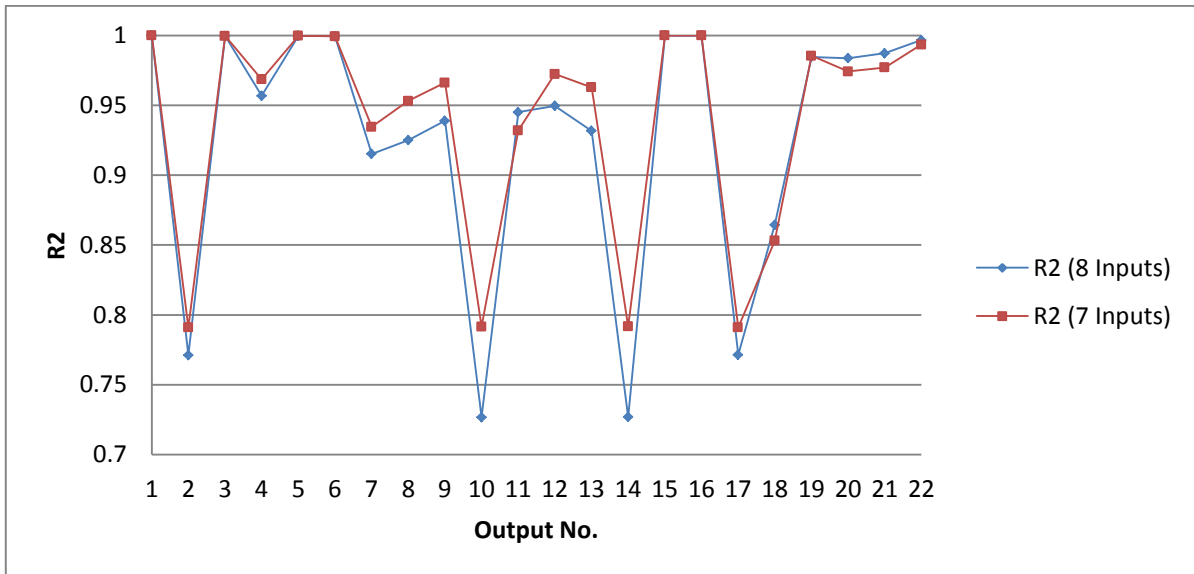
Figure 5-22: O$_2$- Polynomial- 8 Inputs (700 vs. 900)

78

Oxygen Blown ATR (Polynomial)	7 inputs	600, 700, 800, 900, 1000, 1100
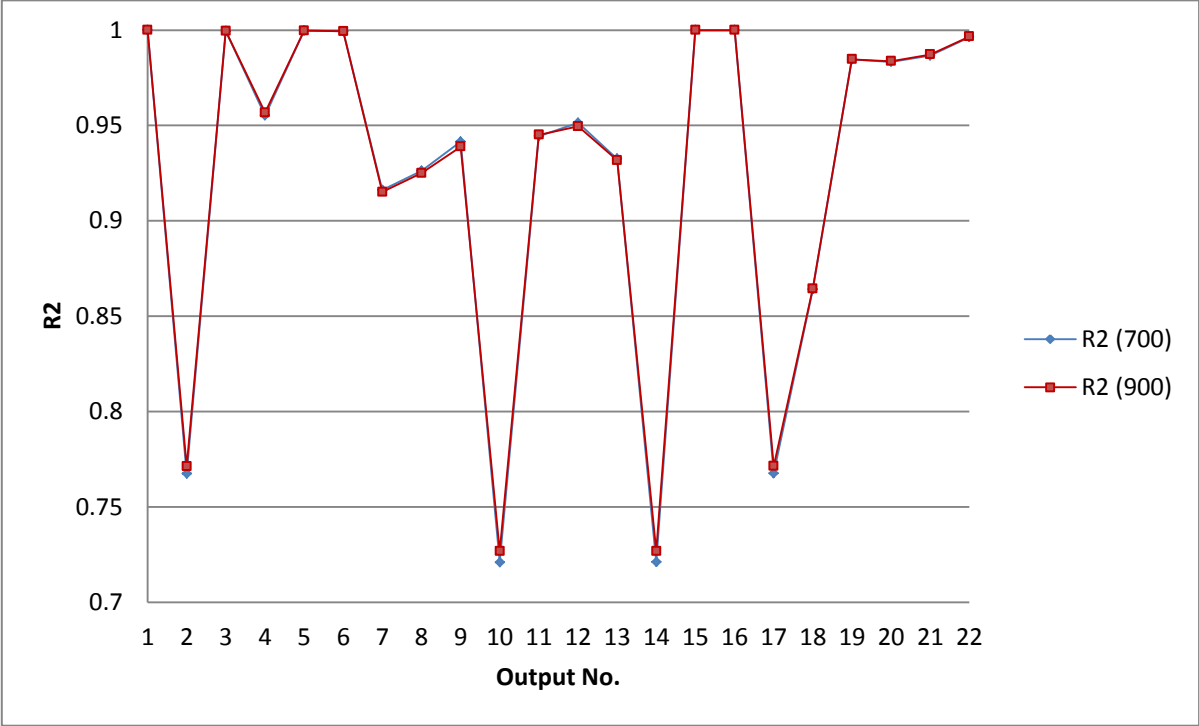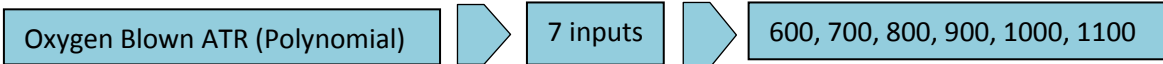
Polynomial models for 7 inputs were made for the same reasons as for the Kriging model. By moving from 8 to 7 inputs, the metamodel fit improved as for the Kriging model (Figure 5-23).

Figure 5-23: O_2- Polynomial- 7 vs. 8 Inputs (900)

The results for the six different sample sizes are given in Figure 5-24. The results for all the sample sizes are more or less the same and not an improvement or deterioration with increasing sample size can be implied from the figure.

Figure 5-24: O_2- Polynomial models (600,700,800,900,1000,1100)
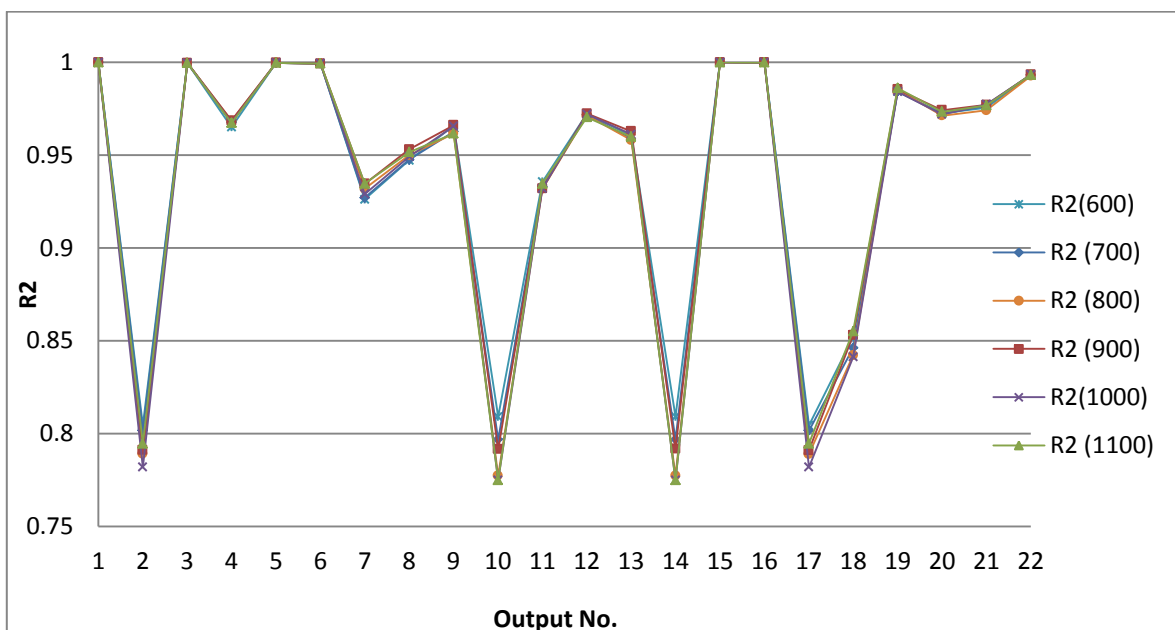
Figure 5-25 shows the average R^2 that are calculated according to Equation 5-1 for the 6 different sample sizes. No discernible pattern can be observed although one expects improvement to the metamodel fit by increasing the sample size. The average R^2 for all the sample sizes are close to each other differ only in parts of thousandths, as the vertical axis of the figure shows. Several researchers also observed the same behaviors towards increasing the sample size. Simpson et al. [27] while comparing Experimental design and metamodel types observed discrepancies among some of their sample sizes. They suggested that the reason is due to over fitting of the function because of its smooth behavior and if it was more nonlinear, taking more points would increase R^2. Laurenceau and Sagaut [54] observed fluctuations in Error of the metamodels by increasing sample sizes.

Figure 5-25: R^2 average O_2 Blown case (Polynomial Model)
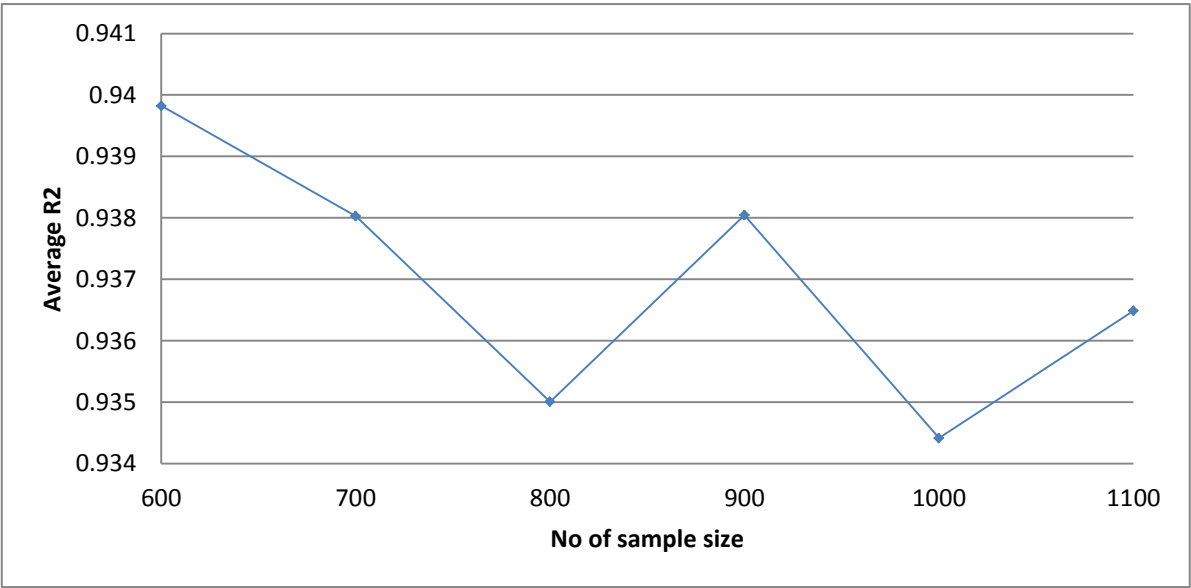
Using 6 input variables:
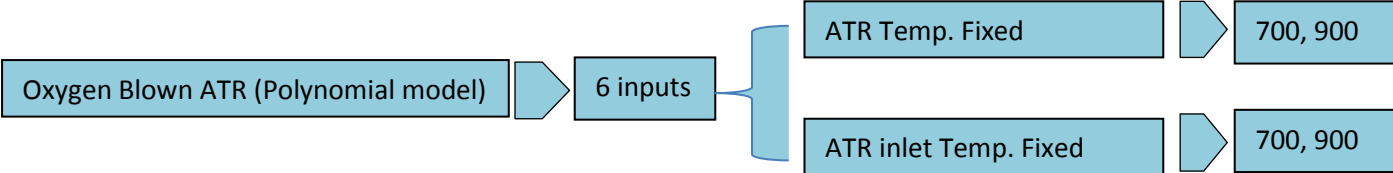
Improvements observed by moving from 8 to 7 inputs, gave this idea that by reducing the number of constraints around ATR, the metamodel fit increases. It is worthwhile to further reduce the number of constraints around ATR. As a first try, the ATR temperature was fixed to 1000°C and metamodels were built for two sample sizes, 700 and 900 points. Figure 5-26 shows the comparison between 7 input model and 6 input model when the ATR temperature is fixed for 900 sample point. As in the Kriging case, the metamodel fit became worse in this case.

Figure 5-26: O$_2$- Polynomial- 700 vs. 900 point model- 6 inputs with ATR Temp. Fixed
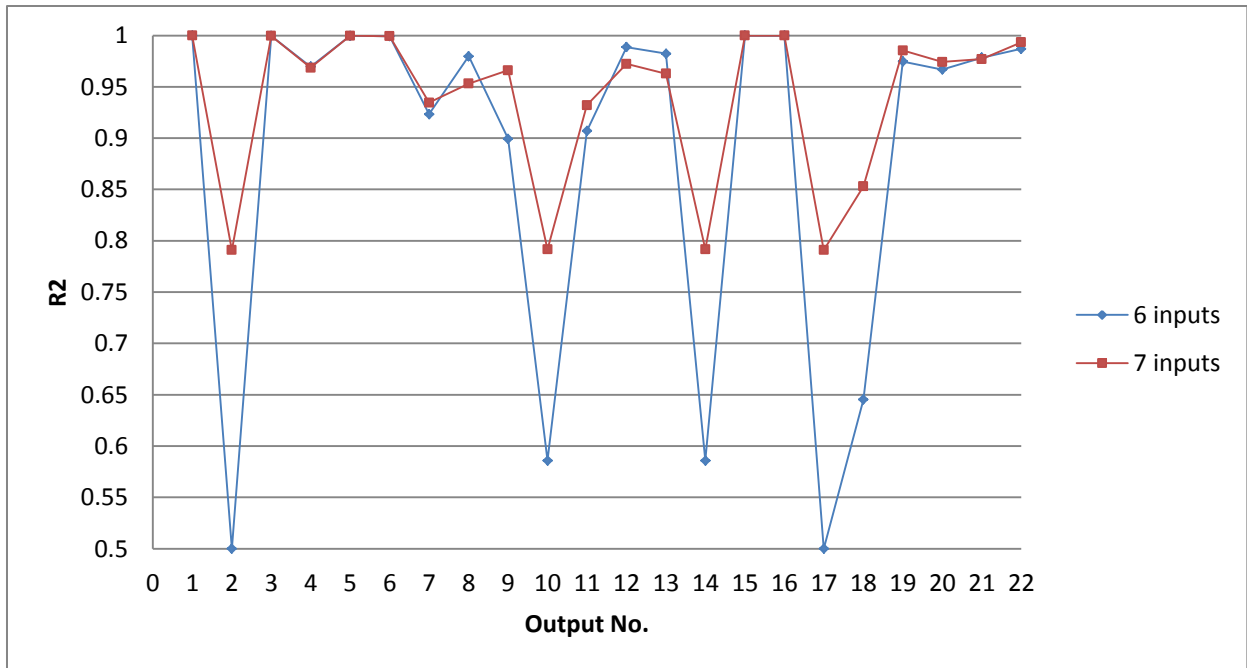
In the next try, ATR inlet temperature was kept constant. The same results were obtained as in the Kriging model and the metamodel fit improved a lot (Figure 5-27). This is the best polynomial fit in oxygen blown case.


Figure 5-27: O$_2$- Polynomial- 6 input (ATR Temp. Fixed) vs. 7 inputs-900 point model
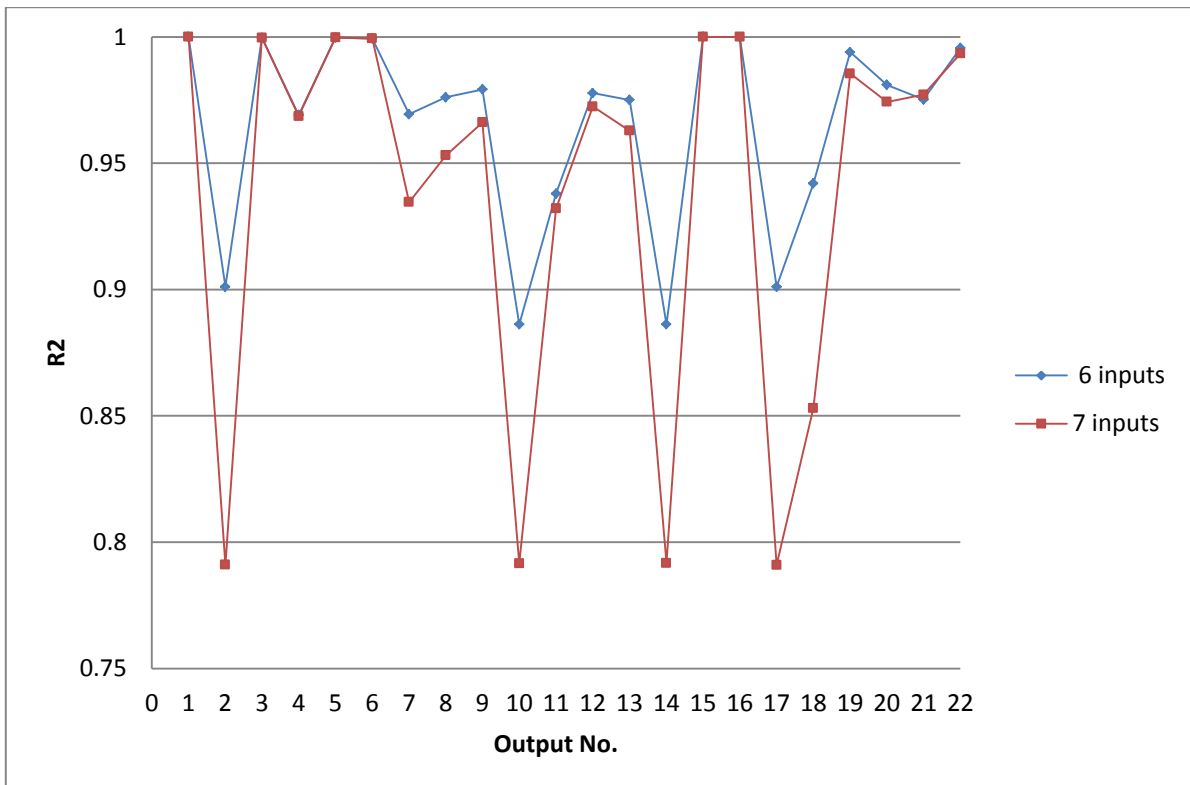
5.1.3 Summary for oxygen blown ATR

The average R^2 for all metamodels in the oxygen blown case is given in Figure 5-28. As mentioned earlier, metamodels made for 6 inputs with ATR inlet temperature fixed show the best behavior among other cases. The metamodels for 6 inputs with ATR temperature fixed show the worst behavior among other cases. The metamodels for 7 inputs show fluctuations in average R^2 with the sample size. Kriging and Polynomial models give close results. Comparison of these two metamodeling types is given in chapter 6.

Figure 5-28: R^2 Average- Oxygen Blown ATR
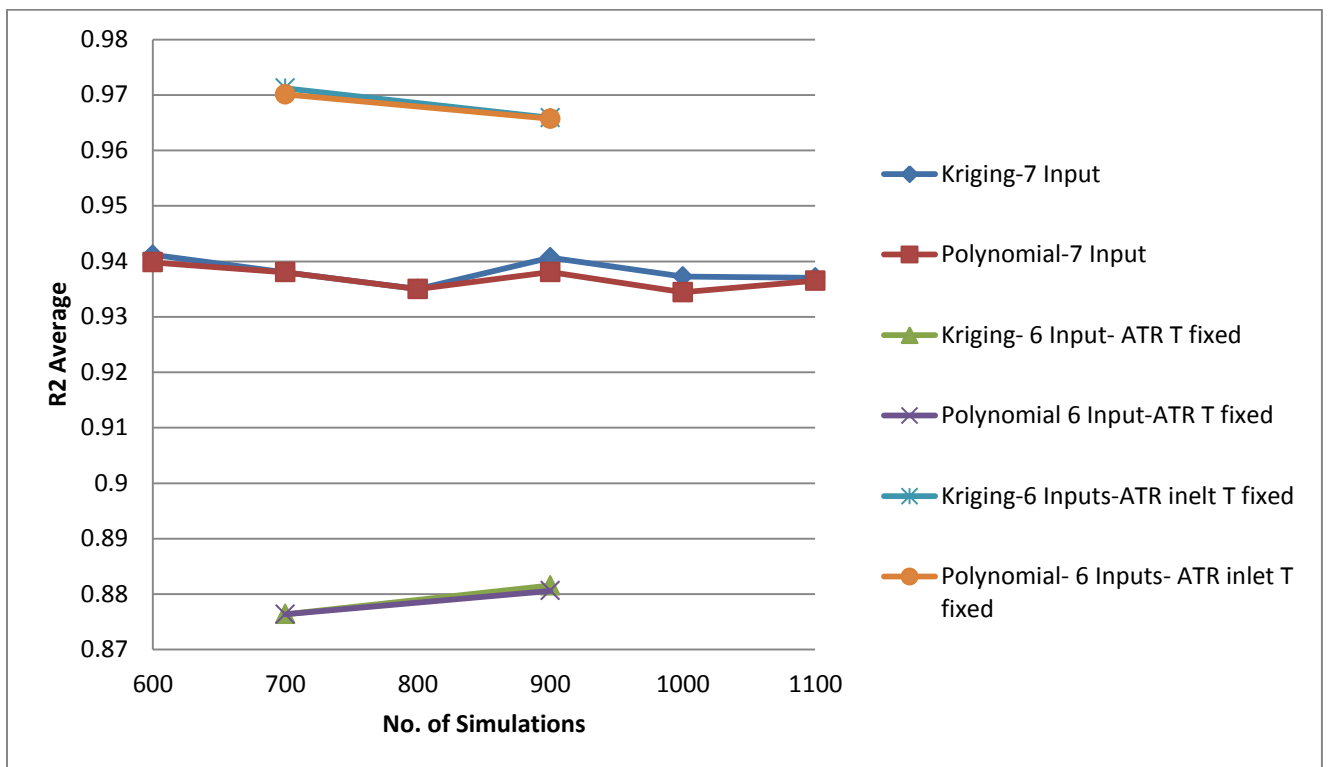
5.2 Air Blown ATR Case

By observing the results for the 8 input O_2 blown case, it was decided to proceed with 7 inputs in the air blown case. Thus the investigation started with 7 inputs. The results of model fitting with 7 inputs were very smooth and satisfactory, unlike the oxygen blown case. Therefore there was no need for investigating 6 inputs. A schematic diagram of the presentation of results is given below:
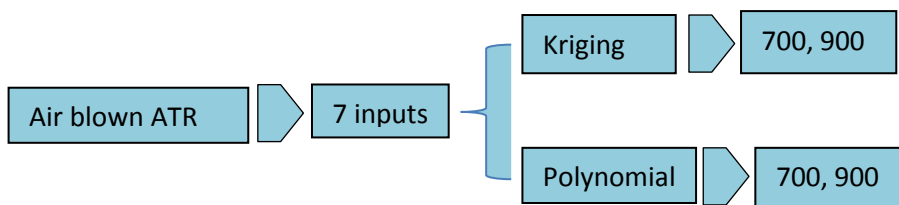
5.2.1 Kriging Metamodel

Metamodels were made for two sample sizes: 700 and 900. The results for comparing these models are given in Figure 5-29. It shows very smooth behavior for all the outputs except output no 10 and 14 which are methane concentration in the ATR outlet and the LTS outlet respectively. The reason for poor behavior of these two outputs is that the Methane Concentration in the ATR and LTS outlets are very low and a slight change in their value will have great impact on R^2. Section 5.3 is dedicated to describe possible reasons for poor model fits and differences in the air blown and the oxygen blown cases.

Figure 5-29: Kriging- Air- 700 vs. 900
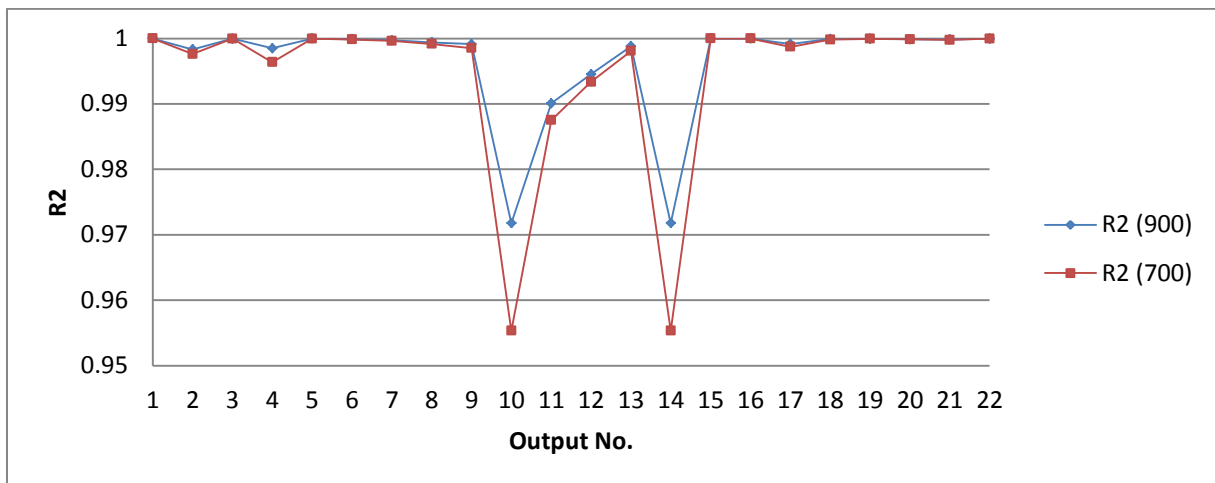
5.2.2 Polynomial Metamodel

Polynomial metamodels for two sample sizes were made: 700 and 900 points. They almost give the same results except for output 10 and 14, in which 900 model show slight improvement (Figure 5-30).

Figure 5-30: Air- Poly- 700 vs. 900
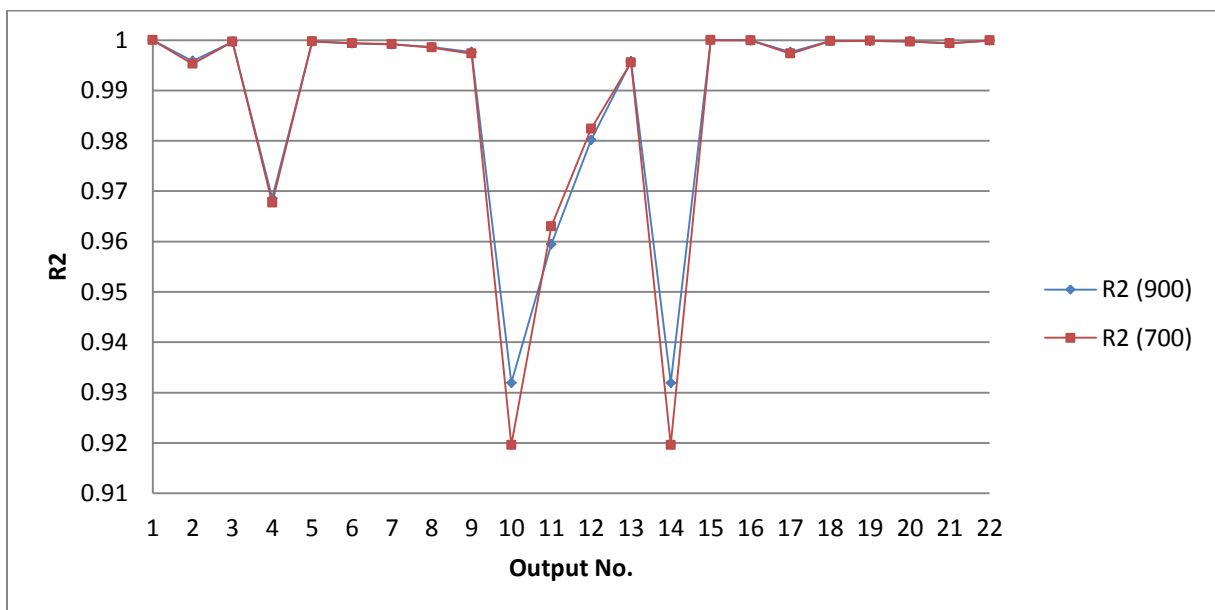
5.2.3 Summary of air blown ATR metamodels:

Average R^2 for the metamodels in the air blown case calculated according to Equation 5-1 is given in Figure 5-31. The Kriging model shows better fit to the data than Polynomial model. Increase in the sample size improves the metamodel fit in air blown case.

Figure 5-31: R^2 Average- Air Blown ATR
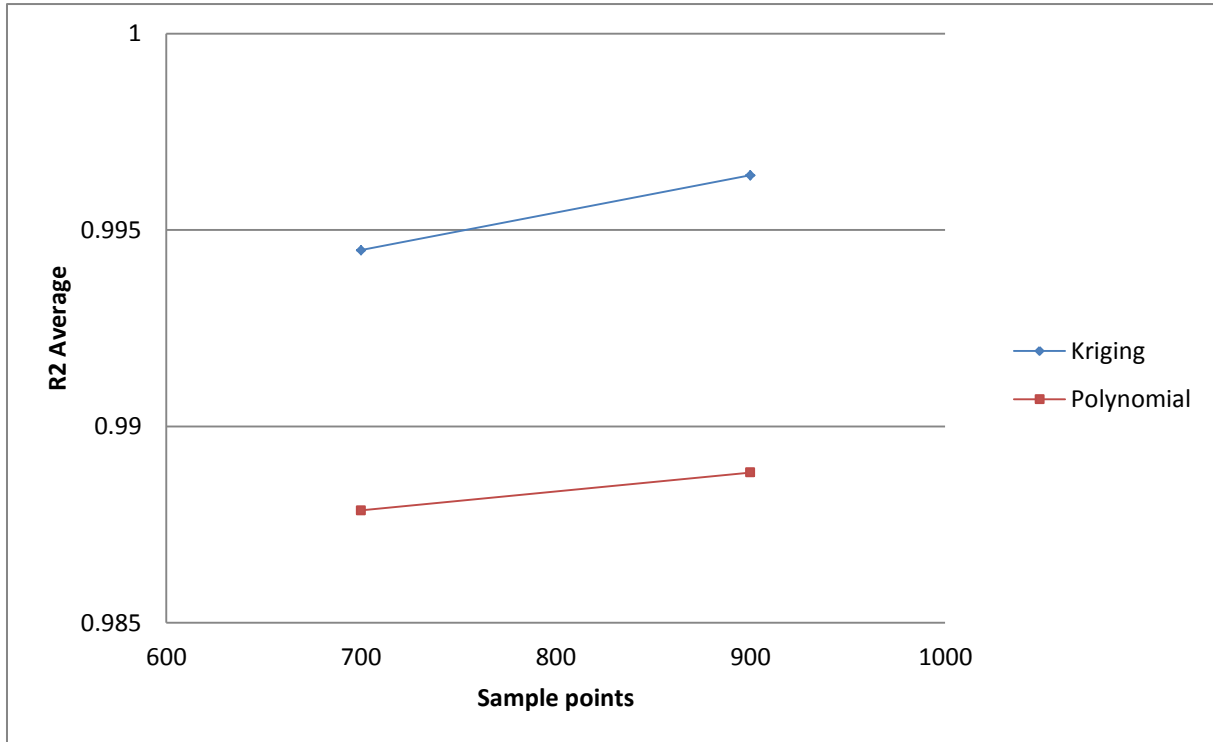
5.3 Reasons for poor fit in O_2 blown case:

So far the results of the oxygen blown and air blown ATR have been presented. In air blown case, for all the outputs, R^2 were more than 0.92 and they were completely fit by the metamodels. In the oxygen blown case, however, some misbehavior in fit was observed. Table 5-8 list the outputs showing the worse behavior towards metamodel fit and Table 5-9 shows the outputs that were completely fit by the metamodel in oxygen blown case.

Table 5-8

Output No.	Variables worse fit by metamodels in O_2 blown case
2	Oxygen to reformer (O_2 flow)
10	CH_4 concentration in ATR outlet
14	CH_4 concentration in LTS outlet
17	Oxygen compression work
18	Reformer product cooling

Table 5-9

Output No.	Variables completely fit by metamodels in O_2 blown case
1	Steam to pre-reformer
3	CO_2 concentration in ATR inlet
5	H_2 concentration in ATR inlet
6	CH_4 concentration in ATR inlet
15	Pre-reformer pre-heat
16	Reformer preheat
22	LTS product cooling

Outputs no.2 and 17 which are O_2 flow to ATR and O_2 compression work are evidently related to each other so that the more O_2 flow, the more compression work is required. Outputs no. 14 is related to output no. 10 where abnormal behavior in methane concentration in ATR outlet will affect methane concentration in LTS outlet. So, in the search to find out why these parameters misbehave, the focus is on three variables: O_2 flow, CH_4 concentration in ATR outlet and reformer product cooling.

In order to investigate the reasons for different metamodel behavior in oxygen and air blown cases, it was decided to run the two HYSYS models for the same inputs. 10 LHS sample points were made for 7 inputs. The respective 10 runs were taken in both air blown and oxygen blown ATR.

The results for the misbehaving outputs in oxygen blown case are presented in the following sections.

5.3.1 Air/O_2 to ATR and Compression Work

Figure 5-32 shows O_2/Air flow to ATR in 10 cases. Very smooth behavior of oxygen blown case is observed unlike air blown case. Why do we see this non linearity in air blown case? One possible explanation is that in air blown case, large amount of nitrogen which is an inert gas enters to the ATR which needs to be heated up to the ATR temperature which is in the range of 850°C- 1000°C. The amount of oxygen to Reformer determines the amount of heat released in ATR. In air blown case, part of the heat is used to heat up the nitrogen and the rest is used to heat up the feed to reformer. This can justify the nonlinear behavior in air blown case.

Now the other question is why metamodels in O_2 blown case show poor fit for output number 2, despite its smooth behavior? One possible answer can be due to very smooth behavior of this output. Consider that the metamodel was made by 6, 7 or 8 inputs and all of them were changing at the same time. If the output variable shows very smooth behavior with all the changes in input variables, it can be difficult to fit a model to it. The same behavior is observed for output no. 17, which is Compression work (Figure 5-33).
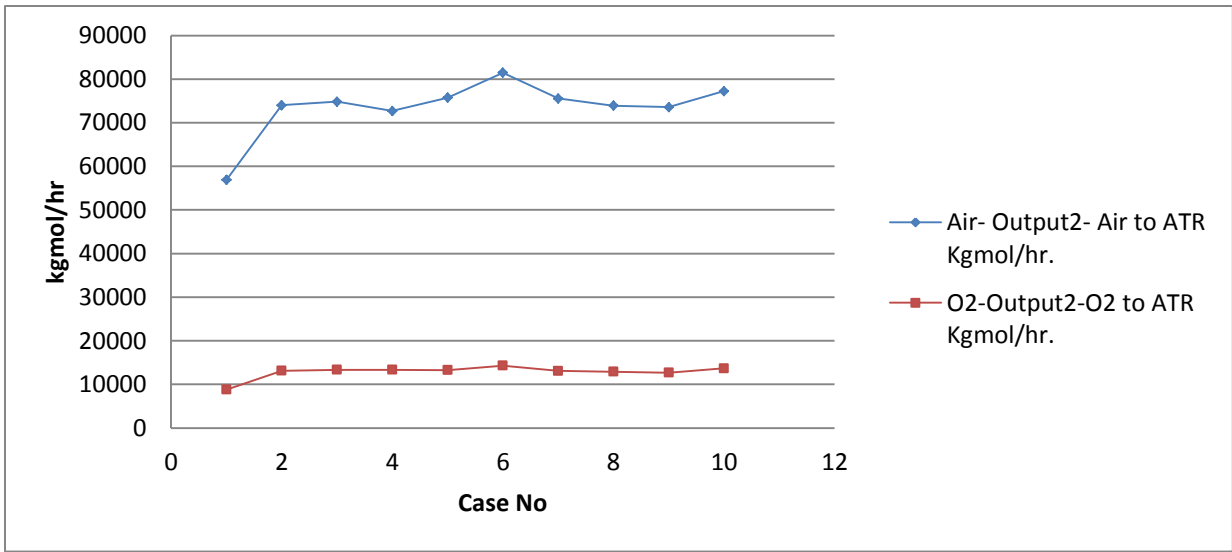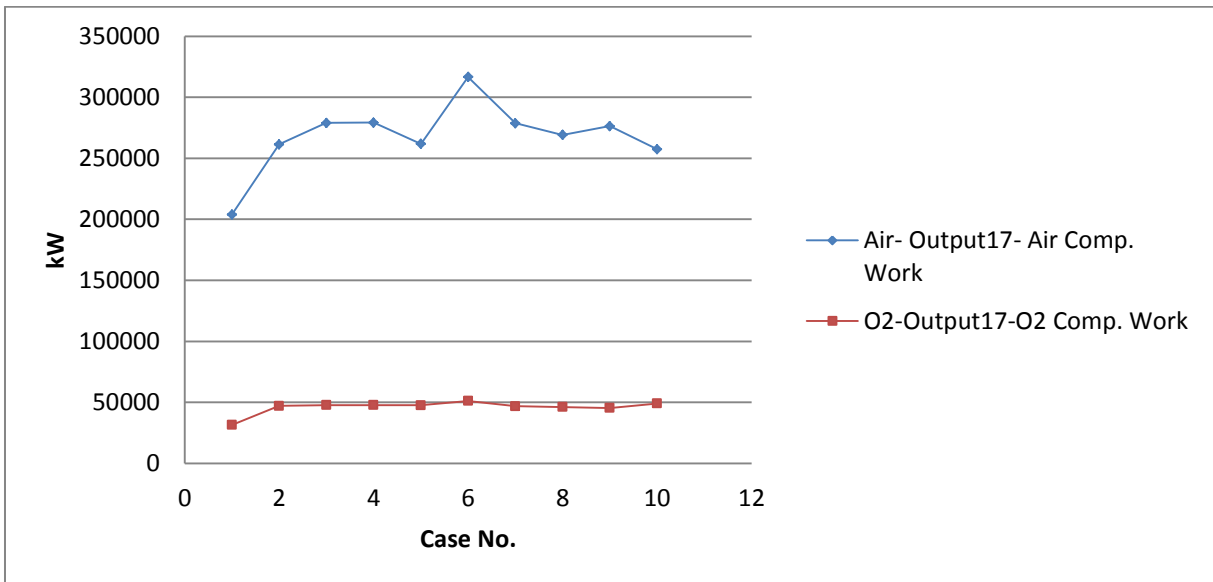
Figure 5-32: Output 2

Figure 5-32: Output 2

Figure 5-33: Output 17

5.3.2 CH$_4$ Concentration in ATR Outlet and LTS Outlet

As Figure 5-34 and Figure 5-35 show, nonlinear behavior is observed for CH$_4$ concentration in ATR and LTS outlets and smoother behavior is observed in air blown case. The possible explanation for air blown case is the diluting effect of nitrogen, since the molar concentrations are plotted, existence of nitrogen damps the effects of change in CH$_4$ concentration. These two outputs are part of the outputs with poor performance in metamodel fit. The reason can be attributed to the fact that methane concentration in ATR outlet is very low and a slight change in its value will have great impact on R^2. The same is true with LTS outlet (output 14), where CH$_4$ is very close to zero.

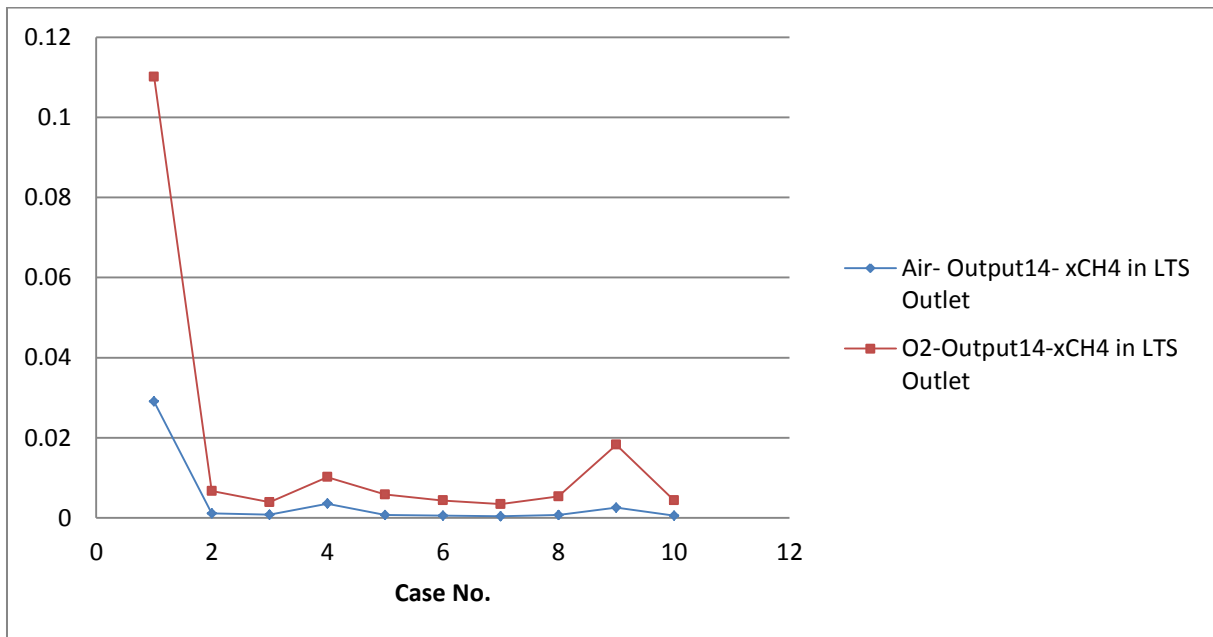Figure 5-34: Output 10

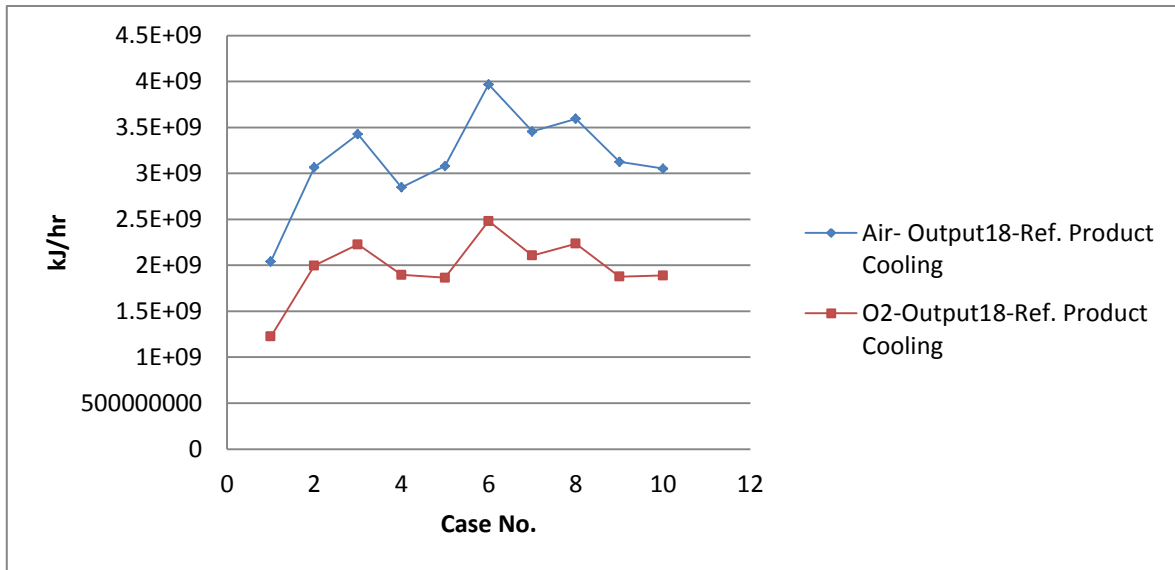Figure 5-34: Output 10
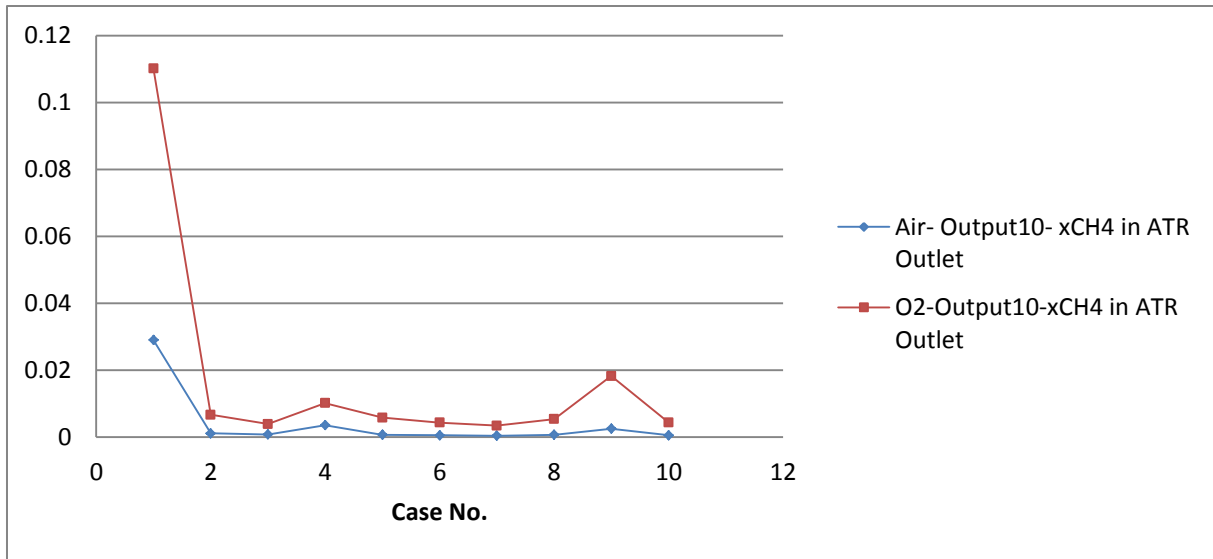
Figure 5-35: Output 14

5.3.3   Reformer Product Cooling

The results of comparison in Figure 5-36 do not give us any hint for bad behavior of metamodel fit in O_2 blown case. Nonlinear behavior of output 18 in air blown case is more than oxygen blown case, but the metamodel fit behaves better in air blown case.
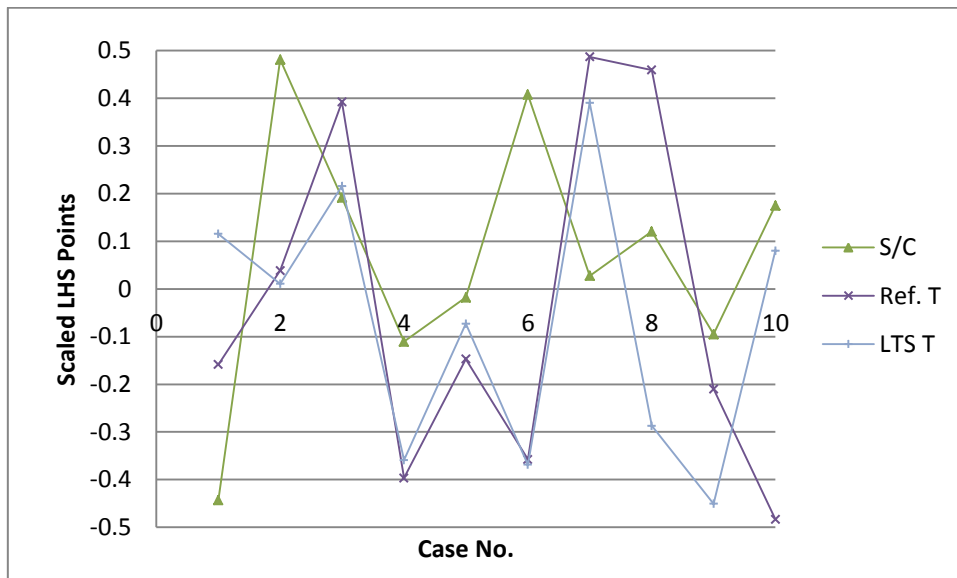
Figure 5-36: Output 18

In order to get a better idea for this behavior, the LHS sample points for 3 input variables that were used for the 10 cases are plotted in Figure 5-37. A lot of variation in the inputs is observed. May be if more points were used instead of 10, better explanation could be made.

Figure 5-37: Scaled LHS sample points for 3 input variables

5.4   Use of Artificial Neural Networks

Artificial Neural Network has been known to be a universal approximator [55]. Neural Network toolbox in MATLAB was used to generate metamodels for the worse behaving outputs, as listed in Table 5-8. The metamodels were made only for the 900 points case to show the potential of this type of metamodeling. For the 900 case, 70% of the points were used for training, 15% for validation and 15% for testing. 15 hidden neurons were chosen to

relate the inputs to the output and Levenberg-Marquardt [56] back propagation was used as the network training function.

| Neural Network making steps	Points used (total=900)
Training	630
Validation	135
Testing	135

The Neural Network diagram for the built metamodels is shown in Figure 5-38. 7 inputs were related to 1 output in each of the ANN metamodels.

Figure 5-38: Neural network diagram
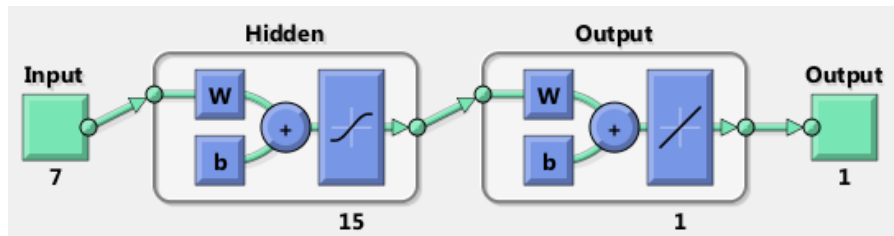
The results comparing Kriging, Polynomial and ANN results are shown in Figure 5-39. The results show much better fit in ANN than Polynomial and Kriging metamodels except for output no. 18. ANN approximations can improve by increasing the number of hidden layers and retraining the model. As mentioned earlier, Kriging models yield equally good or better approximations than polynomial models.

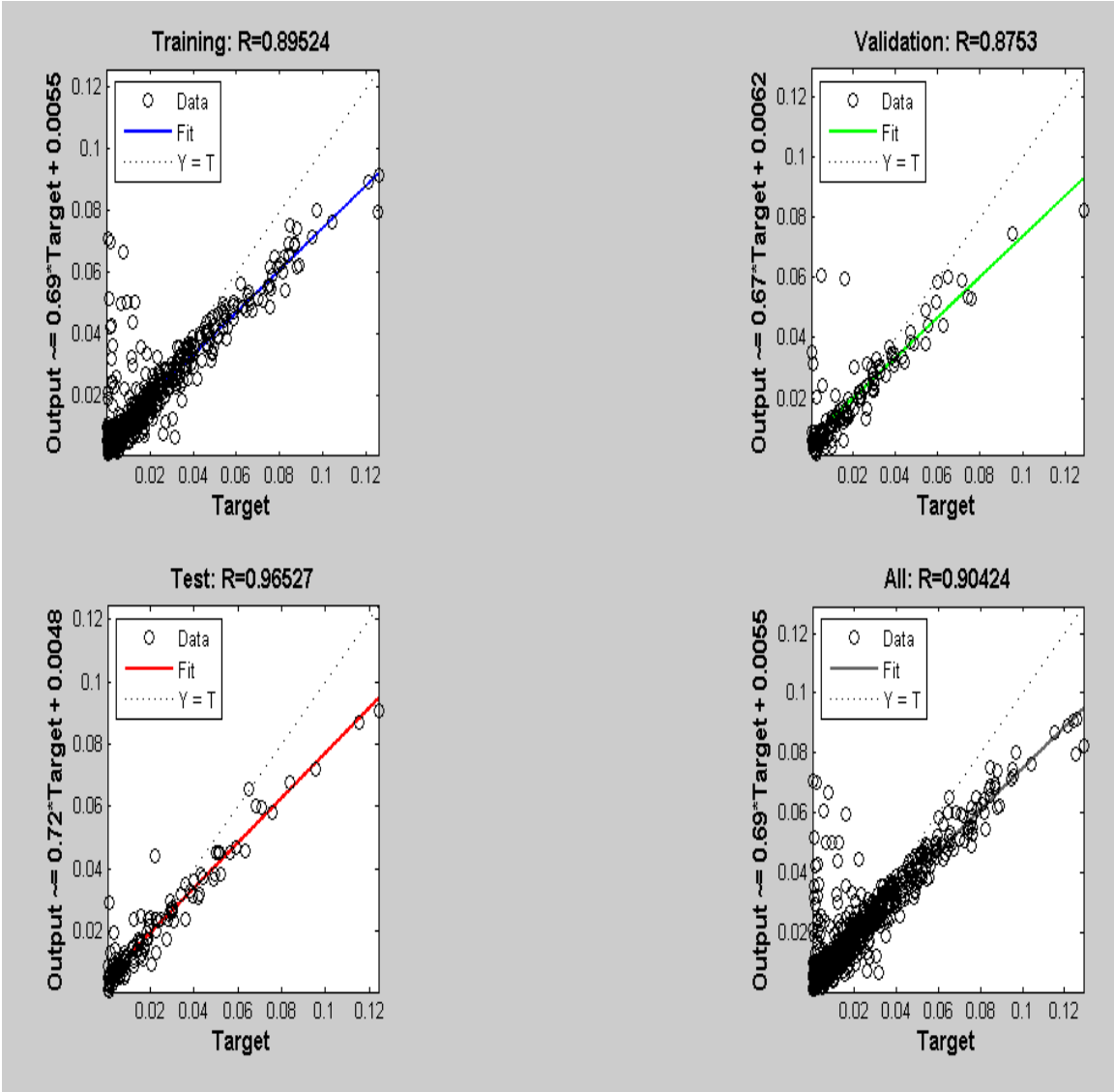Figure 5-39: O_2 Blown- 7 inputs - 900 point model
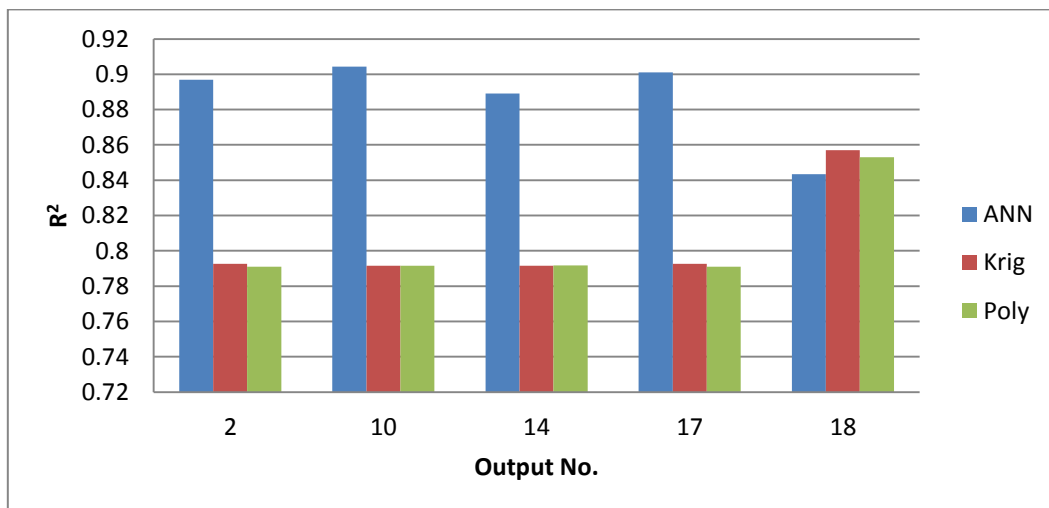
The results of ANN fit to the poor behaving outputs in metamodels are presented in the following sections.
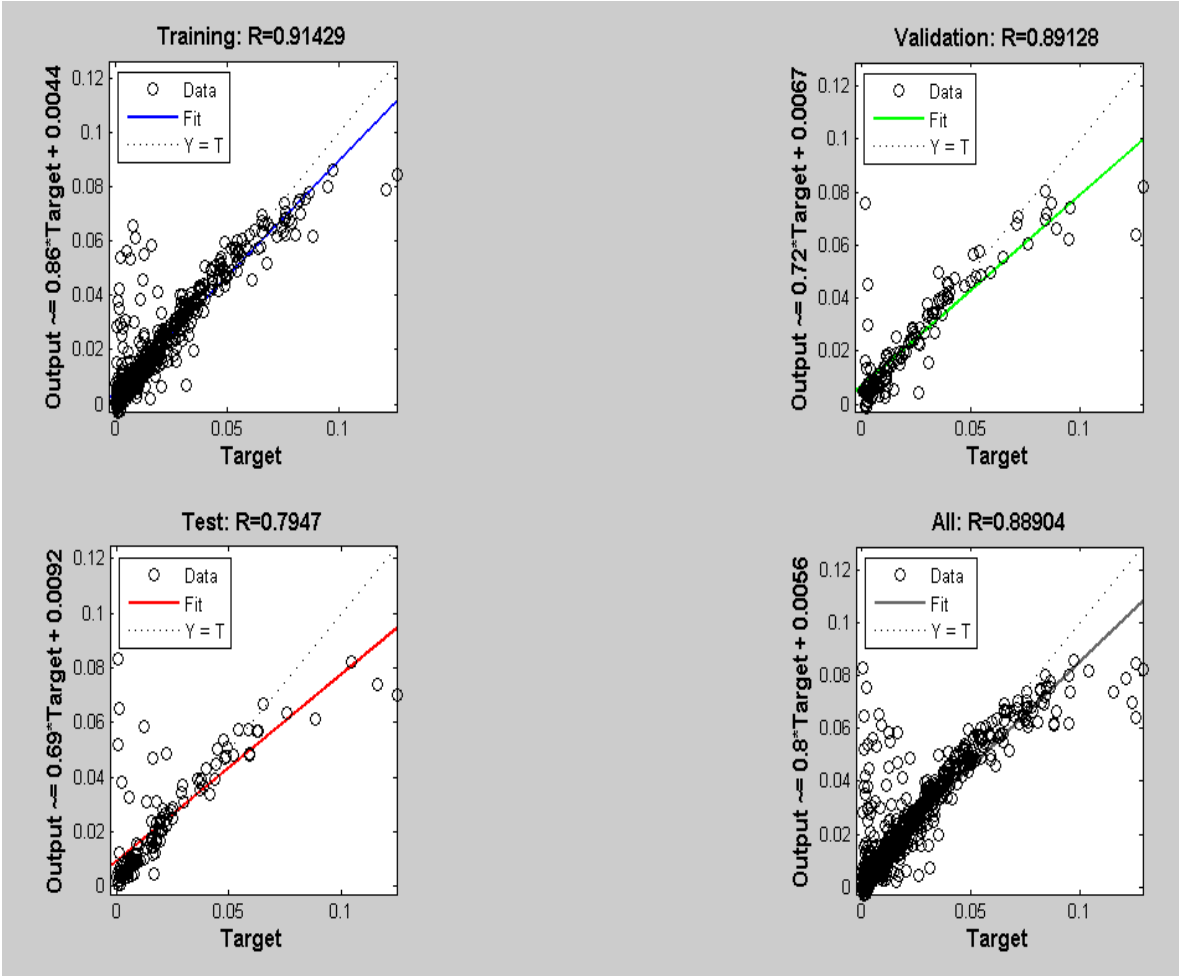
5.4.1 ANN for O_2 Flow: $R^2 = 0.89689$
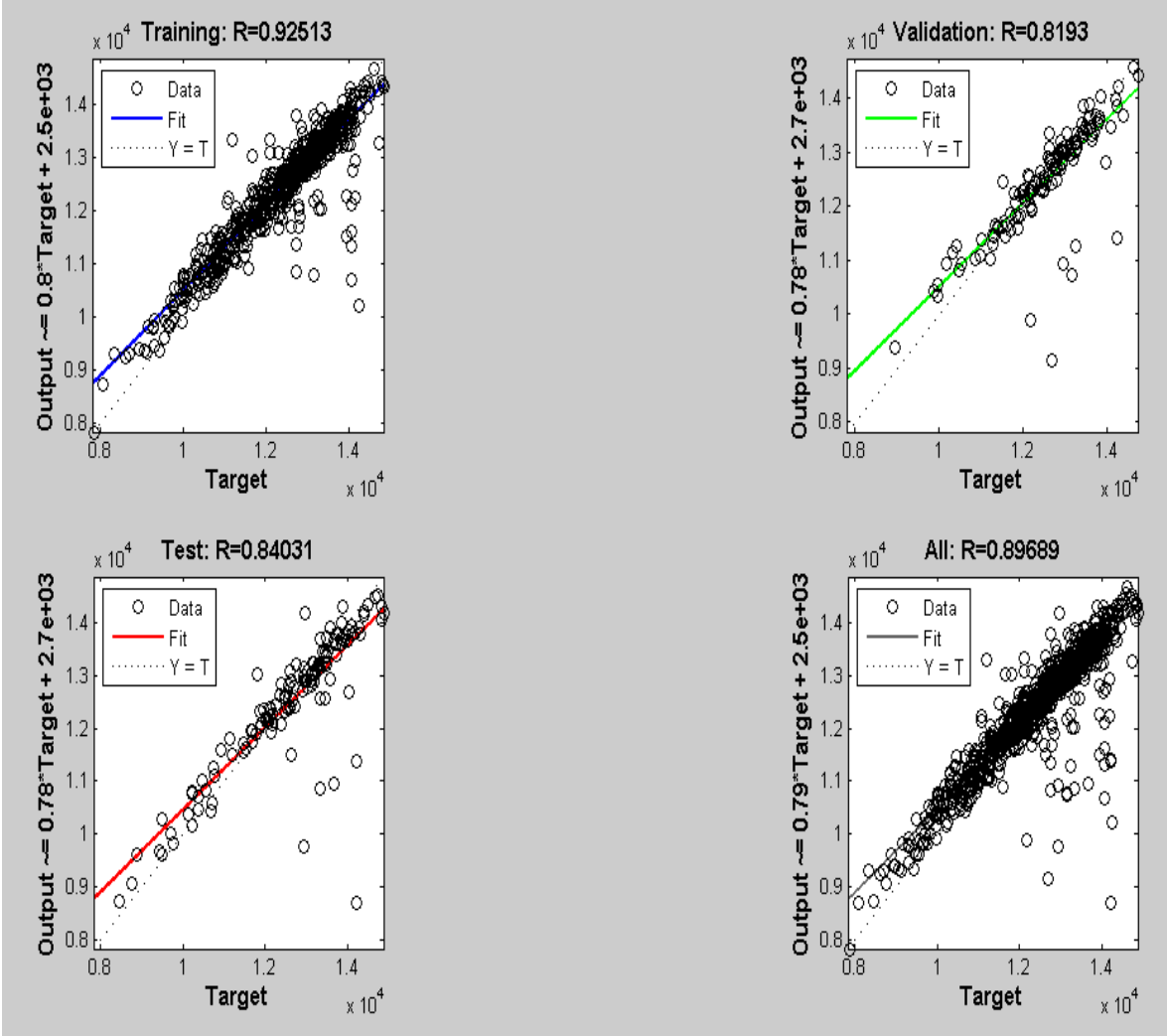
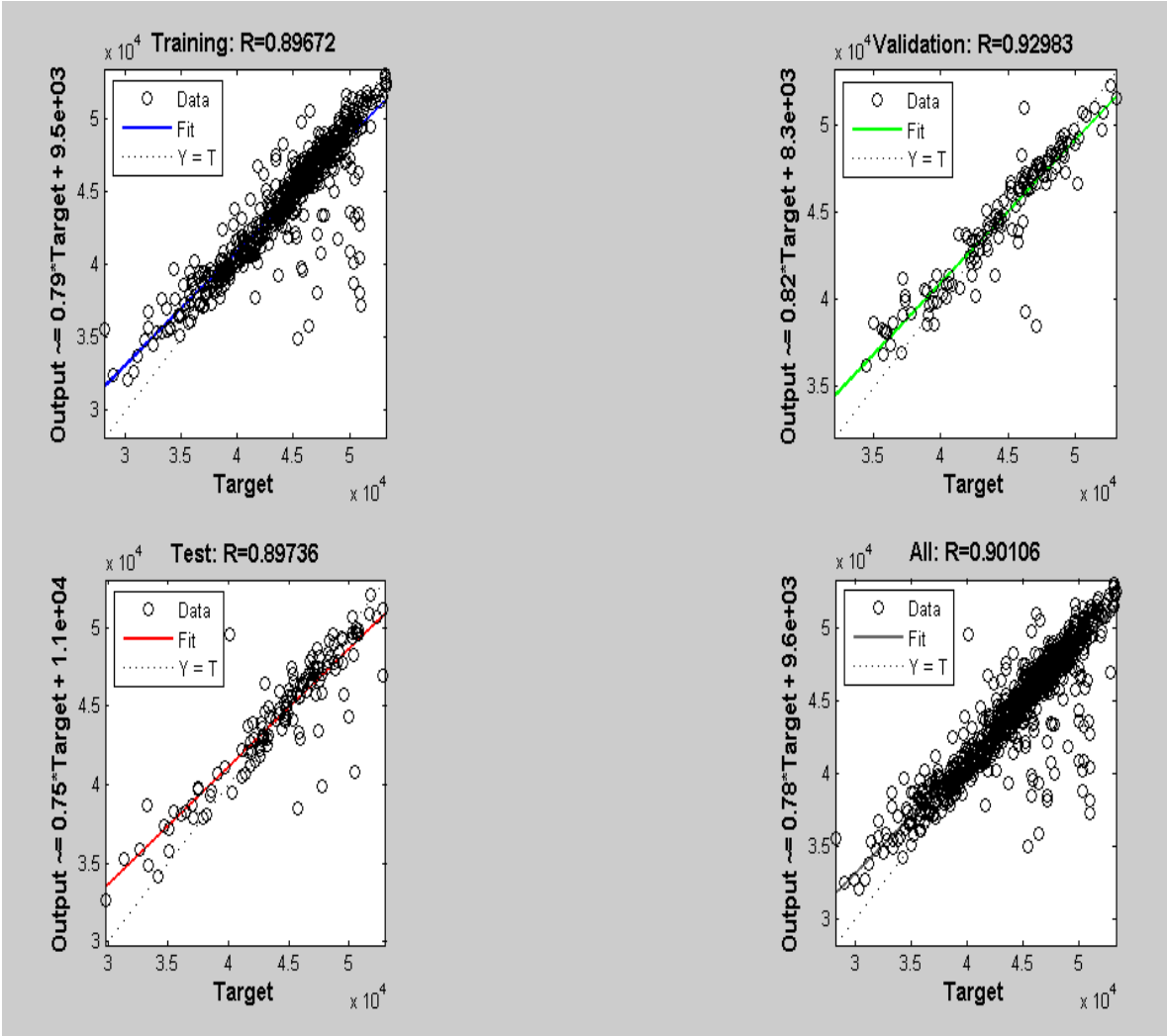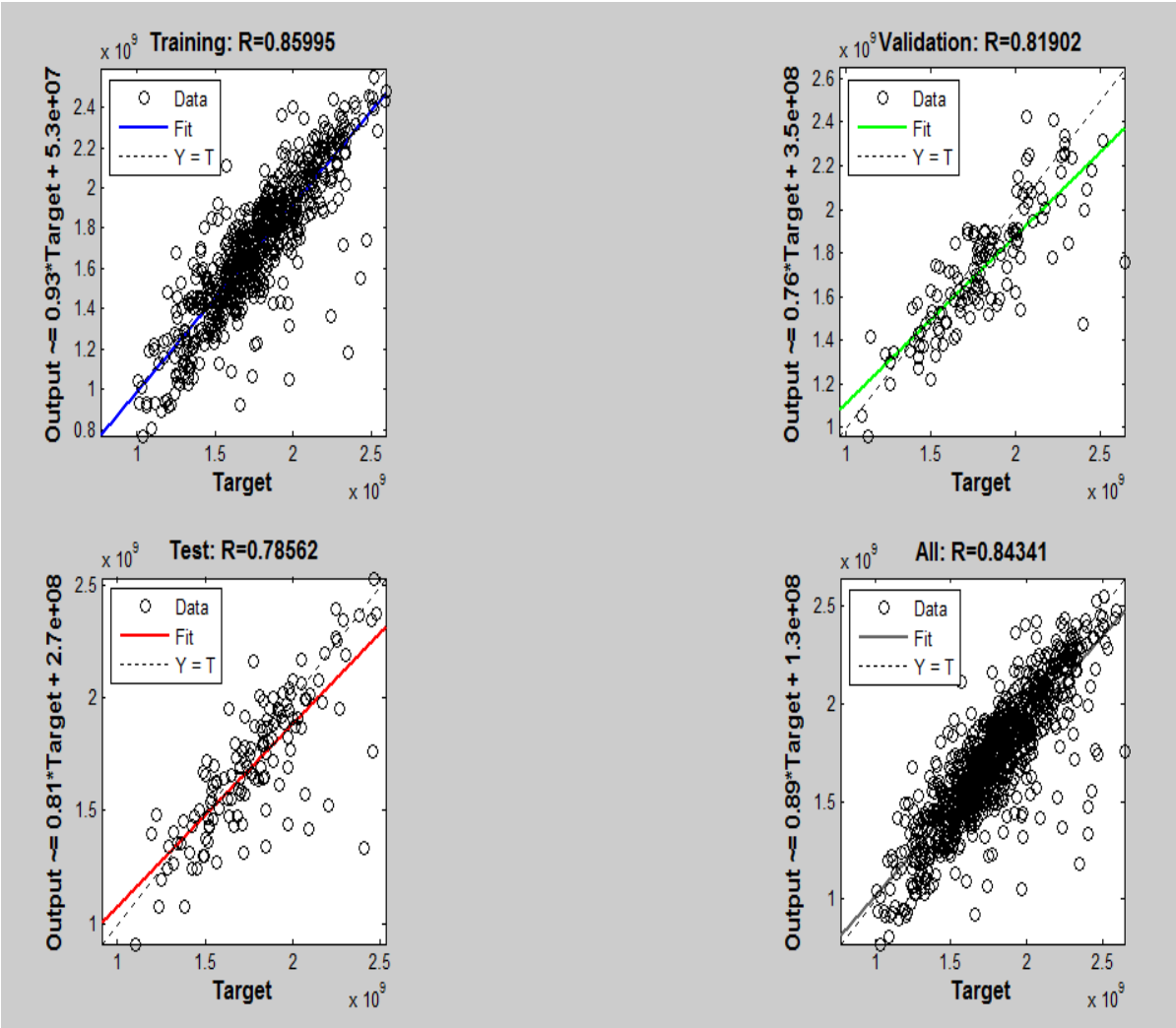## 5.4.2   ANN for CH4 Concentration in ATR Outlet: R²=0.90424

5.4.3 ANN for CH₄ Concentration in LTS Outlet: R²=0.88904

5.4.4 ANN for O_2 Compression Work: R^2= 0.90106

5.4.5 ANN for Reformer Product Cooling: R²= 0. 84341
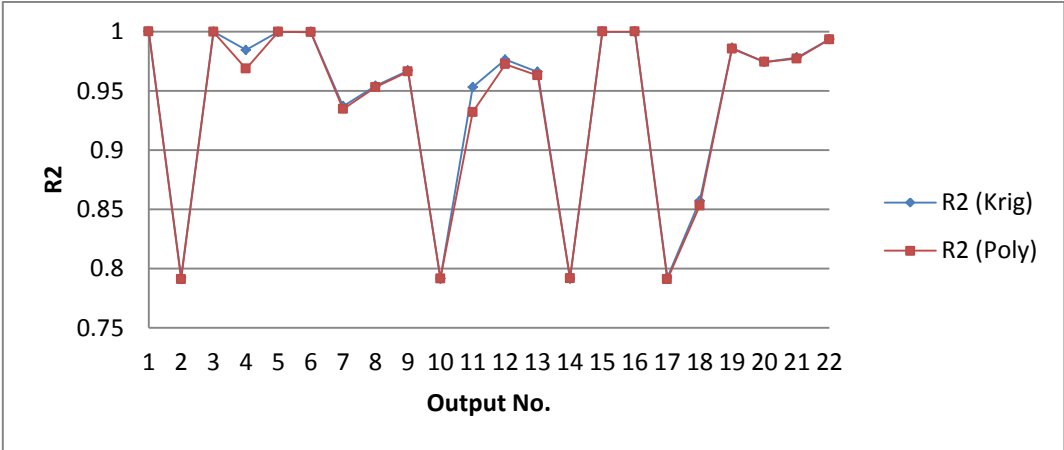
6 Comparison of Polynomial and Kriging Models

Several factors contribute to the success of a given metamodeling technique such as nonlinearity and dimensionality of the problem, data sampling technique and the internal parameter settings of the various modeling techniques [11].

This chapter presents comparison between Polynomial and Kriging models in terms of accuracy and computational cost. In section 6.1 Model accuracies and in section 6.2 computational costs are compared for these two types of metamodels. An overview of comparisons available in the literature is presented in section 6.3.

6.1 Model accuracies

As an example, Polynomial vs. Kriging models generated with 900 points and 7 inputs in oxygen blown case are given in Figure 6-1. Kriging models show slight improvement to the fit.

Figure 6-1: O_2- Polynomial vs. Kriging- 7 Inputs (900)

The case for 1000 point model in oxygen blown case is shown in Figure 6-2. Better fit is given by Kriging models than Polynomial models.

Figure 6-2: O_2- Kriging vs. Polynomial (1000)

95
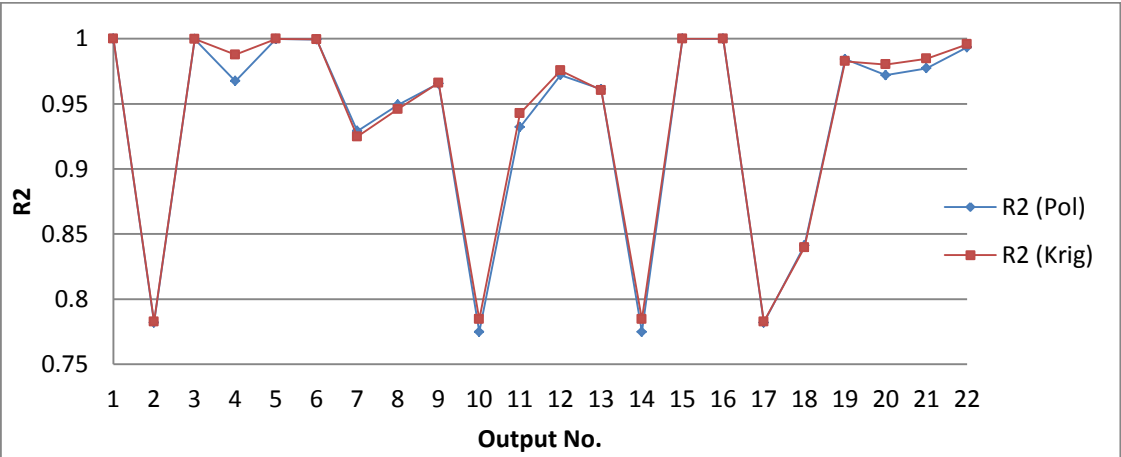
Figure 6-3 shows the comparison between Kriging and Polynomial models for 700 points in air blown case. Again the Kriging models show better behavior than Polynomial models.

Figure 6-3: Air- Polynomial vs. Kriging (900)
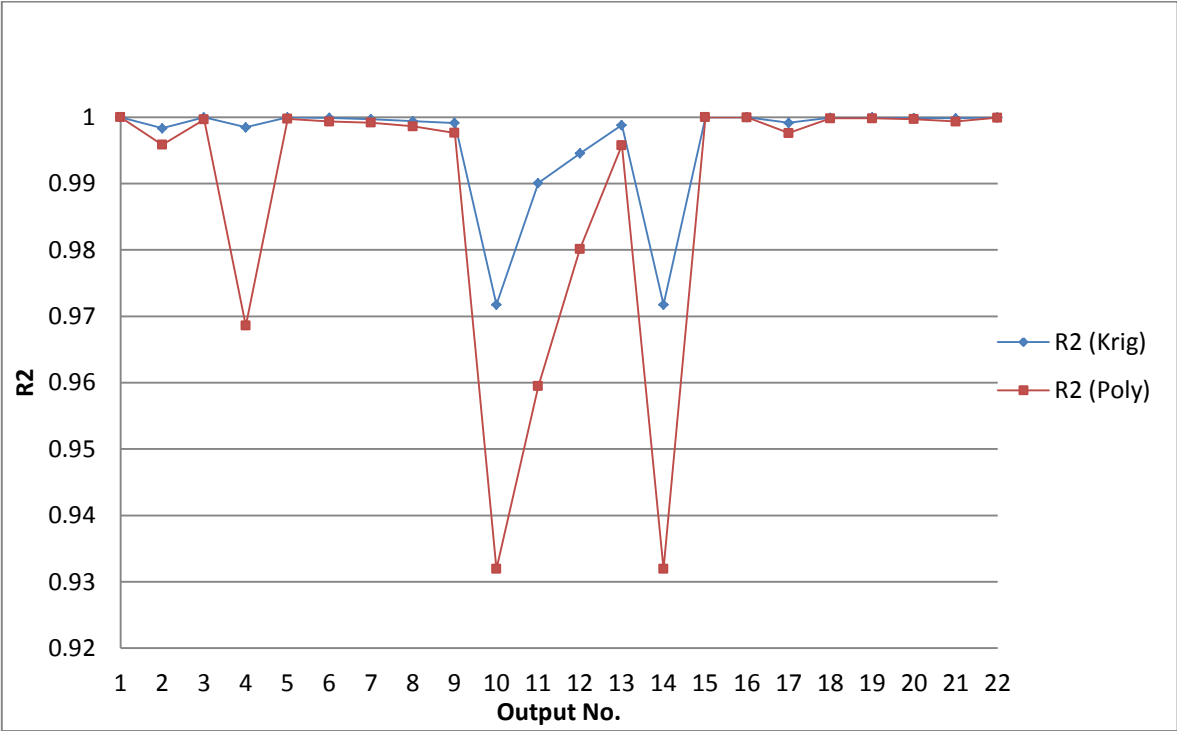
Figure 6-4 shows the R^2 average for 6 sample sizes used for 7 inputs in oxygen blown case. In all the cases Kriging models were behaving equal or better than Polynomial models in terms of model fit to the data.

Figure 6-4: R^2 average for Kriging and Polynomial models with different sample sizes

Increasing the sample size for low order nonlinear functions does not contribute much to the approximation accuracy and the "appropriate" sample size depends on the complexity of the function to be approximated [27]. In general, more sample points offer more information of the function, however, at a higher expense.
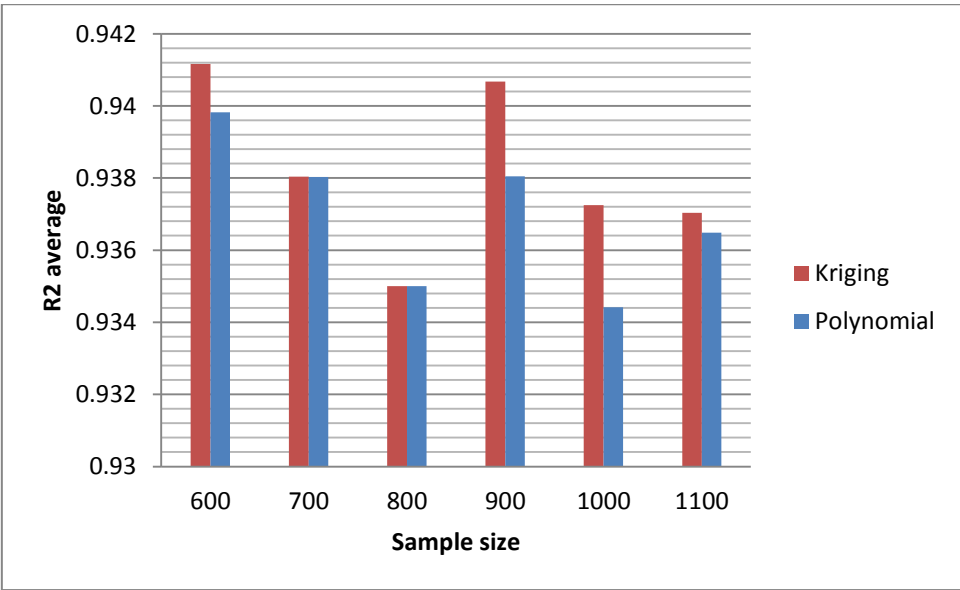
6.2 Computational costs

This project focuses on the development of metamodels for optimization of Integrated Reforming Combined Cycle power plants. An important aspect of metamodels is the computational performance when performing optimization (in addition to accuracy of prediction). Polynomial and Kriging metamodels were used in a simple optimization framework to identify which model has better computational performance. This was performed by Rahul Anantharaman, and his inputs are used here.

The optimization model was built to maximize efficiency defined by:

$$Efficiency = \frac{LHV_{H_2}.F_{H_2} + W_{El}}{LHV_{NG}.F_{NG}}$$

<div align="right">Equation 6-1</div>

The optimization model is formulated as a Non-Linear Program (NLP) with 46 continuous variables. The model was modeled in General Algebraic Modeling Software (GAMS) and solved using CONOPT. The performance of the two metamodels is presented in Table 6-1:

<div align="center">Table 6-1: Computational performance of metamodels</div>

Metamodel type	Computational time (Seconds)
Polynomial	12.2
Kriging	13.0

There is no big difference in the computational performance for a small NLP model. Extrapolating the results from the simple model, it is however expected that for a large MINLP model the polynomial model will perform better.

As the earlier results show that Polynomial models perform similar to Kriging models in predictive accuracy, Polynomials metamodels will be most likely used for optimization of IRCC plants.

6.3   Comparisons of the Kriging and Polynomial models in the literature

By looking into the metamodel literature, a lot of reviews and comparison between metamodels exists. Some of the comparisons and their results are presented here.

Simpson et al. [10] investigated the use of Kriging models as alternatives to the second order polynomial model for constructing global approximations for use in aerospace application. They found that the Kriging models with a constant global model and a Gaussian correlation function, yield global approximations that are slightly more accurate than the polynomial model with minimal added computational expense.

Simpson et al. [27] compared five experimental design types and four metamodel types in making approximations in two engineering applications. They concluded that the Kriging model tend to offer more accurate approximations over a wide range of experimental design types and sample sizes. They observed that second order Polynomial model give average results and perform particularly well when approximating low order non-linear functions. Larger sample sizes generally improve the accuracy, but Simpson et al. [27] observed that for low order non-linear functions taking large samples does not improve the accuracy that much. They observed that due to over fitting of the smooth functions, taking larger sample size results in poor performance of the regression model, but in case of highly nonlinear functions, increasing the number of sample points improves the regression accuracy.

Jin et al. [11] compared Kriging, Polynomial and two other approximating models and concluded that no one model dominated in terms of accuracy, robustness, transparency, etc. They also reported that for low-order nonlinear and small-scale problems, Polynomial models perform best in terms of both average accuracy and robustness.

Giunta and Watson [19] in their comparative study of Polynomial and Kriging models of a test function, concluded that Polynomial models were more accurate. Surprisingly this was true for the highly non-quadratic functions as well as quadratic functions.

Welch & Sacks [26] mentioned shortcomings of Polynomials as metamodels of simulators. Three reasons mentioned are: First, the simulator results are deterministic and lack random error. Second, least squares method produces a smoothed curve through the data which may not necessarily pass through the known data points. Third, poor predictions of polynomial models in several examples were observed. As an alternative, they recommended to use Kriging models instead.

Simpson et al. [10] states that Polynomial models have limited capability to model nonlinear functions of arbitrary shape accurately. Higher order response surface models can be used to approximate nonlinear design space, but instabilities may arise [14].

Kriging regression models may be well suited in describing the relationships between the variables in the IRCC process, but they are more complex and may not be ideal for global optimization.

There is no clear conclusion in literature about which model is definitely superior to the others. The results show that behavior of Kriging and Polynomial models are very case dependent and either of them may behave differently from case to case. But generally Kriging models are more accurate for nonlinear problems but more difficult to make because a global optimization process is applied to identify the maximum likelihood estimators. Kriging is also flexible in either interpolating the sample points or filtering noisy data. On the other hand, a Polynomial model is easy to construct, and cheap to work with but is a little bit less accurate than the Kriging model [15].

7 Conclusions and Future Work

Natural gas combined power plants with CO_2 capture are expected to play an important role in mitigating carbon emissions. Integrated Reforming combined Cycle is a promising route for combined power and hydrogen production with CO_2 capture from natural gas. The reforming part of the IRCC, which is the most important part of an IRCC plant, has been the focus of this study.

The main objective of this work was to develop surrogate models for the reforming section of an IRCC for use in a deterministic optimization framework that reflect a good trade-off between accuracy and computational cost.

Metamodels are found to be a valuable tool for design optimization. Optimization of chemical process simulations is complex and may involve solving of hundreds (or thousands) of nonlinear equations.

The metamodels were successfully made for two different types of reformers in the IRCC process. A total of 30 different cases in terms of number of inputs and sample sizes were considered. The results of this work provided better understanding of the process as well as metamodels behavior. In terms of model accuracy, Kriging models provided equal or better fit than Polynomial models. From computational cost point of view, however, Polynomial models showed better performance.

As the earlier results show, the Polynomial models perform similar to the Kriging models in predictive accuracy, Polynomials metamodels will most likely be used for optimization of IRCC plants.

Several suggestions can be made for further research in future:

First of all, it is better to make metamodels for molar flows rather than concentrations because concentrations are very dependent to the amount of inert gas in the system. As we saw in outputs no. 10 and 14, the effect of inert gas was very sensible. By doing so, the poor performance in some of the outputs may not happen.

Secondly, other DOE types can be investigated, as is done in several other investigations in the literature but not for chemical flow sheets.

Lastly due to the sake of completeness of study, the focus was put on IRCC with standard two shift reactors only and the investigation of the Advanced ECN shift reactor was put for future studies. It would be interesting to look on the behavior of metamodels in that design.

8 Bibliography:

1. Keeling, C. and T. Whorf, *Atmospheric carbon dioxide record from Mauna Loa.* Trends: A Compendium of Data on Global Change. Carbon Dioxide Information Analysis Center, Oak Ridge National Laboratory, Oak Ridge, TN, 2005.
2. Gruenspecht, H., *International Energy Outlook 2011.* Center for Strategic and International Studies, 2010.
3. Palmer, K. and M. Realff, *Metamodeling approach to optimization of steady-state flowsheet simulations: Model generation.* Chemical Engineering Research and Design, 2002. 80(7): p. 760-772.
4. Nord, L.O., R. Anantharaman, and O. Bolland, *Design and off-design analyses of a pre-combustion CO< sub> 2</sub> capture process in a natural gas combined cycle power plant.* International Journal of Greenhouse Gas Control, 2009. 3(4): p. 385-392.
5. Eide, L. and D. Bailey, *Precombustion decarbonisation processes.* Oil & gas science and technology, 2005. 60(3): p. 475-484.
6. Nord, L.O., *Pre-combustion CO2 capture: Analysis of integrated reforming combined cycle*, 2010, Norwegian University of Science and Technology.
7. Aasberg-Petersen, K., et al., *Recent developments in autothermal reforming and pre-reforming for synthesis gas production in GTL applications.* Fuel Processing Technology, 2003. 83(1): p. 253-261.
8. Chiesa, P., G. Lozza, and L. Mazzocchi, *Using hydrogen as gas turbine fuel.* Transactions of the ASME-A-Engineering for Gas Turbines and Power, 2005. 127(1): p. 73-80.
9. Kleijnen, J.P., *Statistical tools for simulation practitioners*1986: Marcel Dekker, Inc.
10. Simpson, T.W., et al., *Kriging models for global approximation in simulation-based multidisciplinary design optimization.* AIAA journal, 2001. 39(12): p. 2233-2241.
11. Jin, R., W. Chen, and T.W. Simpson, *Comparative studies of metamodelling techniques under multiple modelling criteria.* Structural and Multidisciplinary Optimization, 2001. 23(1): p. 1-13.
12. Sobieszczanski-Sobieski, J. and R.T. Haftka, *Multidisciplinary aerospace design optimization: survey of recent developments.* Structural optimization, 1997. 14(1): p. 1-23.
13. Barthelemy, J.-F. and R.T. Haftka, *Approximation concepts for optimum structural design—a review.* Structural optimization, 1993. 5(3): p. 129-144.
14. Barton, R.R. *Metamodels for simulation input-output relations*. in *Proceedings of the 24th conference on Winter simulation*. 1992. ACM.
15. Wang, G.G. and S. Shan, *Review of metamodeling techniques in support of engineering design optimization.* Journal of Mechanical Design, 2007. 129: p. 370.
16. RAMU, M. and R.V. PRABHU, *METAMODEL BASED ANALYSIS AND ITS APPLICATIONS: A.*
17. Simpson, T.W., et al., *On the use of statistics in design and the implications for deterministic computer experiments.* Design Theory and Methodology-DTM'97, 1997: p. 14-17.
18. Simpson, T.W., et al., *Comparison of response surface and kriging models for multidisciplinary design optimization.* AIAA paper 98, 1998. 4758(7).
19. Giunta, A.A., L.T. Watson, and J. Koehler. *A comparison of approximation modeling techniques: polynomial versus interpolating models*. in *Proceedings of the 7th AIAA/USAF/NASA/ISSMO Symposium on Multidisciplinary Analysis and Design*. 1998.
20. Varadarajan, S., W. CHEN∗, and C.J. Pelka, *Robust concept exploration of propulsion systems with enhanced model approximation capabilities.* Engineering Optimization+ A35, 2000. 32(3): p. 309-334.

21. Simpson, T.W., et al., *Metamodels for computer-based engineering design: survey and recommendations.* Engineering with computers, 2001. 17(2): p. 129-150.

22. Palmer, K. and M. Realff, *Optimization and validation of steady-state flowsheet simulation metamodels.* Chemical Engineering Research and Design, 2002. 80(7): p. 773-782.

23. Ge, P. and N. Wang. *DoE study in building surrogate models for complex systems*. in *Proceedings of ASME Design Engineering Technical Conference (DETC2000), Baltimore, ML, USA*. 2000.

24. Kalagnanam, J.R. and U.M. Diwekar, *An efficient sampling technique for off-line quality control.* Technometrics, 1997. 39(3): p. 308-319.

25. McKay, M.D., R.J. Beckman, and W.J. Conover, *Comparison of three methods for selecting values of input variables in the analysis of output from a computer code.* Technometrics, 1979. 21(2): p. 239-245.

26. Sacks, J., et al., *Design and analysis of computer experiments.* Statistical science, 1989. 4(4): p. 409-423.

27. Simpson, T.W., D.K. Lin, and W. Chen, *Sampling strategies for computer experiments: design and analysis.* International Journal of Reliability and Applications, 2001. 2(3): p. 209-240.

28. Koehler, J. and A. Owen, *Computer experiments.* Handbook of statistics, 1996. 13(13): p. 261-308.

29. Palmer, K.D., *Data collection plans and meta models for chemical process flowsheet simulators.* 1998.

30. Box, G.E., W.G. Hunter, and J.S. Hunter, *Statistics for experimenters: an introduction to design, data analysis, and model building.* 1978.

31. Myers, R.H. and C.M. Anderson-Cook, *Response surface methodology: process and product optimization using designed experiments*. Vol. 705. 2009: John Wiley & Sons.

32. Smith, M., *Neural networks for statistical modeling* 1993: Thomson Learning.

33. Cheng, B. and D.M. Titterington, *Neural networks: A review from a statistical perspective.* Statistical science, 1994: p. 2-30.

34. Booker, A.J., et al., *A rigorous framework for optimization of expensive functions by surrogates.* Structural optimization, 1999. 17(1): p. 1-13.

35. Friedman, J.H., *Multivariate adaptive regression splines.* The annals of statistics, 1991: p. 1-67.

36. Hardy, R.L., *Multiquadric equations of topography and other irregular surfaces.* Journal of geophysical research, 1971. 76(8): p. 1905-1915.

37. Dyn, N., D. Levin, and S. Rippa, *Numerical procedures for surface fitting of scattered data by radial functions.* SIAM Journal on Scientific and Statistical Computing, 1986. 7(2): p. 639-659.

38. Box, G.E. and N.R. Draper, *Empirical model-building and response surfaces: Wiley Series in probability and mathematical statistics.* Empirical model-building and response surfaces: Willey series in probability and mathematical statistics, 1987.

39. Giunta, A.A., et al., *Noisy aerodynamic response and smooth approximations in HSCT design* 1994: Department of Computer Science, Virginia Polytechnic Institute and State University.

40. Matheron, G., *Principles of geostatistics.* Economic geology, 1963. 58(8): p. 1246-1266.

41. Cressie, N.A., *Statistics for Spatial Data, revised edition*, 1993, Wiley, New York.

42. Mardia, K.V. and R. Marshall, *Maximum likelihood estimation of models for residual covariance in spatial regression.* Biometrika, 1984. 71(1): p. 135-146.

43. Lophaven, S.N., H.B. Nielsen, and J. Søndergaard, *DACE-A Matlab Kriging toolbox, version 2.0*, 2002.

44. Meckesheimer, M., et al., *Metamodeling of combined discrete/continuous responses.* AIAA journal, 2001. 39(10): p. 1950-1959.

45. Gershenson, C., *Artificial neural networks for beginners.* arXiv preprint cs/0308031, 2003.

46. Lippmann, R., *An introduction to computing with neural nets.* ASSP Magazine, IEEE, 1987. 4(2): p. 4-22.

47.   Haykin, S.S., *Neural networks: a comprehensive foundation*2007: Prentice Hall Englewood Cliffs, NJ.

48.   White, H., *Learning in artificial neural networks: A statistical perspective.* Neural computation, 1989. 1(4): p. 425-464.

49.   Barron, A.R. and R.L. Barron. *Statistical learning networks: a unifying view*. in *Statistics and Computer Science: 1988 Symposium at the Interface*. 1988.

50.   Chen, V.C., et al., *A review on design, modeling and applications of computer experiments.* IIE transactions, 2006. 38(4): p. 273-291.

51.   Montgomery, D.C., E.A. Peck, and G.G. Vining, *Introduction to linear regression analysis*. Vol. 821. 2012: Wiley.

52.   HYSYS, A., *V7. 0, 2009, Aspen HYSYS Simulation Basis; Aspen HYSYS User's Guide.* AspenONEV7. 0 Documentation, AspenTechnology, Inc., Burlington, Massachusetts.

53.   Viana, F. and T. Goel, *SURROGATES toolbox user's guide.* ht tp://fchegury. googlepages. com,[retrieved Dec. 2009], 2010.

54.   Laurenceau, J. and P. Sagaut, *Building efficient response surfaces of aerodynamic functions with kriging and cokriging.* AIAA journal, 2008. 46(2): p. 498-507.

55.   Thompson, M.L. and M.A. Kramer, *Modeling chemical processes using prior knowledge and neural networks.* AIChE Journal, 1994. 40(8): p. 1328-1340.

56.   Moré, J.J., *The Levenberg-Marquardt algorithm: implementation and theory*, in *Numerical analysis*1978, Springer. p. 105-116.